



Annual Report (2010)

No.22

The NOVARTIS Foundation (Japan)
for the Promotion of Science

平成22年度
財団年報 第22号

財団法人 ノバルティス科学振興財団

Contents

I . Introduction	はじめに	7
	Akimichi Kaneko, MD, PhD Chairman of the Board of Trustees	
II . Reports from the Recipients of Novartis Research Grants		
	研究報告	9
1.	Physiological functions of TRIC channels	10
	Hiroshi Takeshima Kyoto University, Graduate School of Pharmaceutical Sciences	
2.	The screening and functional analysis of aerial hyphae inducing signal between soil bacteria	13
	Shinya Kodani Shizuoka University	
3.	Analysis of molecular mechanism underlying ciliary development and maintenance using zebrafish	14
	Yoshihiro Omori Osaka Bioscience Institute	
4.	Functional analysis of the tumor suppressor EXT-like gene <i>EXTL2</i>	17
	Hiroshi Kitagawa Kobe Pharmaceutical University, Department of Biochemistry	
5.	Dissecting mechanisms of cell elimination and epithelial maintenance by cell-cell communications	22
	Tatsushi Igaki Kobe University Graduate School of Medicine	
6.	Design and synthesis of peptide mimetics based on biologically active cyclic depsipeptides	24
	Takayuki Doi Graduate School of Pharmaceutical Sciences, Tohoku University	
7.	Relay Catalysis by Transition Metal Complex/Organic Molecule Binary System for Advanced Molecular Transformation of Nitrogen Containing Compounds	26
	Masahiro Terada Tohoku University	
8.	Analyses of signaling pathway for myelin development by investigating molecular target of demyelinating disease	29
	Junji Yamauchi Department of Pharmacology, National Research Institute for Child Health and Development	

9. Role of leukotriene B4 in allergic airway inflammation	33
Nobuaki Miyahara Department of Allergy and Respiratory Medicine, Okayama University Hospital	
10. The effects of Dickkopf 1, an inhibitor of Wnt signaling pathway, on anti-ageing (anti-wrinkle, whitening and regeneration of pigment, hair and site-specific skin)	36
Yuji Yamaguchi Department of Geriatric and Environmental Dermatology, Nagoya City University Graduate School of Medical Sciences	
11. The Elucidation of transcriptional mechanisms which regulated by gas, one of the smallest unit molecules	40
Taku Yamashita Graduate School of Pharmaceutical Sciences, Osaka University	
12. Development of the method to induce and amplify the ES cell-derived germ layer stem cell	45
Takumi Era Department of Cell Modulation, Institute of Molecular Embryology and Genetics, Kumamoto University	
13. Role of G proteins in the spermatogonial stem cell homing to niche	48
Mito Shinohara Kyoto University, Graduate School of Medicine	
14. Development of New Asymmetric Carbene Ligands toward Contributions to Medicinal Chemistry	54
Kazuhiro Yoshida Chiba University	
15. Role of tissue plasminogen activator for hematopoietic-cell driven neoangiogenesis	57
Beate Heissig Institute of Medical Science University of Tokyo	
16. Identification and characterization of novel prion-like cytoplasmic genetic factors	64
Motomasa Tanaka RIKEN Brain Science Institute	
17. Epigenetic profiling in germ and somatic cells for establishment of induced Germline Stem Cells	67
Kimiko Inoue Bioresource Center, RIKEN	
18. The role of semaphorin in organogenesis during development: Semaphorin 4A navigates intracellular trafficking of retinoids for photoreceptor survival	69
Toshihiko Toyofuku Research Institute for Microbial Diseases, Osaka University	

19. The prevention of postoperative intestinal adhesion by hepatocyte growth factor (HGF)	72
Tomohiro Yoshimoto Laboratory of Allergic Diseases. Institute for Advanced Medical Sciences. Hyogo College of Medicine	
20. Life and death Signalings in fly photoreceptors	76
Akiko Kono Satoh Graduate School of Science, Nagoya University	
21. Crosstalk between arginine methylation of BAD and its phosphorylation by Akt	78
Hiroaki Daitoku Graduate School of Life and Environmental Sciences, University of Tsukuba	
22. Enantioselective synthesis of α -aminophosphonic acid by the process chemistry-oriented method	80
Kaori Ando Gifu University	
23. Impact of GILC1 downregulation on the generation and progression of lung cancer	82
Motoshi Suzuki Nagoya University Graduate School of Medicine, Molecular Carcinogenesis	
24. Molecular basis for regulation of glucosinolate biosynthesis: Cancer preventive sulfur-containing compounds	84
Akiko Maruyama-Nakashita Fukui Prefectural University Faculty of Bioscience	
25. Synthetic Study and Structural Study of Super-carbon-chain Compounds Produced by the Marine Plankton	88
Hiroyoshi Takamura Division of Chemistry and Biochemistry, Graduate School of Natural Science and Technology, Okayama University	
26. Live-imaging studies on the biogenesis of thylakoid membranes in plastids	90
Wataru Sakamoto Institute of Plant Science and Resources, Okayama University	
27. Roles of GABAergic local circuits in the amygdala for emotional memory	94
Hideki Miwa Gunma University Graduate School of Medicine	
28. Dissecting the mechanisms for inhibitory effects of ACE2 on aberrant activation of innate-immune system	96
Keiji Kuba Akita University Graduate School of Medicine	
29. Analysis of molecular function and dynamics of nuclear pore complex protein Rae1 and tumorigenesis.	99
Richard W. Wong Frontier Science Organization, Kanazawa University	

30. Analysis of HNF transcription network in pancreatic β -cells	102
Kazuya Yamagata Department of Medical Biochemistry, Faculty of Life Sciences, Kumamoto University	
31. Study on mechanosensitive calcium channels as mechano-sensors in plants	104
Hidetoshi Iida Tokyo Gakugei University, Faculty of Education, Department of Biology	
32. Role of endoplasmic reticulum stress-induced phosphorylation of translation initiation factor 2 α in metabolic regulation	107
Seiichi Oyadomari Division of Molecular Biology, Institute for Genome Research, The University of Tokushima	
33. Transcription factor networks for maintenance and regeneration of the thymic epithelial stem cells	110
Ryo Goitsuka Tokyo University of Science	
34. Research for regulation mechanism of lymphocyte activation by CARMA1	112
Hiromitsu Hara Saga University	
35. Development of G-quadruplex motifs search in genome by the use of G-q ligands	114
Kazuo Nagasawa Department of Biotechnology and Life Science, Faculty of Technology Tokyo University of Agriculture and Technology	
36. Condition clarification and development of new strategy for the treatment of metabolic syndrome: Role of fatty acid composition and long chain fatty acid elongase Elovl6 in energy metabolism	117
Takashi Matsuzaka Department of Endocrinology and Metabolism, University of Tsukuba	
37. Molecular mechanisms of endoplasmic reticulum stress response in skeletal tissues and development of its regulation.	119
Kazunori Imaizumi Division of Molecular and Cellular Biology, Department of Anatomy, Faculty of Medicine, University of Miyazaki	
38. Structural Analysis of Biomolecules by A Combined Method of Azaelectrocyclization-based Microscale Labeling /Fluorescence Detected Circular Dichroism (FD-CD)	121
Katsunori Tanaka Osaka University	
39. Significance of Transcriptional Control in Vascular Development, Function and Disease	124
Osamu Nakagawa Nara Medical University Advanced Medical Research Center	

40. Severe Dyslipidemia, Atherosclerosis, and Sudden Cardiac Death in Mice Lacking All NO Synthases Fed a High-Fat Die	126
Masato Tsutsui Department of Pharmacology, Faculty of Medicine, University of the Ryukyus	
41. Mechanism of chromosome segregation control by molecules involved in spindle assembly checkpoint	136
Kozo Tanaka Institute of Development, Aging and Cancer, Tohoku University	
42. Molecular mechanism of <i>trans</i> -association of Tie2, a receptor for angiopoietin-1, and its biological significance	139
Shigetomo Fukuhara National Cerebral and Cardiovascular Center Research Institute	
III. Reports from the Recipients of Grants for International Meetings	
研究集会報告	143
1. 2009 29 th INTERNATIONAL SYMPOSIUM ON CANCER	144
Masanori Hatakeyama Hokkaido University	
2. 5 th International Symposium on Autophagy: Molecular mechanism, cellular and physiological functions, and diseases	146
Yasuyoshi Sakai Kyoto University	
3. The 9 th Annual Meeting of the Protein Science Society of Japan	148
Yuriko Yamagata Faculty of Medical and Pharmaceutical Sciences Kumamoto University	
4. The 11th International Symposium on Exocrine Secretion, Tokushima 09 Exocrine Secretion-Mechanism and Disease	150
Kazuo Hosoi Department of Molecular Oral Physiology, Institute of Health Bioscience, The University of Tokushima Graduate School	
5. 16th International Conference on Cytochrome P450	154
Hirofumi Shoun Tokyo University	
6. Satellite Symposium, XXXVIth International Union of Physiological Sciences (IUPS)	156
Gozoh Tsujimoto Department of Genomic Drug Discovery Science, Graduate School of Pharmaceutical Sciences Kyoto University	

IV.	The 23nd (fiscal year 2009) Promotion Report 第 23 期(2009 年度)助成事業報告	158
V.	The 23nd (fiscal year 2009) Financial Report 第 23 期(2009 年度)財務報告	161
VI.	List of the Board Members 役員名簿	162
VII.	Information from the Secretariat 事務局便り	165

Introduction

“Selection of the objective of individual research”



Akimichi Kaneko, MD, PhD
Chairman of the Board of Trustees

This annual report includes research and meeting reports written by the 2009 grantees. From these reports, you can vividly feel their passion and seriousness in pursuing research activities. Their passion is the source of energy to promote their activity. I strongly believe that the aim of the Foundation is to help keeping their passion and I would like to do our best toward this goal. I sincerely appreciate the assistance and warm encouragement extended by the members of the Board of Trustees, the auditors, the Board of Councilors and the Selection Committee. The powerful support by the Novartis Pharma KK enabled us to sustain our activity without interruption.

How do individual investigators select their research objectives? The most popular reason may be that they are “interested” in that particular topic. I believe this is the most reasonable way and this reason is perfectly acceptable for “amateur scientists”. However, professional researchers have responsibilities for their research which is supported by various funds. Often the objectives of researchers’ activity would be to “publish” their results, and they wish to publish as many papers as possible. In this situation they may select popular and easy targets for this purpose.

I believe that the most important aspect of selecting research objectives is to consider the value of their research outcome. I do not mean its applicability. It is important to pick up the topic that many researchers wish to know. Even if the topic is difficult to achieve because the necessary technique is unavailable, one has to break through the difficulty by their original idea. If the number of publications will be limited because of the difficulty, the outcome will be very valuable. Our Foundation will support such valuable research.

はじめに

「何を研究するか」

理事長 金子章道

本年度もこの財団年報に 2009 年度助成金を受けられた方々の報告書を収録いたしました。受賞者の皆様の研究に対する熱い思い、真摯な取り組み態度が感じられる素晴らしいエッセイ集です。このような研究に対する熱い思いが研究を推進していく上で非常に大事なエネルギーの源です。この熱意を冷まさないよう多少なりとお力添えをすることが研究助成金の目的と考え、努力を続けて行きたいと思っております。また、そのために尽力されている当財団関係者の皆様に深く感謝いたします。とりわけノバルティスファーマ社の継続した強力な経済的支援に御礼申し上げたいと思います。

さて、研究者の皆さんはその研究テーマをどのようにして選んでおられるのでしょうか。「自分が面白いと思ったから」というのが多くの方々の選択理由の一つでしょう。私もこれが研究の原点だと思います。アマチュアサイエンティストであればこれで十分なのですが、研究を職業としておられる方々はそれだけでいいのでしょうか。当然どこからか研究費をもらって研究を行っておられると思います。ですからそれに対する責任があります。ややもすると「論文を出す」ことが研究の目的になり、多数の論文が書けるような研究をするということになっていないでしょうか。そうすると「やり易く、早く結果が出る」研究課題を選ぶことになってしまいます。

研究テーマを選択する上で重要な視点はその研究がもたらす「知的価値」ではないかと思えます。私は研究成果が応用につながることを言っているわけではありません。多くの人たちが「知りたい」と考えていることを取り上げることで。現存の実験技術では解決できないと尻込みせず、それを創意工夫で解決してゆく、いわゆるブレークスルーを作り出すことが最重要だと思います。仮にそのために論文の数が少なくなっても、そのようにして生み出された研究成果は価値の高いものになりましょう。当財団ではそのような研究を支援したいと考えております。

II.

Reports from the Recipients of Novartis Research Grants

Physiological functions of TRIC channels

Hiroshi Takeshima

Kyoto University, Graduate School of Pharmaceutical Sciences
takeshim@pharm.kyoto-u.ac.jp

Abstract

TRIC channels function as monovalent cation-specific channels and mediate counter-ion movements coupled with ryanodine receptor-mediated Ca^{2+} release from intracellular stores in muscle cells. Mammalian tissues differentially contain two TRIC channel subtypes; TRIC-A is abundantly expressed in excitable cells, while TRIC-B is ubiquitously expressed throughout tissues. Here, we report the physiological role of TRIC-B channels in mouse perinatal development. TRIC-B-knockout neonates were cyanotic due to respiratory failure and died shortly after birth. In the mutant neonates, the deflated lungs exhibited severe histological defects, and alveolar type II epithelial cells displayed ultrastructural abnormalities. The metabolic conversion of glycogen into phospholipids was severely interrupted in the mutant type II cells, and surfactant phospholipids secreted into the alveolar space were insufficient in the mutant neonates. Moreover, the mutant type II cells were compromised for Ca^{2+} release mediated by inositol-trisphosphate receptors, despite Ca^{2+} overloading in intracellular stores. Our results indicate that TRIC-B channels take an active part in Ca^{2+} signalling to establish specialised functions of type II cells and are thus essential for perinatal lung maturation.

Keywords: alveolar epithelial cells, surfactant phospholipids, TRIC channels.

Introduction

Ca^{2+} is an essential second messenger in cellular signal-transduction pathways, and Ca^{2+} release from intracellular stores regulates a myriad of physiological functions including cell-fate decisions and cellular maturation. Ryanodine and inositol 1,4,5-trisphosphate (IP_3) receptor subtypes on the sarco/endoplasmic reticulum (SR/ER) comprise a unique family of intracellular Ca^{2+} release channels that mediate Ca^{2+} mobilisation in response to various stimuli. When Ca^{2+} cations are released from the SR/ER, a negative potential is generated on the luminal side, which likely inhibits subsequent Ca^{2+} release processes. Therefore, in addition to the Ca^{2+} uptake and storage functions of intracellular stores, counter-ion movements seem to be essential for efficient Ca^{2+} release in order to balance the membrane potential.

We have been conducting a survey of the molecular components supporting SR/ER multi-functions and recently identified two TRIC (trimeric intracellular cation) channel subtypes, namely TRIC-A and TRIC-B. TRIC-A protein contain three putative transmembrane segments and assemble into a bullet-shaped homo-trimer to function as a monovalent cation-selective channel. Knockout mice lacking both TRIC-A and TRIC-B channels suffer embryonic cardiac failure, and the mutant cardiac myocytes display severe dysfunction in SR Ca^{2+} handling. Moreover, the SR from TRIC channel-

deficient skeletal muscle shows reduced K^+ permeability and weakened Ca^{2+} release. Therefore, TRIC channels function as counter-ion channels that synchronise with ryanodine receptor-mediated Ca^{2+} release in striated muscle cells. The role of TRIC channels expressed in non-muscle cells, however, remains to be studied. We studied the neonatal lethality that occurs in TRIC-B-knockout mice, and unveiled an essential role for TRIC-B in perinatal lung maturation.

Results

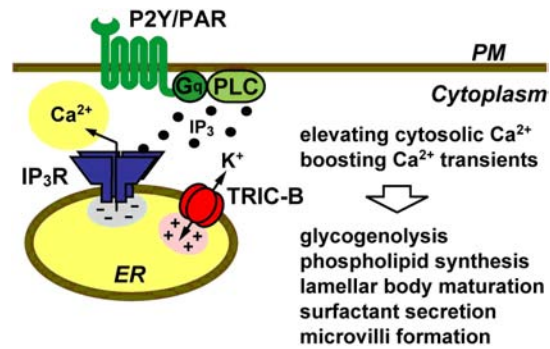
TRIC-B-knockout neonates show several abnormalities as described below.

- 1) TRIC-B-knockout neonates were delivered with the expected Mendelian frequency, but died shortly after birth. The mutant mice die due to severe hypoxia and acidosis resulting from respiratory failure. Histological data demonstrated that alveolar hypoplasia seems to be the major cause of death in the mutant neonates.
- 2) Alveolar type II epithelial cells responsible for surfactant synthesis were normally developed in TRIC-B-knockout mice. However, electron-microscopic observations indicated that glycogen deposits are accumulated and surfactant phospholipids are poorly synthesized in type II cells from TRIC-B-knockout neonates. Moreover, the surfactant phospholipids were insufficiently secreted into the alveolar space of the TRIC-B-knockout lung.
- 3) In type II cells from TRIC-B-knockout mice, Fura-2 Ca^{2+} imaging detected three major defects; 1) resting Ca^{2+} levels in the mutant cells were significantly lower than those in wild-type cells in a normal bathing solution, 2) agonist-induced Ca^{2+} transients is significantly impaired, 3) intracellular stores are Ca^{2+} -overloaded. The abnormal Ca^{2+} handling is closely linked to the morphological and biochemical defects in TRIC-B-knockout type II cells during perinatal maturation.

Discussion & Conclusion

TRIC-A protein forms a monovalent cation-selective channel in lipid bilayer membranes and functions as a counter-ion channel coupled with ryanodine receptor-mediated Ca^{2+} release in striated muscle cells. In our current collaborative study, recombinant TRIC-B protein displayed a similar channel-forming activity. Knockout mice lacking TRIC-A channels are fertile, while TRIC-B-knockout mice show neonatal lethality. Double-knockout mice lacking both TRIC subtypes are embryonic lethal, and the aggravated lethality indicates *in vivo* compensatory functions between the subtypes. In this study, we found weakened IP_3 receptor-mediated Ca^{2+} release from Ca^{2+} -overloaded intracellular stores in TRIC-B-knockout alveolar type II cells. These abnormalities in store Ca^{2+} handling closely resemble those observed in embryonic cardiomyocytes lacking both TRIC channel subtypes. Therefore, TRIC-B channels predominantly expressed in the neonatal lung seem to function as counter-ion channels synchronised with IP_3 receptor-mediated Ca^{2+} release and to support efficient agonist-induced Ca^{2+} responses in alveolar type II cells (see an attached figure

below). In addition to muscle and alveolar type II cells, TRIC channel subtypes likely contribute to physiological Ca^{2+} release in various cell types.



References

- 1) Yamazaki, D., Komazaki, S., Nakanishi, H., Mishima, A., Nishi, M., Yazawa, M., Yamazaki, T., Taguchi, R. & Takeshima, H. Essential role of TRIC-B channel in Ca^{2+} - handling of alveolar epithelium and perinatal lung maturation. *Development* **136**, 2355-2361, 2009.

The screening and functional analysis of aerial hyphae inducing signal between soil bacteria

Shinya Kodani
Shizuoka University
askodan@ipc.shizuoka.ac.jp

Abstract

The aerial hyphae inducing compound was isolated from *Streptomyces hawaiiensis*. The molecular weight of the compound was deduced to be 262Da by ESI-MS analysis. The partial chemical structure of the compound was determined by NMR analyses.

Keywords: streptomycetes, aerial hyphae induction, bioactive compound

Introduction

It is known that soil bacteria, streptomycetes, have the similar life cycle with that of fungi. Aerial hyphae-spore formation followed by spore formation is an important strategy for the streptomycetes, resisting to dryness and the shortage of nutrition. The purpose of this study is to discover the aerial hypha inducing compounds to clarify the development mechanism.

Results

The culture media of *Streptomyces hawaiiensis* was extracted by acetone. The reversed phase open column chromatography with aqueous MeOH system was used after the concentration of the extract. The active compound was isolated using HPLC with ODS column. By ESI-MS analysis on the compound, the ion peak was observed at $[M+H]^+$ m/z 263. The compound was barely soluble in distilled water or various organic solvents. On HPLC analysis of the compound, two exchangeable peaks were detected, which showed same molecular weight in ESI-MS measurement. Therefore, the analysis of two dimensional NMR was performed after acetylating of the compound was done to eliminate exchanging between two structures. The compound was converted into one steady structure, and the partial structure was decided by two dimensional NMR.

Discussion & Conclusion

The aerial hyphae inducing compound was isolated from *Streptomyces hawaiiensis*. The molecular weight of the compound was deduced to be 262Da by ESI-MS analysis. The partial chemical structure of the compound was determined. The complete determination of the gross structure is now on going.

Analysis of molecular mechanism underlying ciliary development and maintenance using zebrafish

Yoshihiro Omori

Osaka Bioscience Institute

omori@obi.or.jp

Abstract

A photoreceptor cell develops a photo-sensitive outer segment on the apical side of the cell body. A cilium with a microtubule axoneme connects the outer segment and the photoreceptor cell body. Ciliary integrity is crucial for survival of photoreceptor cells, because large amounts of proteins involved in photo-transduction are transported from the photoreceptor cell body to the outer segments thorough cilia. In human, functional disruption of several ciliary proteins causes photoreceptor cell death and progressive blindness called as retinitis pigmentosa (RP). However, molecular mechanisms underlining ciliary formation and maintenance in photoreceptors have been poorly understood. In order to investigate molecular mechanisms of photoreceptor formation and maintenance, we performed an ENU-mutagenesis screen using a transgenic zebrafish line expressing GFP under control of the rhodopsin promoter. The GFP labels photoreceptor cells specifically in the zebrafish retina. We carried out an early-pressure screen by observing morphological integrity of the GFP labeled photoreceptors. We identified four recessive mutants defective in formation of photoreceptor outer segments. We found that these mutations were also defective in the ciliary formation of inner ear hair cells and olfactory cells.

Keywords: Zebrafish, cilium, retina, photoreceptor

Introduction

Cilia are microtubule-based hair-like organelles which extend from apical surface of the eukaryotic cells. Since cilia protrude from cell surface, they can act as “ antennae” which receive signals from the periphery. The transport of proteins in the cilium is dependent on intraflagellar transport (IFT). IFT is not only necessary for transport of axonemal components, but is also important for the sensory activity of cilia.

In human, Ciliary defects cause various disease. Defect of the photoreceptor cilia in the retina causes progressive blindness, retinitis pigmentosa (RP). Defects of ciliary function also cause obesity, polydactyly, cystic kidney, sperm immotility and situs inversus. Zebrafish develops cilia in the sensory organs, kidney and CNS similar to Mammals. Cilia in the sensory neurons such the retina, inner ear, nasal pit and lateral lines are develop between 24hpf to 72hpf in the zebrafish embryos. In the developing zebrafish embryo, these ciliated cells are easy to access for observation. Previously we found that a IFT component, Elipsa is interact with Rab8 through Rabaptin5 and play a crucial role for ciliary protein transport (Omori et al., 2008). We also identified that an apico-

basal polarity determinant, *crb3a*, is essential for ciliary integrity of inner ear hair cells (Omori et al., 2006).

Results

To identify mutations affecting development and maintenance of photoreceptors, we performed genetic screen using ENU-based mutagenesis screen. We used a transgenic line which expresses GFP in the photoreceptor specifically. In this line, GFP is expressed specifically in the rod photoreceptor cells under the control of rhodopsin promoter. We performed early pressure screen for 450 lines. We isolated several mutations which affect photoreceptor development at 5 dpf. We found that these mutations affect in the ciliogenesis of other sensory neurons including olfactory cells in the nasal pit and hair cells in the inner ear.

In the wild type photoreceptors, opsin localizes to the outer segment of photoreceptors. However, in the mutant photoreceptors, opsin does not localize to the outer segment and accumulates to the surface of cell bodies. GEP226 and GEP263 show obvious cystic kidney phenotype. GEP226 shows curly tail similar to *elipsa* mutant. GEP226 has ciliary defects in the photoreceptor, hair cells and olfactory cells. GEP263 shows progressive photoreceptor cell death and cystic kidney. GEP263 does not show curly tail. GEP263 might to be categorized different group from IFT mutants such as *elipsa*.

To observe ciliary phenotype in the mutants, we stained with the anti- acetylated alpha-tubulin antibody. GEP305 has ciliary defects in the photoreceptor, hair cells and olfactory cells. We roughly mapped GEP305 on zebrafish chromosomes. Fine mapping of this gene is currently in progress.

On a related issue, recently we also showed that *Blimp1* suppresses *Chx10* expression in differentiating retinal photoreceptor precursors (Kato, Omori et al., 2010). Furthermore, we also identified that a novel photoreceptor-specific ankyrin repeat protein, *Panky*, is a transcriptional cofactor that suppresses CRX-regulated photoreceptor genes (Sanuki, Omori et al., 2010).

Discussion & Conclusion

We identified four recessive mutants defective in formation of photoreceptor outer segments. We found that these mutations were also defective in the ciliary formation of inner ear hair cells and olfactory cells. These mutations did not cause obvious curly tail, a common feature of IFT mutants such as *elipsa* and *oval* (Omori et al., 2008). These results suggest that the mutated genes encode molecules essential for ciliary formation of sensory neurons.

References

- 1) Omori Y, Zhao Z, Saras A, Mukhopadhyay S, Kim W, Furukawa T, Sengupta P, Veraksa A, Malicki J
elipsa is an early determinant of ciliogenesis that links the IFT particle to membrane-associated small GTPase Rab8 *Nat Cell Biol.* 2008 **10**(4):437-44

- 2) Omori Y, Malicki J. *oko meduzy* and related crumbs genes are determinants of apical cell features in the vertebrate embryo. *Curr Biol.* 2006 **16** (10):945-957.
- 3) Katoh K, Omori Y, Onishi A, Sato S, Kondo M, Furukawa T. Blimp1 suppresses Chx10 expression in differentiating retinal photoreceptor precursors to ensure proper photoreceptor development. *J Neurosci* 2010, **30**(19):6515-26.
- 4) Sanuki R, Omori Y, Koike C, Sato S, Furukawa T. Panky, a novel photoreceptor-specific ankyrin repeat protein, is a transcriptional cofactor that suppresses CRX-regulated photoreceptor genes. *FEBS letter* 2010 Feb 19;**584**(4):753-8.

Functional analysis of the tumor suppressor EXT-like gene *EXTL2*

Hiroshi Kitagawa

Kobe Pharmaceutical University, Department of Biochemistry
kitagawa@kobepharma-u.ac.jp

Abstract

Heparan sulfate (HS) is synthesized by HS co-polymerases encoded by the *EXT1* and *EXT2* genes, which are known as causative genes for hereditary multiple exostoses, a dominantly inherited genetic disorder characterized by multiple cartilaginous tumors. It has been thought that the heterooligomeric EXT1-EXT2 complex is the biologically relevant form of polymerase and that targeted deletion of either *EXT1* or *EXT2* leads to a complete lack of HS synthesis. Here we show, unexpectedly, that two distinct cell lines defective in *EXT1* expression indeed produce small but significant amounts of HS chains. The HS chains produced without the aid of EXT1 decreased in length compared with HS chains formed in concert with EXT1 and EXT2. In addition, biosynthesis of HS in *EXT1*-defective cells was notably blocked by knockdown of either EXT2 or EXTL2, but not of *EXTL3*. Then, to examine the roles of EXTL2 in the biosynthesis of HS in *EXT1*-deficient cells, we focused on GlcNAc transferase activity of EXTL2, which is involved in the initiation of HS chains by transferring the first GlcNAc to the linkage region. Although EXT2 alone synthesized no heparan polymers on the synthetic linkage region analogue GlcUA β 1-3Gal β 1-*O*-C₂H₄NH-benzyloxycarbonyl, marked polymerization by EXT2 alone was demonstrated on GlcNAc α 1-4GlcUA β 1-3Gal β 1-*O*-C₂H₄N-benzyloxycarbonyl, which was generated by transferring a GlcNAc residue using recombinant EXTL2 on GlcUA β 1-3Gal β 1-*O*-C₂H₄NH-benzyloxycarbonyl. These findings indicate that the transfer of the first GlcNAc residue to the linkage region by EXTL2 is critically required for the biosynthesis of HS in cells deficient in *EXT1*.

Keywords: Heparan sulfate, proteoglycan, glycosaminoglycan, hereditary multiple exostoses

Introduction

Heparan sulfate (HS) proteoglycans are ubiquitously found at the cell surface and in the extracellular matrix, affecting a variety of biological processes, including specific signaling pathways. The biosynthesis of HS chains is initiated by construction of the tetrasaccharide linkage region, GlcUA β 1-3Gal β 1-3Gal β 1-4Xyl β 1-, where Xyl is attached to a serine residue in the core protein. Next, the HS chain backbone is synthesized by HS polymerases encoded by *EXT1* and *EXT2* in the *EXT* (exostosin) gene family, which were first identified as causative genes of a genetic bone disorder, hereditary multiple exostoses, and subsequently demonstrated to function as tumor suppressor genes. Both EXT1 and EXT2 encode bifunctional glycosyltransferases with *N*-acetylglucosaminyltransferase II (GlcNAcT-II) and glucuronyltransferase II (GlcAT-II) activities that catalyze the polymerization of HS. EXT1 and EXT2 form a heterooligomeric complex *in vivo*,

leading to higher glycosyltransferase activity than EXT1 and EXT2 alone. Thus, it is suggested that the EXT1-EXT2 heterocomplex represents the biologically functional form of HS polymerases.

The *EXT* gene family consists of five members, *EXT1*, *EXT2*, and three additional members, designed *EXTL1-3* (*EXT-like 1-3*), based on the amino acid sequence similarity of their gene products to EXT1 and EXT2 proteins. The *EXTL* genes have not been linked to hereditary multiple exostoses, although the chromosomal loci of the genes imply that they might also encode tumor suppressors. All three *EXTL* proteins possess glycosyltransferase activities related to HS biosynthesis; however, in view of the recent findings that *in vitro* HS polymerization was induced on tetrasaccharide-linkage analogs as acceptor substrates by the enzyme complex of human EXT1-EXT2 without the aid of *EXTL* proteins, the biological roles of mammalian *EXTL*s in HS biosynthesis are less clearly defined. *EXTL2*, the shortest member of the *EXT* family, is an *N*-acetylhexosaminyltransferase that transfers not only GlcNAc but also GalNAc to the linkage region. Here we present the evidence that the transfer of the first GlcNAc residue to the linkage region by *EXTL2* is critically required for the biosynthesis of HS in cells deficient in *EXT1*.

Results

Gro2C Cells Defective in EXT1 Synthesize Small Amounts of HS

Previous studies have shown that gro2C cells, a mouse L cell mutant, are deficient in the expression of *EXT1*, which encodes a glycosyltransferase related to the formation of the HS backbone and thereby synthesizes no HS chains. In this study, however, characterization of GAGs isolated from L and gro2C cells with a mixture of heparinase and heparitinase revealed that gro2C cells synthesized a small but significant amount of HS, which was ~15% of the amount produced by L cells. Then, to examine whether the decrease in the amount of HS in gro2C cells was the result of a reduction in the length of HS, HS chains obtained by reductive β -elimination using alkali from L and gro2C cells were subjected to gel filtration chromatography, revealing that gro2C cells produced shorter HS chains than L cells.

HL60 cells defective in EXT1 also synthesize HS chains

It has been reported that transcriptional inactivation of *EXT1* by CpG island promoter hypermethylation occurs in HL60 cells, leading to loss of *EXT1* expression. In fact, *EXT1* mRNA was not expressed in HL60 cells, whereas *EXT2*, *EXTL2* and *EXTL3* were produced. We next examined whether HL60 cells also synthesize a small number of HS chains. We found that HL60 cells indeed produced a detectable amount of HS without the assistance of *EXT1* as well as gro2C cells. HL60 cells synthesized about 10% of the amounts of HS synthesized in HL60 cells treated with a DNA demethylating agent, AZA, by which the epigenetic loss of *EXT1* function can be restored. Furthermore, the length of HS chains synthesized in HL60 cells was examined. The results indicated that there was a decrease in the amount of HS chains with lengths of 8~37 kDa produced in HL60 cells compared with cells treated with AZA. These results suggest that *EXT1*-deficient cells can produce shorter HS chains.

EXTL2 plays an important role in HS biosynthesis in EXT1-deficient cells

As EXT2 alone exhibits no HS polymerization activity in the synthetic linkage region analogue GlcUA β 1-3Gal β 1-*O*-C₂H₄NH-benzyloxycarbonyl, we next investigated the involvement of EXTLs in HS biosynthesis in gro2C cells. *EXTL1* mRNA was expressed at a very low level in gro2C and HL60 cells; therefore, we examined whether EXTL2 or EXTL3 might contribute to HS biosynthesis in *EXT1*-deficient cells. Gro2C cells stably transfected with either a mouse EXT2, EXTL2, or EXTL3 shRNA-expressing vector were established. Knockdown of *EXT2* decreased the amount of HS by approximately 75%, suggesting that EXT2 may function as HS polymerase in gro2C cells. A decrease in the expression level of *EXTL2* reduced the amount of HS by >50%. In contrast, knockdown of *EXTL3* had little effect on amount of HS synthesis. These results indicate that EXT2 and EXTL2 work together to produce HS chains in *EXT1*-deficient cells.

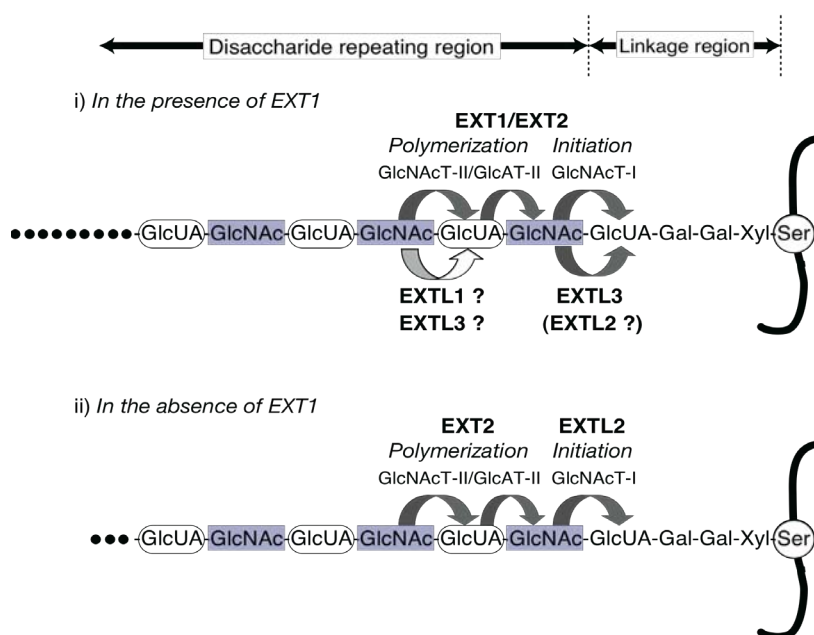


Figure 1 Role of EXTL2 in HS biosynthesis in *EXT1*-deficient cells

In the presence of *EXT1*, an *EXT1-EXT2* complex has dual functions to initiate HS biosynthesis and polymerize HS chains. *EXTL3* is also involved in transferring the first GlcNAc to the tetrasaccharide linkage region as GlcNAc-I. *EXTL3* might be indispensable for HS biosynthesis, and regulate the number and length of HS chains. In the absence of *EXT1*, *EXT2* alone cannot execute HS polymerization because of a lack of GlcNAc-I activities. Thus, *EXTL2* is required for initiation of HS biosynthesis. Given that the first GlcNAc is transferred to the linkage region by *EXTL2*, *EXT2* can polymerize HS chains. The length of HS chains produced without the aid of *EXT1* is shorter than that synthesized by the *EXT1-EXT2* complex.

EXTL2 acts as GlcNAc-I to initiate HS biosynthesis in *EXT1*-deficient cells

It has been reported that recombinant soluble enzymes expressed by the co-transfection of *EXT1* and *EXT2* exhibit polymerization activities and synthesize heparan polymer on the synthetic linkage region analog, GlcUA β 1-3Gal β 1-*O*-C₂H₄NH-benzyloxycarbonyl. In contrast, no significant polymerization was reported to occur on GlcUA β 1-3Gal β 1-*O*-C₂H₄NH-benzyloxycarbonyl by individually expressed *EXT1* and *EXT2*. Thus, we speculated that even *EXT1* and *EXT2* alone could polymerize HS chains to some extent, provided that the first GlcNAc has been transferred to the linkage region by *EXTL2*. For this analysis, GlcNAc α 1-4GlcUA β 1-3Gal β 1-*O*-C₂H₄NH-

benzyloxycarbonyl, which was generated by recombinant EXTL2. Separately expressed EXT1 or EXT2 alone could utilize GlcNAc α 1-4GlcUA β 1-3Gal β 1-O-C₂H₄NH-benzyloxycarbonyl as an acceptor and exhibited weaker yet significant polymerization activities compared with co-expressed EXT1-EXT2. However, the chain length of the products formed by EXT1 or EXT2 alone was shorter than that formed by co-expressed EXT1-EXT2. These results demonstrate that EXT2 alone can achieve HS polymerization with the aid of GlcNAcT-I activities of EXTL2 even in the absence of EXT1 (Fig. 1).

Discussion & Conclusion

Three *EXT-like* (*EXTL*) genes that share significant sequence homologies with *EXT1* and *EXT2* have been identified. All *EXTL1*, *EXTL2*, and *EXTL3* encode proteins with glycosyltransferase activities related to HS biosynthesis; however, their roles in HS biosynthesis *in vivo* remain unclear. In this study, we demonstrated that GlcNAcT-I activities of EXTL2 were required for HS synthesis in *EXT1*-deficient cells. RNA interference of *EXT2* or *EXTL2* depressed HS biosynthesis in *gro2C* cells to a similar extent, suggesting a distinct function of EXT2 and EXTL2 in HS biosynthesis in *EXT1*-deficient cells. We therefore thought that transfer of the first GlcNAc residue to the tetrasaccharide linkage by EXTL2 might be needed for the HS polymerization process by EXT2 alone. As expected, EXT2 alone could form no heparan polymers on the synthetic linkage analog GlcUA β 1-3Gal β 1-O-C₂H₄NH-benzyloxycarbonyl, but the transfer of GlcNAc to the synthetic linkage analog by EXTL2 allowed EXT2 to synthesize HS chains. In contrast, knockdown of *EXTL3* had little effect on the amount of HS in *EXT1*-deficient cells, although EXTL3 also possesses GlcNAcT-I activities as well as EXTL2. In fact, the amounts of HS were markedly decreased by knockdown of *EXTL3* in *EXT1*-expressing L cells. In addition, *EXTL3* knockout mice have been generated and HS biosynthesis is reported to be severely reduced in *EXTL3*^{-/-} embryos. These results suggest that EXTL3 might mainly function as a GlcNAcT-I in the presence of EXT1 (Fig. 1).

The functional importance of GlcNAcT-I activities in HS biosynthesis has been demonstrated in several *in vivo* model animals. In *Drosophila*, there are three orthologs of mammalian *EXT* genes, *EXT1* (*ttv*), *EXT2* (*sotv*) and *EXTL3* (*botv*). Biochemical and immunohistochemical studies on *Drosophila* have revealed that HS levels are markedly reduced or abolished in the absence of *ttv*, *sotv*, or *botv*. Although TTV/SOTV complex can catalyze the HS polymerization reaction *in vitro*, the complex exhibits no GlcNAcT-I activity required for the initiation of HS in contrast to human EXT1/EXT2 complex, indicating that BOTV, corresponding to human EXTL3, which possesses GlcNAcT-I activity, is indispensable for HS biosynthesis in *Drosophila*. In this regard, Han *et al.* demonstrated that *botv*-null embryos exhibited stronger segment polarity phenotypes than *ttv*- or *sotv*-null embryos and that Wg signaling is defective only in the *botv* mutant or *ttv-sotv* double mutant but not in the *ttv* or *sotv* mutant. These results together suggest that BOTV is essential for the initiation of HS and that all three EXT members, *ttv*, *sotv*, and *botv*, are required for HS biosynthesis

in *Drosophila*. In mammals, the enzyme complex of human EXT1/EXT2 without the aid of EXTL proteins can synthesize HS chains; however, in view of our results, the transfer of the first GlcNAc residue to the tetrasaccharide-linkage region by EXTL2 is thought to trigger HS biosynthesis in the absence of EXT1.

References

- 1) Okada, M., Nadanaka, S., Shoji, N., Tamura, J., and Kitagawa, H. (2010) Biosynthesis of heparan sulfate in EXT-1-deficient cells. *Biochem. J.*, in press.

Dissecting mechanisms of cell elimination and epithelial maintenance by cell-cell communications

Tatsushi Igaki

Kobe University Graduate School of Medicine

igaki@med.kobe-u.ac.jp

Abstract

Most cancers arise from a single cell of origin in an epithelial sheet. Therefore, a newly emerged oncogenic cell has to confront anti-tumor selective pressures in the host tissue. We found in *Drosophila* imaginal epithelia that surrounding normal cells activate non-apoptotic JNK signaling in response to the emergence of oncogenic cells. This JNK activation leads to activation of the phagocytic pathway, thereby eliminating oncogenic neighbors by engulfment.

Keywords: cancer, *Drosophila*, Cell-cell communication.

Introduction

Most cancers arise from a single cell that acquired multiple oncogenic alterations. Therefore, in the early stages of neoplastic development, pre-malignant oncogenic cells emerge as clones that are surrounded by normal cells. While cell-cell communication between oncogenic cells and surrounding normal cells can create a context that promotes tumor growth and progression, surrounding cells often exert anti-tumor effects. However, the molecular events at the interface between oncogenic cells and surrounding normal cells are largely unknown.

Results

Loss of apico-basal polarity is frequently associated with epithelial cancer development. Indeed, evolutionarily conserved apico-basal polarity genes such as *scribble* (*scrib*) and *discs large* (*dlg*) have been shown to function as tumor suppressors. For instance, human Scrib protein is down-regulated by proteasome-mediated degradation in tumors associated with human papillomavirus E6 infection, and loss of Scrib is correlated with the aggressiveness of late stage breast and colon cancers. Furthermore, depletion of *scrib* gene in mouse mammary epithelia has been shown to promote tumorigenesis. Similarly, in *Drosophila* epithelia, loss-of-function mutations in *scrib* or *dlg* result in tumorous overgrowths. Intriguingly, in *Drosophila* imaginal epithelia, clones of these mutant cells induced within wild-type tissue do not overproliferate but instead are eliminated from the tissue (Igaki et al., 2006; Igaki et al., 2009). This elimination of mutant cells occurs only when mutant cells are surrounded by wild-type cells, as removal of surrounding wild-type tissue by inducing cell death allows mutant tissue to overgrow (Brumby and Richardson, 2003). This suggests that normal imaginal tissue exerts an anti-tumor effect that eliminates oncogenic polarity-deficient cells. Previous studies have shown that these neoplastic tumor-suppressor mutant clones undergo

JNK-dependent cell death (Brumby and Richardson, 2003; Igaki et al., 2006; Igaki et al., 2009). However, the mechanism underlying elimination of oncogenic cells by surrounding normal cells, possibly through cell-cell communication, has remained unknown. In this study, we found that normal imaginal cells activate non-apoptotic JNK signaling in response to the emergence of polarity-deficient oncogenic clones. Furthermore, we found that this JNK activation in surrounding cells promotes elimination of oncogenic neighbors by activating the engulfment pathway (Fig. 1) (Ohsawa et al., submitted).

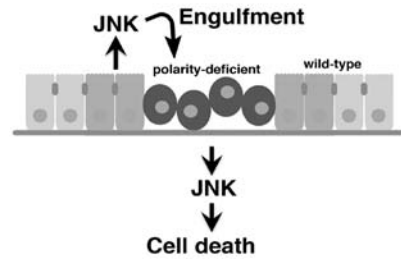


Fig 1

Discussion & Conclusion

Loss of epithelial integrity, particularly apico-basal polarity, is often associated with tumor development and malignancy. To counteract this, normal epithelial tissue seems to exert anti-tumor effects against such oncogenic cells. In this study, we found that normal imaginal epithelial cells exert an anti-tumor effect through activation of the JNK-mediated engulfment pathway. Our data indicate that JNK-mediated cell engulfment could be an evolutionarily conserved intrinsic tumor suppression mechanism that eliminates pre-malignant cells from epithelia.

References

- 1) Brumby, A.M., and Richardson, H.E. (2003). scribble mutants cooperate with oncogenic Ras or Notch to cause neoplastic overgrowth in *Drosophila*. *EMBO J* **22**, 5769-5779.
- 2) Igaki, T., Pagliarini, R.A., and Xu, T. (2006). Loss of cell polarity drives tumor growth and invasion through JNK activation in *Drosophila*. *Curr Biol* **16**, 1139-1146.
- 3) Igaki, T., Pastor-Pareja, J.C., Aonuma, H., Miura, M., and Xu, T. (2009). Intrinsic tumor suppression and epithelial maintenance by endocytic activation of Eiger/TNF signaling in *Drosophila*. *Dev Cell* **16**, 458-465.

Design and synthesis of peptide mimetics based on biologically active cyclic depsipeptides

Takayuki Doi

Graduate School of Pharmaceutical Sciences, Tohoku University

doi_taka@mail.pharm.tohoku.ac.jp

Abstract

Peptide mimetics of beauveriolide III designed on the basis of SAR study were synthesized. The mimetics exhibited inhibitory activity for lipid droplet accumulation in macrophages as well as for ACAT.

Keywords: cyclic peptide, mimetics, natural products

Introduction

Beauveriolide III, a 13-membered cyclic depsipeptide, is an inhibitor of lipid droplet accumulation in macrophages and is expected to be a drug candidate for treating atherosclerogenesis. We have already reported for a combinatorial synthesis of its analogues and elucidated structure-activity relationships [1]. The three-dimensional configuration of the side chains of beauveriolide is of importance for biological activity.

Results

The synthesis of a 6-membered ring compound, a bicyclic compound, and a 10-membered ring compound in which the substituents may have similar three-dimensional position to the side chains in beauveriolide III was planned. Toward the high-speed synthesis of a variety of these peptide mimetics, solid-phase synthesis was utilized. The first moiety was attached on the polymer-support by acetal formation. After coupling with two synthetic fragments with above polymer-supported amine, the cyclization precursor was cleaved from the polymer-support by weak acid. Concomitant Mannich-type cyclization provided a 6-membered ring compound, a bicyclic compound, and a 10-membered ring compound. These products exhibited potent inhibitory activity for lipid droplet accumulation in macrophages as well as that for ACAT.

Discussion & Conclusion

We have demonstrated the synthesis of a new bicyclic ring and a 10-membered ring we originally designed. Since the products exhibited potent inhibitory activity for lipid droplet accumulation, these new skeletons could have potential in the point of view of drug discovery. Further study for a library synthesis on the basis of these skeletons is underway.

References

- 1) H. Tomoda and T. Doi, *Acc. Chem. Res.*, **41**, 32 (2008).

Relay Catalysis by Transition Metal Complex/Organic Molecule Binary System for Advanced Molecular Transformation of Nitrogen Containing Compounds

Masahiro Terada

Tohoku University

mterada@mail.tains.tohoku.ac.jp

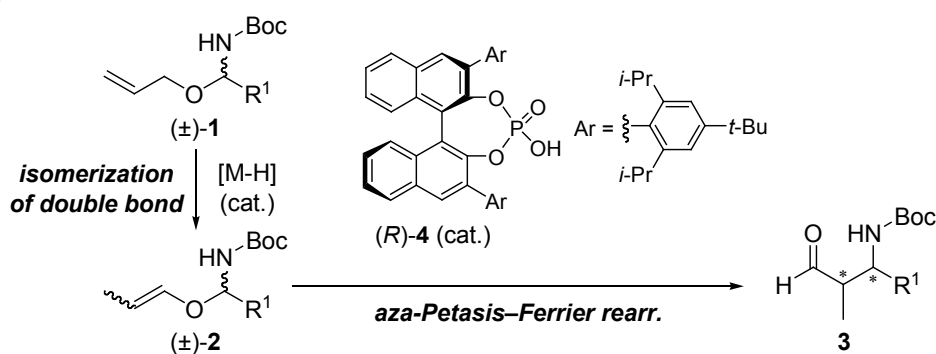
Abstract

Highly *anti*- and enantioselective synthesis of β -amino aldehydes having an aliphatic substituent at the β -position was accomplished by combination of two catalytic reactions, that is, an initial Ni(II) complex-catalyzed isomerization of a double bond followed by a chiral phosphoric acid-catalyzed aza-Petasis-Ferrier rearrangement, using hemiaminal allyl ethers as the initial substrate.

Keywords: asymmetric synthesis, catalysis, organocatalysts

Introduction

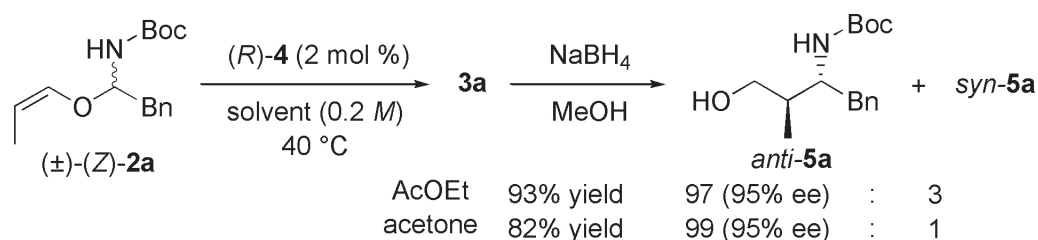
Considerable efforts have been devoted to the development of *syn*- or *anti*-selective synthesis of β -amino aldehydes in an optically active form, which are versatile synthetic precursors of amino alcohols, amino acids, β -lactams, and amino sugars, among others. The enantioselective direct Mannich reaction of aliphatic aldimines has largely been unexploited because these aldimines are readily isomerized to their enamine form. To overcome this intrinsic problem, we envisioned an alternative strategy to furnish optically active β -amino aldehydes having an aliphatic substituent (R^1) at the β -position by combination of two catalytic reactions (Scheme 1). The sequence involves initial metal-catalyzed isomerization of a double bond followed by a chiral Brønsted acid-catalyzed aza-Petasis-Ferrier rearrangement,¹ using readily available hemiaminal allyl ethers (**1**) as the initial substrate. Herein we report the sequential transformation of racemic **1** to optically active β -amino- β -alkylaldehydes (**3**) via intermediary vinyl ethers (**2**) in a highly diastereo- and enantioselective manner.



Results

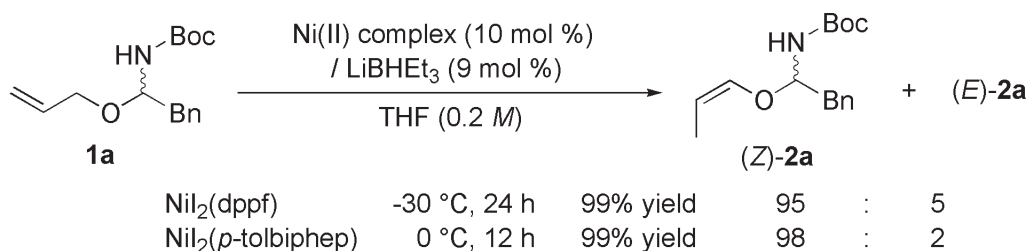
To the best of our knowledge, no previous reports have described enantioselective catalysis in aza-Petasis-Ferrier rearrangement, even considering chiral metal complexes, despite the wide applicability of **3** to the synthesis of a diverse array of nitrogen containing compounds. We therefore began by investigating diastereo- and enantioselective aza-Petasis-Ferrier rearrangement of hemiaminal vinyl ethers (**2**) using chiral phosphoric acids (**4**) as a catalyst.²

An initial experiment was performed using an (*Z*)-**2a** and 2 mol % of (*R*)-**4** at 40°C. Delightfully, **2a** was transformed cleanly to the desired β-amino aldehyde (**3a**: R¹ = Bn). Among the solvents examined, AcOEt and acetone were the best in terms of both chemical yields and enantioselectivities (Scheme 2).



Scheme 2

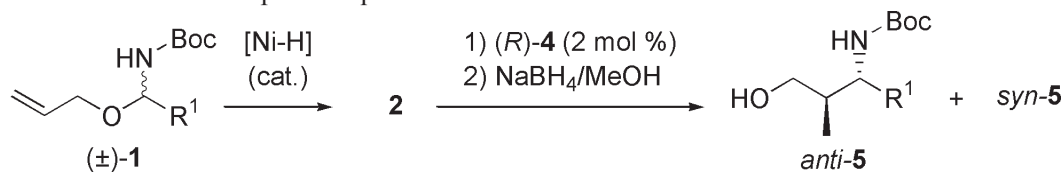
In an effort to establish a sequential protocol that combined the two catalytic reactions without the need for separation of the geometrical isomers of **2**, we next attempted (*Z*)-selective isomerization of **1** using a Ni(II) complex. NiCl₂ complexes having a phosphine ligand, such as PPh₂Me and dppb, can be utilized as efficient catalysts for isomerization of double bonds.³ However, the typical NiCl₂ complexes were not effective in the present case and **2a** was obtained with insufficient (*Z*)-selectivity. After thorough optimization of the ligands, counter anions of the nickel salts, and reaction temperature, a NiI₂ complex having a bidentate phosphine ligand, dppf or *p*-tolbiphep, was found to be the best, giving **2a** in high (*Z*)-selectivity (Scheme 3).



Scheme 3

Having identified (*Z*)-selective isomerization, we combined this with an enantioselective aza-Petasis-Ferrier rearrangement to develop a sequential transformation without the need for separation of the geometrical isomers of **2**. As shown in Table 1, the present sequential protocol is applicable to a variety of hemiaminal allyl ethers (**1**).

Table 1 Substrate Scope of Sequential Transformation of **1** to Amino Alcohols^a



entry	1(R ¹)	2(Z)/(E)	conditions ^b	5	yield (%) ^c (<i>anti/syn</i>)	ee (%) ^d
1	1a: Bn	98:2 ^e	acetone, 40 °C, 7 h	5a	70 (95:5)	94
2	1b: Me	97:3 ^f	AcOEt, 40 °C, 2 h	5b	86 (91:9)	76
3	1c: <i>n</i> -pentyl	96:4 ^f	acetone, 40 °C, 7 h	5c	76 (93:7)	97
4	1d: isobutyl	96:4 ^f	AcOEt, 40 °C, 3 h	5d	55 (95:5)	97
5	1e: <i>c</i> -hexyl	95:5 ^f	AcOEt, 40 °C, 3 h	5e	75 (95:5)	>99
6	1f: Ph	96:4 ^f	AcOEt, 40 °C, 3 h	5f	87 (93:7)	98

^a All reactions were carried out using 0.25 mmol of **1**.

^b Reaction conditions of enantioselective aza-Petasis-Ferrier rearrangement.

^c Combined yield of *anti/syn*-**5** from **1** (3 steps).

^d For major *anti*-**5**. Determined by chiral HPLC analysis.

^e Isomerization of **1** using NiL₂(*p*-tolbiphep).

^f Isomerization of **1** using NiL₂(dppf).

Discussion & Conclusion

In conclusion, we have demonstrated highly *anti*- and enantioselective synthesis of β-amino aldehydes having an aliphatic substituent at the β-position by combining two catalytic reactions, a Ni(II) complex-catalyzed isomerization of a double bond and a chiral phosphoric acid-catalyzed aza-Petasis-Ferrier rearrangement.

References

- (a) Frauenrath, H.; Arenz, T.; Raabe, G.; Zorn, M. *Angew. Chem., Int. Ed. Engl.* 1993, **32**, 83-85. (b) Arenz, T.; Frauenrath, H.; Raabe, G.; Zorn, M. *Liebigs Ann. Chem.* 1994, 931-942. (c) Tayama, E.; Otoyama, S.; Isaka, W. *Chem. Commun.* 2008, 4216-4218.
- Activation of hemiaminal ethers, see: Terada, M.; Machioka, K.; Sorimachi, K. *Angew. Chem., Int. Ed.* 2009, **48**, 2553-2556.
- (a) Wille, A.; Tomm, S.; Frauenrath, H. *Synthesis* 1998, 305-308. (b) Yamamoto, Y.; Kurihara, K.; Yamada, A.; Takahashi, M.; Takahashi, Y.; Miyaura, N. *Tetrahedron* 2003, **59**, 537-542.

Analyses of signaling pathway for myelin development by investigating molecular target of demyelinating disease

Junji Yamauchi

Department of Pharmacology, National Research Institute
for Child Health and Development
jyamauchi@nch.go.jp

Abstract

Charcot-Marie-Tooth (CMT) disease is the most frequent peripheral neuropathy affecting the Schwann cells and neurons. CMT disease type 2 (CMT2) neuropathies are characterized by peripheral nerve aberrance. Four missense mutations of Rab7, a small GTPase of the Rab family involved in intracellular vesicular trafficking, are associated with the CMT2B phenotype. Despite a growing body of evidence concerning the gene structures responsible for genetically heterogenous CMT2B and other CMT2 neuropathies, little is known about the *in-vitro* neuropathy model and how CMT2B-associated mutation-caused aberrant neuritogenesis is properly reversed. Here, we show that compound A improves defective neurite formation in N1E-115 neuroblastoma cells regardless of which CMT2B-associated Rab7 mutant protein is expressed. Furthermore, compound A has similar effects in dorsal root ganglion (DRG) neurons expressing any of the four mutant Rab7 proteins. Thus, compound A has a previously unknown potential to improve defective neuritogenesis associated with CMT2B *in vitro*.

Keywords: Demyelination, CMT disease, Myelination

Introduction

Charcot-Marie-Tooth (CMT) disease is the most common inherited neuropathy of the peripheral nervous system (PNS) and is genetically and clinically heterogenous. CMT disease is characterized by progressive sensory neuron loss and by weakness, beginning in the legs and manifesting later in the hands. Based on nerve electrophysiology, most patients with CMT are categorized into two major types: CMT disease type 1 (CMT1) and CMT disease type 2 (CMT2) (Shy et al. 2002; Suter and Scherer 2003; Nicholson 2006; Barisic et al. 2008). Recent molecular genetic investigations have demonstrated that the clinical and neurophysiological features of the CMT subtypes are strongly associated with defective genes of different types (Nicholson 2006; Barisic et al. 2008). In CMT1, nerve conduction velocity is less than 38 m/s. The genes involved in CMT1 participate in Schwann cell development and maintenance of myelin structure. CMT2 is associated with normal nerve conduction velocity but decreased action potentials, and frequent loss of nerve fibers. The genes responsible for CMT2 appear to code for the molecular connections necessary for axonal stability. While many of the genes and mutations responsible for CMT disease have been identified, we still do not know what compound protects against nerve fiber loss, nor how it may be reversed.

CMT2B is characterized by profound loss of pain sensation with mild to severe loss of sensory neuron fibers but is often complicated by infections and arthropathy, and it is associated with high rates of amputation. CMT2B is also associated with motor neuron degradation. To date, four CMT2B-associated missense mutations have been identified in the *rab7* gene (Verhoeven et al. 2003; Houlden et al. 2004; Meggouh et al. 2006). The Rab7 protein is a small GTPase of the Rab family and controls membrane transport from early endosomes to late endosomes and lysosomes. Rab7 is perhaps the only known lysosomal Rab GTPase. Like Ras and Rho GTPases (Schmidt and Hall 2002; Rossman et al. 2005; Miyamoto and Yamauchi 2010), Rab GTPases act as molecular switches (Bucci and Chiariello 2006; Fukuda 2008). They are active when bound to GTP and can bind to downstream effector proteins, though they are inactive when bound to GDP. This transition is strictly regulated by two types of regulatory proteins: guanine-nucleotide exchange factors (GEFs) and GTPase-activating proteins (GAPs). When transfected with Rab7 harboring each of the CMT2B-associated mutations, N1E-115 cells exhibit defective neurite formation. Therefore, we used N1E-115 cells expressing the CMT2B-associated Rab7 mutants to perform a rescue experiment attempting to correct abnormal neurite formation by small molecule compounds. We report here that compound A improves defective neurite formation in N1E-115 cells. Similar effects are seen in dorsal root ganglion (DRG) neurons expressing a CMT2B-associated mutant Rab7. Thus, compound A is now known to improve peripheral neuropathy in an *in-vitro* model.

Results

To investigate whether the CMT2B-associated Rab7 mutants actually inhibit the formation of neurites, we transfected plasmids, each of which encoded one of the four known Rab7 proteins harboring CMT2B-associated mutations (L129F, K157N, N161T, or V162M; Verhoeven et al. 2003; Houlden et al. 2004; Meggouh et al. 2006), into N1E-115 cells. Typically, following their differentiation with reducing serum, approximately 40% of these N1E-115 cells exhibit neurites longer than two cell bodies at 48 hours. Wild type Rab7, like control transfection, did not have a significant effect on neurite behavior. In contrast, all Rab7 mutants inhibited neurite formation by more than 80%, supporting the conclusion made elsewhere that the functional deficiency of all four CMT2B-associated, mutated Rab7 proteins is biochemically equivalent (De Luca et al. 2008; Spinosa et al. 2008). Transfection with Rab7L129F, Rab7K157N, Rab7N161T, or Rab7V162M did not induce cell death, as revealed by the observation that transfected cells incorporating trypan blue made up less than 5% of all cells under these experimental conditions. Thus, N1E-115 cells can serve as a useful *in-vitro* model to reproduce the loss of neurite formation caused by all known CMT2B-associated mutations.

We next examined whether compound A has a protective effect on cells transfected with a CMT2B-associated mutant Rab7. We found that compound A stimulated neurite formation, leading to an increase of approximately 40%. These levels were comparable to those seen under

normal differentiation conditions. We did not observe an obvious toxic effect of compound A on cells. Thus we present compound A as the first chemical compound that can repair the neurite formation process after it has been damaged by a CMT2B-associated mutant Rab7 *in vitro*.

We next examined the effect of compound A in primary rat DRG neurons. When DRG neurons were transfected with a plasmid encoding a CMT2B-associated mutant Rab7, all mutated Rab7 constructs displayed largely blocked neurite formation. Thus, CMT2B-associated mutant Rab7 proteins had the ability to inhibit neurite formation. Meanwhile, treatment with compound A reduced the severity of these deficits by approximately 50%

Discussion & Conclusion

To date, four missense mutations in the *rab7* gene have been identified in CMT2B; these are associated with sensory neuron fiber loss and sometimes with motor neuron degradation. While Rab7 has multiple cellular functions in the endocytotic pathways, its primary function is in controlling late endocytotic traffic, that is, in transporting substances from early to late endosomes and to lysosomes. Rab7 is ubiquitously expressed in tissues and is perhaps the only lysosomal Rab GTPase. Recent biochemical evidence demonstrates that CMT2B-associated mutations of Rab7 can result in unregulated guanine nucleotide exchange reactions or inadequate GTPase activity. Yet the restriction, in most cases, of the disease phenotype associated with CMT2B-associated mutations of Rab7 to neurons with long neurites is thought to be due to the fact that none of these mutations, which exist outside of the guanine nucleotide binding domain, cause a complete loss of Rab7 activity; rather, they render it incomplete. Before beginning this study, we experimented with the human neuroblastoma cell lines NB1 and SHSY-5Y as potential *in-vitro* models, but could not observe any changes in neurite outgrowth in cells expressing a CMT2B-associated mutant Rab7. One reason for this may be that NB1 and SHSY-5Y cells are not able to extend long neurites, at least, not as long as those of N1E-115 cells. These results are consistent with the observation that CMT2B phenotypes are restricted to neurons with long neurites. In the current study, we have found that compound A repairs neurite formation processes that have been damaged through transfection of N1E-115 cells and primary DRG neurons with disease-associated mutant Rab7 proteins. As far as we have been able to ascertain, this is the first report identifying a chemical compound that can repair CMT2B-associated aberrant neurite behavior, as well as the first report establishing an *in-vitro* CMT2B peripheral neuropathy model.

References

- 1) Barisic N, Claeys KG, Sirotković-Skerlev M, Löfgren A, Nelis E, De Jonghe P, Timmerman V. 2008. Charcot-Marie-Tooth disease: a clinico-genetic confrontation. *Ann. Hum. Genet.* **72**:416-441.
- 2) De Luca A, Progida C, Spinosa MR, Alifano P, Bucci C. 2008. Characterization of the Rab7K157N mutant protein associated with Charcot-Marie-Tooth type 2B. *Biochem. Biophys. Res. Commun.* **372**:283-287.

- 3) Houlden H, King RH, Muddle JR, Warner TT, Reilly MM, Orrell RW, Ginsberg L. 2004. A novel RAB7 mutation associated with ulcero-mutilating neuropathy. *Ann. Neurol.* **56**:586-590.
- 4) Meggouh F, Bienfait HM, Weterman MA, de Visser M, Baas F. 2006. Charcot-Marie-Tooth disease due to a de novo mutation of the RAB7 gene. *Neurology* **67**:1476-1478.
- 5) Miyamoto Y, Yamauchi, J. 2010. Cellular signaling of Dock family proteins in neural function. *Cell. Signal.* **22**:175-182.
- 6) Nicholson GA. 2006. The dominantly inherited motor and sensory neuropathies: clinical and molecular advances. *Muscle Nerve* **33**:589-597.
- 7) Rossman KL, Der CJ, Sondek J. 2005. GEF means go: turning on RHO GTPases with guanine nucleotide-exchange factors. *Nat. Rev. Mol. Cell Biol.* **6**:167-180.
- 8) Schmidt A, Hall A. 2002. Guanine nucleotide exchange factors for Rho GTPases: turning on the switch. *Genes Dev.* **16**:1587-1609.
- 9) Shy ME, Garbern JY, Kamholz J. 2002. Hereditary motor and sensory neuropathies: a biological perspective. *Lancet Neurol.* **1**:110-118.
- 10) Spinosa MR, Progida C, De Luca A, Colucci AM, Alifano P, Bucci C. 2008. Functional characterization of Rab7 mutant proteins associated with Charcot-Marie-Tooth type 2B disease. *J. Neurosci.* **28**:1640-1648.
- 11) Suter U, Scherer SS. 2003. Disease mechanisms in inherited neuropathies. *Nat. Rev. Neurosci.* **4**:714-726.
- 12) Verhoeven K, De Jonghe P, Coen K, Verpoorten N, Auer-Grumbach M, Kwon JM, FitzPatrick D, Schmedding E, De Vriendt E, Jacobs A, Van Gerwen V, Wagner K, Hartung HP, Timmerman V. 2003. Mutations in the small GTP-ase late endosomal protein RAB7 cause Charcot-Marie-Tooth type 2B neuropathy. *Am. J. Hum. Genet.* **72**:722-727.

Role of leukotriene B4 in allergic airway inflammation

Nobuaki Miyahara

Department of Allergy and Respiratory Medicine, Okayama University Hospital
miyahara@md.okayama-u.ac.jp

Abstract

The role of leukotriene B4 in already established asthma has not been well defined. In the present study, blockade of leukotriene B4 receptor 1 significantly suppressed late phase airway development of AHR and inflammation in previously sensitized and challenged mice. Control of leukotriene B4 and BLT1 may be beneficial for the treatment of already established asthma.

Keywords: Leukotriene B4, BLT1, asthma

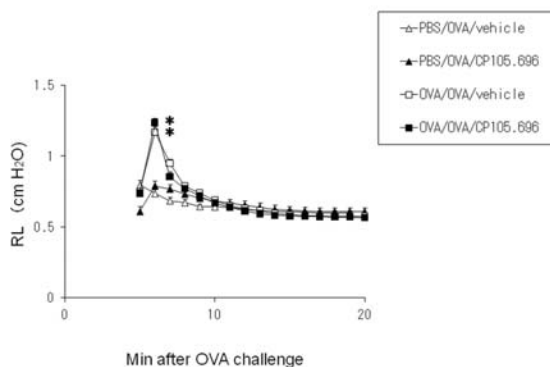
Introduction

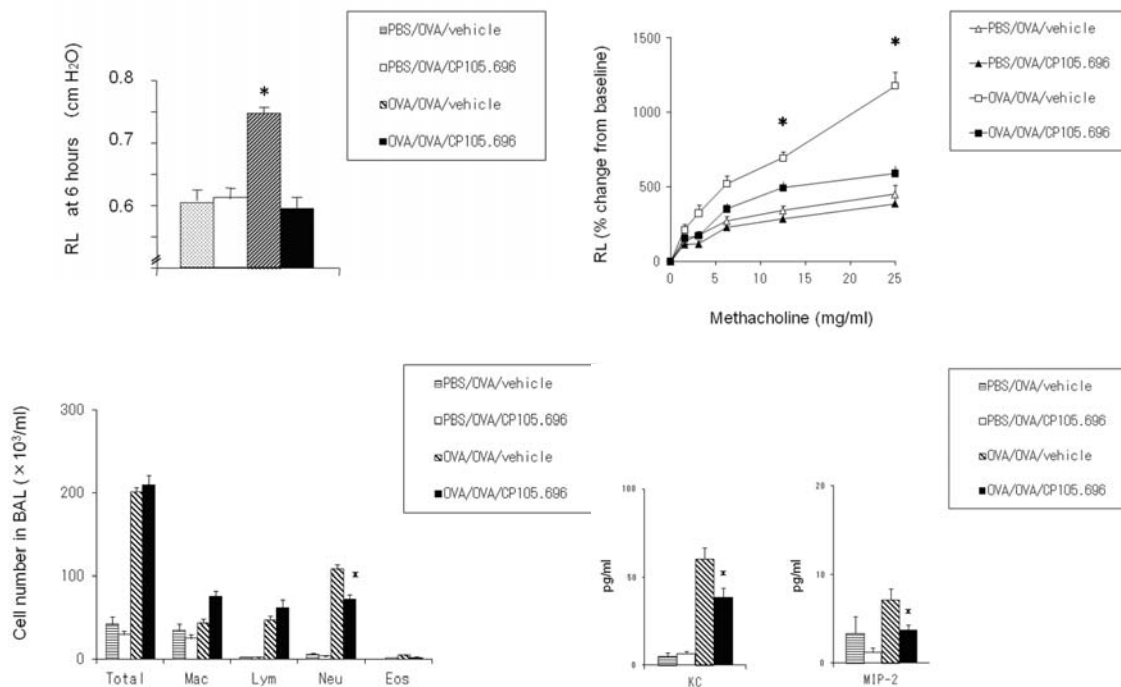
Most of the studies investing the effectiveness of blocking the leukotriene B4 (LTB4) receptor 1, BLT1, have been performed in models of primary allergen challenge. The role of the LTB4-BLT1 pathway in secondary challenge models, where airway hyperresponsiveness (AHR) and airway inflammation have already been established, has not been defined. We investigated the effects of blocking BLT1 on early and late phase airway development of AHR and inflammation in previously sensitized and challenged mice.

Results

Female BALB/c mice were sensitized (days 1 and 14) and challenged (primary, days 28-30) with OVA. Six weeks later (day 72), mice were challenged (secondary) with a single OVA aerosol and the early and late phase of development of AHR and inflammation were determined. Specific blockade of BLT1 was attained by oral administration of BLT1 antagonist (CP105,696) on days 70-72.

CP105,696 administration inhibited the secondary OVA challenge-induced changes in lung resistance during the late but not early phase. CP105,696 administration decreased bronchoalveolar lavage neutrophilia 6h after secondary challenge, which was associated with decreased levels of KC and MIP-2 in the airway.





Discussion & Conclusion

These data identify the importance of the LTB₄-BLT1 pathway in the development of late phase allergen-induced airway responsiveness following secondary airway challenge, that is, in mice with already established airway disease.

References

- 1) Busse WW., Lemanske RF Jr. Asthma. *New Engl. J. Med.* 2001;**344**:350-62.
- 2) Lewis RA, Austen KF, Soberman RJ. Leukotrienes and other products of the 5-lipoxygenase pathway. Biochemistry and relation to pathobiology in human diseases. *N Engl J Med.* 1990;**323**: 645-55
- 3) Miyahara N, Takeda K, Kodama T, Joetham A, Taube C, Park JW, Miyahara S, Balhorn A, Dakhama A, Gelfand EW. Contribution of antigen-primed CD8⁺ T cells to the development of airway hyperresponsiveness and inflammation is associated with IL-13. *J Immunol.* 2004;**172**:2549-58.
- 4) Miyahara N, Swanson BJ, Takeda K, Taube C, Miyahara S, Kodama T, Dakhama A, Ott VL, Gelfand EW. Effector CD8(+) T cells mediate inflammation and airway hyper-responsiveness. *Nat Med.* 2004;**10**:865-9.
- 5) Miyahara N, Miyahara S, Takeda K, Gelfand EW. Role of the LTB₄/BLT1 pathway in allergen-induced airway hyperresponsiveness and inflammation. *Allergology International.* 2006;**55**:91-7.
- 6) Miyahara N, Takeda K, Miyahara S, Taube C, Joetham A, Koya T, Matsubara S, Dakhama A, Tager AM, Luster AD, Gelfand EW. Leukotriene B₄ (BLT1) is essential for allergen-mediated recruitment of CD8⁺ T cells and airway hyperresponsiveness. *J Immunol.* 2005;**174**:4979-84.

- 7) Miyahara N, Takeda K, Miyahara S, Matsubara S, Koya T, Matsubara S, Joetham A, Krishnan E, Dakhama A, Haribabu B, Gelfand EW. Requirement for the Leukotriene B4 Receptor-1 in Allergen-Induced Airway Hyperresponsiveness *Am J Respir Crit Care Med.* 2005;**172**:161-7.

The effects of Dickkopf 1, an inhibitor of Wnt signaling pathway, on anti-ageing (anti-wrinkle, whitening and regeneration of pigment, hair and site-specific skin)

Yuji Yamaguchi

Department of Geriatric and Environmental Dermatology,
Nagoya City University Graduate School of Medical Sciences
yujin@med.nagoya-cu.ac.jp

Abstract

Palms of the hands and soles of the feet (Palmoplantar areas) are generally less pigmented and thicker than the other sites of the body. We hypothesized and proved that mesenchymal-epithelial interactions, especially the influences by mesenchymal factors, play important roles in determining and maintaining the site-specificity (anatomical difference) of the skin. We previously proved that cultured dermal fibroblasts derived from palmoplantar skin express higher levels of dickkopf 1 (DKK1) than the rest of the body at mRNA and protein levels. We also proved that DKK1 inhibits melanocyte function and growth via Wnt/beta-catenin signaling and that enhances keratinocyte growth. Since there is no report regarding the expression patterns of DKK1 in vivo, we obtained biopsied specimens, which include palmoplantar and non-palmoplantar skin simultaneously. We developed rabbit polyclonal antibodies detecting four different epitopes against DKK1 and immunologically examined the expression patterns. Western blotting and immunohistochemistry showed that the expression of DKK1 is high in palmoplantar skin in vivo. We conclude that the expression of DKK1 is upregulated in vivo as well as in vitro, explaining why palmoplantar skin is non-hair bearing, thick and hypopigmented skin. These series of studies suggest the usefulness of DKK1 as an anti-ageing reagent.

Keywords: dermatology, regenerative medicine, anti-ageing, pigment cell research

Introduction

We have proved that mesenchymal-epithelial interactions (effects of the underlying dermal fibroblasts on the overlying epidermal cell types) determine the site-specificity of the skin (the topographical differences of the skin) in human adult tissues as well as embryos(1-5). For example, palms of the hands and soles of the feet (palmoplantar areas) are anatomically different from the other sites of the body in terms of the thickness of the epidermis(6, 7), the structure of appendixes including hair follicles and the pigmentation of the skin color(8, 9). We found that Dickkopf 1 (DKK1), an inhibitor of canonical Wnt signaling pathway, is highly expressed in palmoplantar dermis (mesenchyme) (10) and that DKK1 suppresses melanocyte function and growth by inhibiting Wnt/beta-catenin signaling pathway(10, 11), which also plays pivotal roles in hair morphogenesis(12). DKK1 also thickens the epidermal thickness and suppresses the melanin uptake via PAR2 expressed

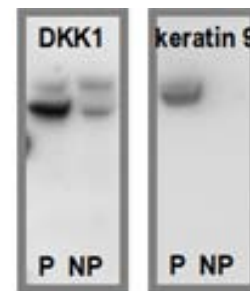
in keratinocytes (13, 14). Since DKK1 is proved to be highly expressed in palmoplantar dermal fibroblasts only in culture conditions, the expression levels of DKK1 *in vivo* were examined using human skin obtained during plastic surgery.

Results

The studies were approved by Institutional Review Board. We used human skin derived from the same subjects. Five subjects were used in the studies. We obtained the border including the sole of the feet and the adjacent non-palmoplantar skin (hyperpigmented and hairy skin). We extracted protein and examined the expression patterns of DKK1, keratin 9(, which is exclusively expressed in palmoplantar area,) and beta-catenin measured by Western blotting. We also investigated immunohistochemical analysis.

This investigation was necessary since there was a report at the academic meeting that the expression of DKK1 was surprisingly decreased in palmoplantar skin *in vivo* measured by Western blotting and by RT-PCR, although we proved that DKK1 expression is highly observed in palmoplantar fibroblasts *in vitro* as compared with non-palmoplantar fibroblasts.

We could successfully develop four different rabbit polyclonal antibodies, which detect four different epitopes. The expression levels of DKK1 and keratin 9 were clearly upregulated in palmoplantar skin as compared with non-palmoplantar skin measured by Western blotting (Figure 1). The expression level of



P: palmoplantar skin
NP: non-palmoplantar skin

Figure 1. Western blotting. The extracts of palmoplantar skin and non-palmoplantar skin were examined for the expressions of DKK1, keratin 9 and beta-catenin.

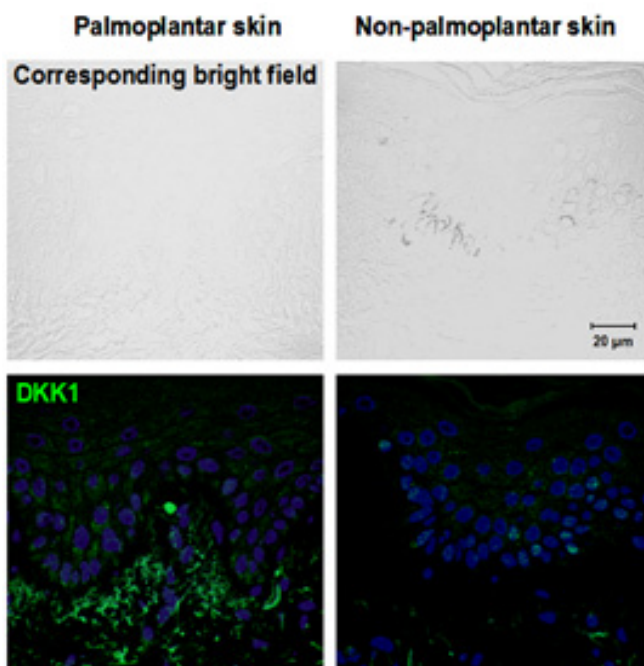


Figure 2. Immunohistochemistry The expression of DKK1 was upregulated in fibroblasts under palmoplantar epidermis and its expression was downregulated under non-palmoplantar epidermis.

beta-catenin was not downregulated as expected, but slight decrease was observed in palmoplantar skin.

We next checked the expression levels of DKK1 measured by immunohistochemistry (Figure 2). We found that the DKK1-positive cells were exclusively observed under palmoplantar epidermis *in vivo*. Additionally we could find the intense DKK1 expression under the hypopigmented epidermis. Finally, strong DKK1-positive cells were observed around the sweat gland ducts, very close to keratin 9-positive cells.

Discussion & Conclusion

We could prove that DKK1 expression was observed in the dermis under the thick and hypopigmented skin *in vivo* as well as *in vitro*. DKK1 suppresses melanocyte growth and pigmentation (9-11). It also suppresses the melanin receptor (PAR2) in keratinocytes and increases keratinocyte growth (13). It also suppresses hair morphogenesis (15).

These series of studies indicate that DKK1 could be used as a reagent for treating skin ageing. For example DKK1 could be used as an anti-wrinkle drug by thickening epidermis, as a hypopigmenting reagent by suppressing melanocyte function and growth and by suppressing the expression of PAR2 in keratinocytes and as a vellus hair remover by suppressing hair morphogenesis. It also could be used to treat intractable wounds since it increases keratinocyte growth and makes thick skin. Conversely, anti-DKK1 could be used to treat alopecia. Future studies will focus on the clinical application of DKK1.

References

- 1) Yamaguchi, Y., Kubo, T., Tarutani, M., Sano, S., Asada, H., Kakibuchi, M., Hosokawa, K., Itami, S. & Yoshikawa, K. (2001) *Arch Dermatol* **137**, 621-8.
- 2) Yamaguchi, Y., Yoshida, S., Sumikawa, Y., Kubo, T., Hosokawa, K., Ozawa, K., Hearing, V. J., Yoshikawa, K. & Itami, S. (2004) *Br J Dermatol* **151**, 1019-28.
- 3) Yamaguchi, Y., Hearing, V. J., Itami, S., Yoshikawa, K. & Katayama, I. (2005) *J Dermatol Sci* **40**, 1-9.
- 4) Yamaguchi, Y., Sumikawa, Y., Yoshida, S., Kubo, T., Yoshikawa, K. & Itami, S. (2005) *Br J Dermatol* **152**, 664-72.
- 5) Yamaguchi, Y., Itami, S. & Yoshikawa, K. (2005) in *Wound healing: science and practice*, eds. Falabella, A. & Kirsner, R. (Marcel Dekker, New York), pp. 535-544.
- 6) Yamaguchi, Y., Itami, S., Tarutani, M., Hosokawa, K., Miura, H. & Yoshikawa, K. (1999) *J Invest Dermatol* **112**, 483-8.
- 7) Yamaguchi, Y. & Yoshikawa, K. (2001) *J Dermatol* **28**, 521-34.
- 8) Yamaguchi, Y. & Hearing, V. J. (2006) in *From melanocytes to malignant melanoma: the progression to malignancy*, eds. Hearing, V. J. & Leong, S. P. L. (Humana Press, Totowa), pp. 101-115.
- 9) Yamaguchi, Y., Brenner, M. & Hearing, V. J. (2007) *J Biol Chem* **282**, 27557-61.
- 10) Yamaguchi, Y., Itami, S., Watabe, H., Yasumoto, K., Abdel-Malek, Z. A., Kubo, T., Rouzaud, F., Tanemura, A., Yoshikawa, K. & Hearing, V. J. (2004) *J Cell Biol* **165**, 275-85.
- 11) Yamaguchi, Y., Passeron, T., Watabe, H., Yasumoto, K., Rouzaud, F., Hoashi, T. & Hearing, V. J. (2007) *J Invest Dermatol* **127**, 1217-25.
- 12) Suzuki, K., Yamaguchi, Y., Villacorte, M., Mihara, K., Akiyama, M., Shimizu, H., Taketo, M. M., Nakagata, N., Tsukiyama, T., Yamaguchi, T. P., Birchmeier, W., Kato, S. & Yamada, G. (2009) *Development* **136**, 367-72.

- 13) Yamaguchi, Y., Passeron, T., Hoashi, T., Watabe, H., Rouzaud, F., Yasumoto, K., Hara, T., Tohyama, C., Katayama, I., Miki, T. & Hearing, V. J. (2008) *Faseb J* **22**, 1009-20.
- 14) Yamaguchi, Y. & Hearing, V. J. (2009) *Biofactors* **35**, 193-9.
- 15) Yamaguchi, Y., Morita, A., Maeda, A. & Hearing, V. J. (2009) *J Investig Dermatol Symp Proc* **14**, 73-5.

The Elucidation of transcriptional mechanisms which regulated by gas, one of the smallest unit molecules

Taku Yamashita

Graduate School of Pharmaceutical Sciences, Osaka University

taku@phs.osaka-u.ac.jp

Abstract

CooA is one of the gas-sensors, and regulates transcriptional activation with CO gas. Notably, CooA has an unprecedented ligand, Pro2 was provided as one of the axial ligands to the other subunit. In the previous works, we have reported that Pro2 could be replaced by CO, and then the C-helix was changed the orientation with the “roll-and-slide” mechanism. Here, we focused on the conformational changes which were induced by CO-binding. In order to clarify the mechanism in details, we performed ultrafast spectroscopic measurements with time-resolved spectroscopy in the ferrous and CO-bound forms of CooA. Internal ligand rebinding was really disturbed by the mutation on the one axial ligand, His 77, as expected. Moreover, only three mutants, D72N, L116Q, and truncated, showed mono-exponential rebinding, however wild-type and H77A were fitted bi-exponentially. On the other hand, CO-rebinding was perturbed in the variants. Although H77A showed higher escape of CO than wild-type, highest escape was observed in the L116Q mutant. It could support the proposed activation mechanism with C-helix reorientation. In addition, some mutants indicated varied aspects, and it will be discussed later.

Keywords: Hemeprotein, Gas sensor, Time-resolved spectroscopy

Introduction

Gas sensor is the novel member of heme proteins, and it has been reported that several gas molecules were discriminated by the heme environment with surrounded amino acids. In the previous works, we have studied on oxygen sensor proteins with spectroscopic methods. FixL is known to be involved in the nitrogen fixation with histidinekinase activity which regulated by oxygen. We have investigated on the ligand binding of FixLH with the time-resolved spectroscopic measurements (1). Second, we have studied also on DosH with the same procedures. Dos has been reported to indicate phosphodiesterase activity which is dependent on either oxygen or oxidative state of the heme iron. On Dos, we aimed to solve the role of methionine position at 95 (2), and also succeeded to measure on full-length Dos in order to clarify the function (3). These studies suggested that the time-resolved spectroscopic measurements could be useful tool in order to investigate structural features on the activated mechanisms.

In 1990, a novel transcriptional activator was reporter as a first example of heme containing regulator. Remarkably, CooA was activated by CO gas, and the small molecule induces the large conformational changes in the protein moiety. Since the crystal structure of CooA was solved as a

dimeric protein in 2000 (Figure 1), the activation mechanism has not been fully elucidated yet. In our previous works, we have targeted on the heme axial ligands, His 77 and Pro 2. Notably, Pro 2 is provided by the other subunit, and the ligand could be replaced by the external ligand, CO. We had studied with spectroscopic measurements in the steady-states, and clarified not only the Pro 2 residue was replaced by CO as expected but also the His 77 residue could be crucial to lead CO to the proper distal side (4). On the other hand, we also had aimed

on C-helix, which constructed an interface between dimers. In the work, we introduced mutations on each amino acid, thoroughly, and investigate on the DNA-binding abilities, CO binding affinities, and the surrounding of bound-CO. The result showed us that Leu 116, Gly 117, and Leu 120 could face to the other subunit, and that suggested the C-helix orientations could be disturbed by the binding of CO. Finally, we proposed the model of activation mechanism as the “roll-and-slide” (5).

Recently, several CO sensor proteins, NPAS2 and Per2, have been reported in human brain (6,7). However the physiological functions are extremely interesting, these proteins have never solved the structures and it could be hard to elucidate the activation mechanisms without structural features. Here we have targeted CooA in order to clarify the earlier stage of activation mechanism; how the replaced external ligand lead the conformational change in the protein moiety.

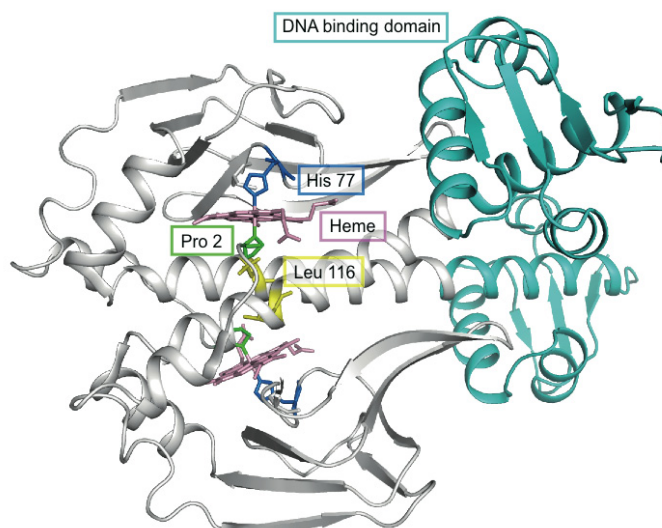


Figure 1. The dimeric structure of CooA in the ferrous (inactive) state (pdb:1ft9).

The heme axial ligands and the mutated leucine 116 were depicted as sticks colored in green, blue, and yellow, respectively. The region colored in cyan indicated the DNA binding domain, which was deleted in the truncated mutant.

Results

Purification of wild-type and mutated CooA

CooA was constructed the procedure in order to purify the protein. E.coli strain was streaked on the LB plate again, and culture in 10 L LB medium in each. the extractions of proteins from the cells were performed with ultrasonication, and separated CooA fraction with ultracentrifuge. Soluble fractions were purified with ion-exchange and gel-filtration columns, and finally CooAs were obtained (200 μ M~1.5 mM). In order to investigate on the effect of DNA-binding domain, we prepared also the “truncated” mutant which was constructed 1-131 amino acids. The purities and properties of purified CooAs were confirmed with SDS-PAGE and UV-visible spectroscopic measurements.

Time-resolved spectra in the ferrous state

In order to investigate on the ferrous states of CooA variants, we have used sodium dithionite and ascorbic acid. The reduced CooA were measured with the multicolour dye-laser system in femtosecond absorption spectroscopy as 30 fs pump pulse centered at 560 nm with <30 fs white light probe pulse. Spectral changes were recorded in the range from 420 to 470 nm, and the kinetics were monitored the absorbance at 438.5 nm (Figure 2). As shown, wild-type (WT) indicated bi-exponential rebinding, and the time constants were estimated as 6.4 and 12 ps. Those amplitudes

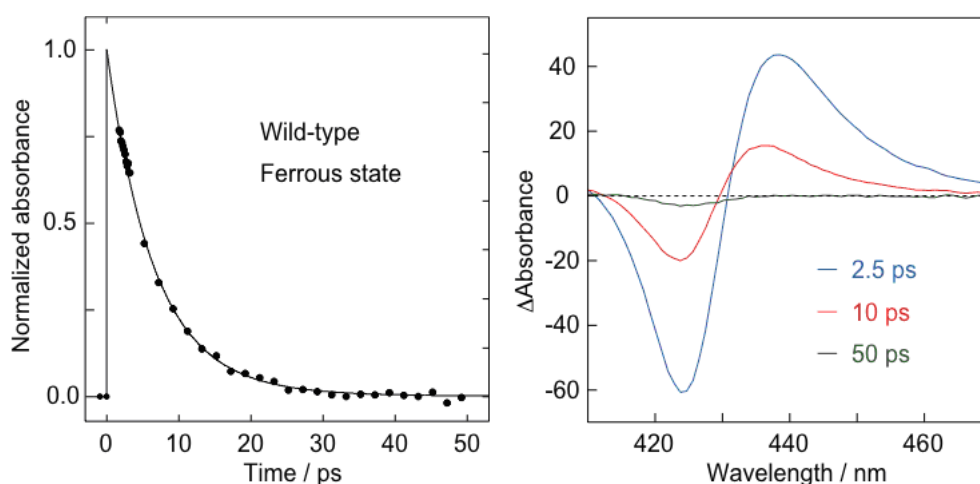


Figure 2. Internal ligand rebinding for the wild-type CooA in the ferrous state. Normalized kinetics on the wild-type CooA was detected with the alteration of absorbance at 438 nm (left). The decay-associated spectra were recorded in the different delay times, 2.5, 10, and 50 ps (right).

were also calculated and fast phase was assigned as 92%. Although the H77A mutant, His 77 was replaced by alanine, also showed bi-exponential rebinding, the truncated, the D72N, and the L116Q mutants indicated mono-exponential rebinding of the dissociated internal ligand (Table 1).

Table 1. Fit parameters of internal ligand rebinding kinetics in the CooA variants. The absorbance changes were fitted mono- and/or bi-exponentially, and the fitted equations gave us the following time constants and amplitudes.

	Fitted equations	τ_1 / ps	τ_2 / ps
Wild-type	Bi-exponential	6.4 (92)	12 (8)
H77A	Bi-exponential	6.4 (90)	71 (10)
Truncated	Mono-exponential	6.5	
D72N	Mono-exponential	6.9	
L116Q	Mono-exponential	6.9	

The values in the parentheses indicate the amplitudes (%).

Time-resolved spectra in the ferrous CO-bound state

We measured the kinetics of CooA in the ferrous-CO bound forms. The measured instruments were completely same except for the monitored range from 4 ps to 4 ns. The rebinding of CO in WT was measured and fitted as 3rd exponential decay as shown in the Figure 3. All mutant was also fitted as 3rd exponential decays (Table 2). Notably, the truncated and the D72N mutants showed less escape than that of WT, however the H77A and the L116Q mutants indicated higher values.

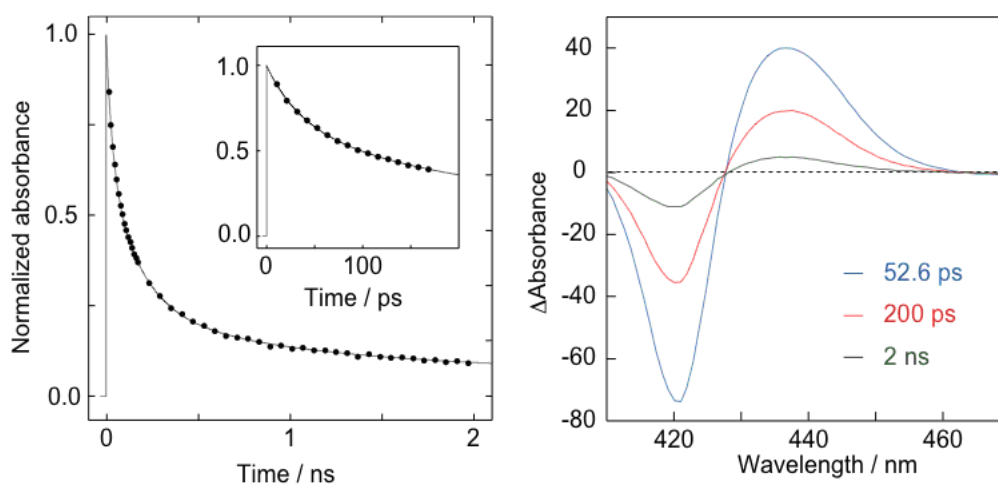


Figure 3. Rebinding of dissociated CO to heme for the wild-type CooA.

Normalized kinetics on the wild-type CooA was detected with the alteration of absorbance at 438.5 nm (left). The decay-associated spectra were recorded in the different delay times, 52.6 ps, 200 ps, and 2 ns (right).

Table 2. Fit parameters of CO rebinding kinetics in the CooA variants

	τ_1 / ps	τ_2 / ps	τ_3 / ns	Residual (%)
Wild-type	34 (37.4)	174 (40.3)	1.1 (16.3)	6.0
H77A	5.8 (40.8)	78 (25.7)	0.50 (21.7)	11.8
Truncated	35 (33.7)	140 (47.7)	0.76 (15.2)	3.4
D72N	3.5 (61.9)	90 (18.7)	0.66 (15.0)	4.4
L116Q	20 (16.9)	175 (31.8)	0.94 (29.6)	21.7

The values in the parentheses indicate the amplitudes (%).

Moreover, the kinetics of the D72N and the H77A mutants suggested that the CO-rebinding were totally faster than those of WT. Especially, the 1st rates were extremely rapid as the internal ligand rebinding.

Discussion & Conclusion

The relationship between heme axial ligands and DNA-binding domain

As mentioned above, in the CO rebinding, the truncated and the D72N mutants showed less escape than that of WT. It inspired that the direct interaction between heme-binding and DNA-binding domains caused unrestricted form in the CO-bound structure, and the heme surrounding was not so fixed a space in order to escape CO from the pocket. On the other hand, the D72N and the H77A mutants showed totally rapid rebinding. It could be explained that the mutated positions were involved in the heme-binding domain, and caused unexpected effect for CO-rebinding. The further investigations can be required in order to clarify the mechanism on CO-binding in detail.

The axial ligands for the heme

In the internal ligand rebinding, the H77A mutant showed the distinguishable result from WT. especially, the slower phase was delayed with the mutation. It indicated that the dissociated Pro 2 was orientated farer from the heme, and the rebinding caused a steric distortion than that of WT.

Finally, we concluded that the rebinding of the internal and the external ligands were complicated. However, the results suggested that the mutated internal ligand disturbed the rebinding of not only

the internal ligand but also external one. The introduced mutation on the DNA-binding domain and an interactive position also caused serious effect not to the internal ligand but external ligand rebinding.

Acknowledgement

We thank The Novartis Foundation for the Promotion of Science to give chance to graduated students in order to work abroad for 10 days. They could have irreplaceable experience, and actually, one of them will be employed by Novartis pharma K. K. from the next spring. I hearty appreciate again for your support.

References

- 1) Kruglik, S. G., Jasaitis, A., Hola, K., Yamashita, T., et al. (2007) *Proc. Natl. Acad. Sci. U. S. A.* **104**, 7408-7413
- 2) Yamashita, T., et al. (2008) *J. Biol. Chem.* **283**, 2344-2352
- 3) Lechauve, C., Bouzhir-Sima, L., Yamashita, T., et al. (2009) *J. Biol. Chem.* **284**, 36146-36159
- 4) Yamashita, T., et al. (2004) *J. Biol. Chem.* **279**, 21394-21400
- 5) Yamashita, T., et al. (2004) *J. Biol. Chem.* **279**, 47320-47325
- 6) Fu, L., Pelicano, et al. (2002) *Cell* **111**, 41-50
- 7) McNamara, P., et al. (2001) *Cell* **105**, 877-889

Development of the method to induce and amplify the ES cell-derived germ layer stem cell

Takumi Era

Department of Cell Modulation, Institute of Molecular Embryology and Genetics,
Kumamoto University
tera@kumamoto-u.ac.jp

Abstract

Pluripotent stem cells such as embryonic stem (ES) and induced pluripotent stem (iPS) cells have attractive attention as a source of cells for use in therapeutic application. However, as the *in vitro* differentiation culture does not provide efficiently positional information for cell type definition, this system definitely requires visible markers to identify and monitor the intermediates that present on the way of differentiation. Here, we have shown that the cell surface markers against the mesoderm and mesenchymal cells in the ES cell culture can visualize the cell lineages and allow us to isolate the specific cell types that is considered to be useful for the application of regenerative medicine. Using the cell purification in combination with gene subtraction method, we have isolated the molecules whose function are unclear and have identified their function in embryogenesis.

Keywords: ES cell, mesoderm, in vitro differentiation

Introduction

ES cell have the multiple potentials to give rise to a whole cell types in mouse body and to undergo unlimited symmetrical divisions with maintaining its pluripotency(1). The high ability for differentiation and unlimited growth capacity lead us to expect to utilize it as the source of cell therapies such as transplantation(2). Moreover, the forced differentiation system of ES cell in vitro has been expected to use as a good tool to find the developmental pathways into the specific cell lineage and to dissect them from others. However, as ES cell differentiation culture does not provide usefully positional information for cell type definition, this system definitely requires visible markers to identify and monitor the intermediates that present on the way of differentiation(3).

To overcome the obstacles, we have been developing the visible markers to define the intermediates on the way of ES cell differentiation and elucidate the differentiation pathways in the ES cell culture. In embryogenesis, Vascular Endothelial Growth Factor Receptor 2 (VEGFR2, FLK1) that marks the subtypes of mesoderm cells with a potential to give rise to hematopoietic cells (HPCs) and endothelial cells (ECs) facilitates our understanding on the developmental pathways of these lineages(4). In fact, the population expressing VEGFR2 in the differentiated ES cells can give rise to vascular endothelial and hematopoietic cells under a proper condition. Another important surface marker involving in mesoderm development is Platelet-derived growth factor receptor alpha (PDGFR α) that is mainly expressed in paraxial mesoderm during mouse embryogenesis(5). In this

study, we have shown to clarify the differentiation pathway of mesoderm-like cells in ES cell culture and to establish the serum- free culture condition that provide the mesoderm-like cells efficiently from undifferentiated ES cells.

Results, Discussion & Conclusion

Our previous result obtained from in vitro ES cell culture shows that day4 differentiated ES cells are divided into four population by VEGFR2 and PDGFR α expression patterns, PDGFR α ⁺VEGFR2⁺ cell (DP), PDGFR α ⁺VEGFR2⁻(PSP), PDGFR α ⁻VEGFR2⁺(VSP) and PDGFR α ⁻VEGFR2⁻ cell (DN). DP population initially appears at day 3.5 ES cell culture is a common precursor for PDGFR α ⁺VEGFR2⁻(PSP) and PDGFR α ⁻VEGFR2⁺(VSP) cells (Fig.1). DP purified from ES cell culture can give rise to both PSP and VSP populations. To characterize these populations, we purified them from the differentiated ES cells on day 4 and examined the lateral and paraxial

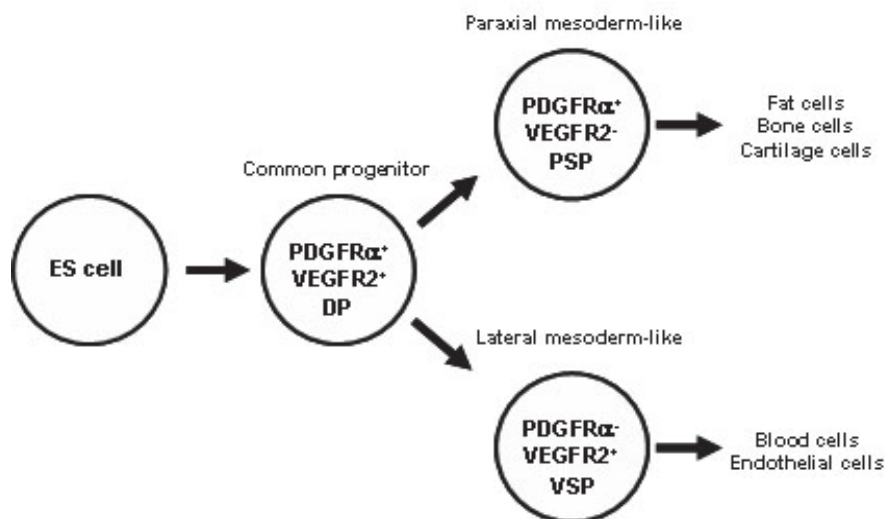


Figure 1

markers by RT-PCR. As expected, the expression pattern indicated that, while PSP corresponds to paraxial mesoderm, VSP represent to lateral mesoderm culture in mouse embryogenesis. Based on the results of in vitro fate analysis, we found a new differentiation pathway in which the DP gives rise to both the PSP and the VSP that eventually differentiate into bone and cartilage cells, and HPCs and ECs, respectively(Fig.1). These indicate that PSP and VSP populations represent the paraxial and lateral mesoderm populations in actual mouse embryo, respectively.

We next sought to define condition in which the mesoderm-like cells are enriched in ES cell culture. BMP4 and Activin are shown to be potent inducer for mesoderm generation in actual Xenopus embryos. While activin in combination with BMP4 efficiently induce DP as well as VSP, BMP4 alone can stimulate the PSP generation under serum-free condition.

To investigate the molecular processes underlying mesoderm development in ES cell culture, we conducted the gene expression analyses by DNA microarrays and tried to isolate the new molecules

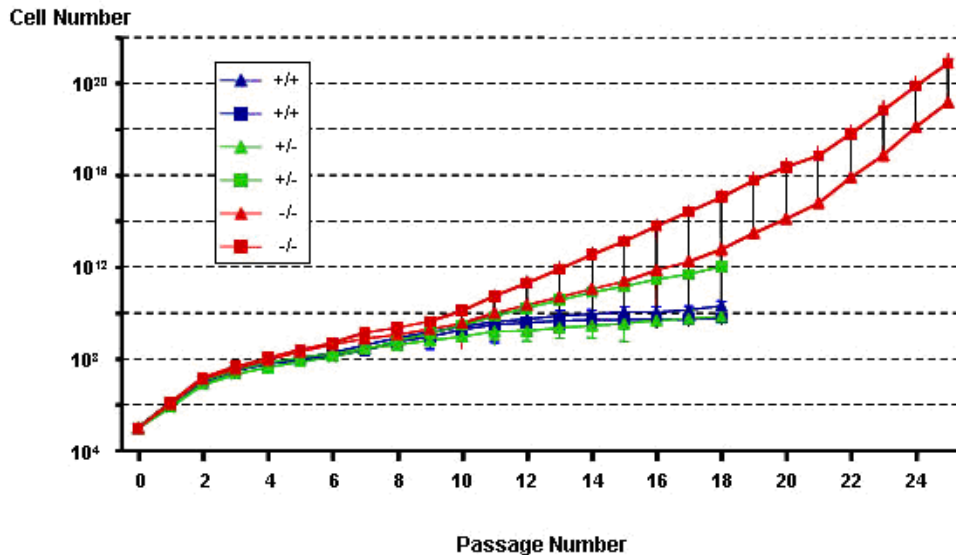


Fig.2

that are involved in mesoderm and/or mesenchymal differentiation. As shown in Fig., the new molecules involved in mesenchymal growth in embryogenesis are identified from in vitro ES cell culture. The null embryonic fibroblasts are shown to undergo the sustained growth in vitro (Fig.2). These results suggested that the in vitro ES cell culture system is a powerful for understanding the differentiation pathways and molecular processes in the early development.

References

- 1) Niwa H How is pluripotency determined and maintained? *Development* **134**, 635-646, 2007.
- 2) Keller G. Embryonic stem cell differentiation: emergence of a new era in biology and medicine. *Genes Dev* **19**, 1129-1155,2005.
- 3) Nishikawa S-I, Jakt LM, Era T ES cell culture as a tool for developmental cell biology. *Nature Rev. Mol. Cell Biol.* **8**: 502-507, 2007.
- 4) Nishikawa, S. I., Nishikawa, S., Hirashima, M., Matsuyoshi, N. and Kodama, H. Progressive lineage analysis by cell sorting and culture identifies FLK1+VE-cadherin+ cells at a diverging point of endothelial and hemopoietic lineages. *Development* **125**,1747-1757, 1998.
- 5) Kataoka, H., Takakura, N., Nishikawa, S., Tsuchida, K., Kodama, H., Kunisada, T., Risau, W., Kita, T. and Nishikawa, S. I. Expressions of PDGF receptor alpha, c-Kit and Flk1 genes clustering in mouse chromosome 5 define distinct subsets of nascent mesodermal cells. *Dev Groeth Differ* **39**, 729-740, 1997.

Role of G proteins in the spermatogonial stem cell homing to niche

Mito Shinohara

Kyoto University, Graduate School of Medicine

mshinoha@virus.kyoto-u.ac.jp

Abstract

Spermatogonial stem cells (SSCs) migrate into niches after transplantation into infertile testes. Transplanted SSCs attach to Sertoli cells and transmigrate through the blood-testis barrier (BTB), which is formed by inter-Sertoli tight junctions, towards niches on the basement membrane. Previously, we showed that β 1-integrin is involved in the regulation of SSC homing, and that it regulate SSC binding to the basement membrane. In this study, we extended the previous study and found the involvement of Rac1 in SSC transmigration through BTB, the most critical step of SSC homing. SSCs deleted in Rac1 gene did not colonize the adult testes, but they reinitiated spermatogenesis when transplanted into pup testes without a BTB. Moreover, a dominant-negative Rac1 construct increased the number of cell divisions and frequency of differentiating division, as revealed by serial transplantation. Thus Rac1 is a critical regulator of SSC homing and self-renewal.

Keywords: Stem cell, spermatogenesis, homing

Introduction

Spermatogonial stem cells (SSCs) are the source of spermatogenesis throughout adult life. SSCs are not randomly distributed in the testis, but that they reside within special microenvironments called niches where they can remain undifferentiated (Chiarini-Garcia et al., 2001). Self-renewal factors secreted from the niche are considered to maintain SSCs in the undifferentiated state, and this unique microenvironment is a prerequisite for undergoing self-renewal division. Despite their close relationship, the relationship between SSCs and niche is dynamic. In germ cell transplantation into testis, SSCs from a donor animal recolonize the seminiferous tubules when microinjected into the seminiferous tubules of infertile animals (Brinster and Zimmermann, 1994). Transplanted SSCs attach to the Sertoli cells, and within a few days migrate to the basal compartment following passage through the BTB between Sertoli cells. SSCs then proliferate and differentiate to produce donor-derived spermatogenesis (Nagano et al., 1999). Thus, SSCs have the ability to migrate toward the niche in a manner similar to hematopoietic stem cells (HSCs).

Recently, we showed that β 1-integrin expression in SSCs plays a critical role in their homing ability (Kanatsu-Shinohara et al., 2008). In these experiments, the function of adhesion molecules in SSC homing was examined by taking advantage of β 1-integrin conditional knockout (KO) mice. SSCs from β 1-integrin knockout mice cannot make germ cell colonies and disappear after transplantation. Loss of β 1-integrin expression probably prevented SSCs from attaching to the basal membrane, because SSCs without β 1-integrin could neither attach to laminin in vitro nor migrate into the niche

even when transplanted into pup testes without a BTB. These experiments identified β 1-integrin as a homing receptor for SSCs.

In this study, we examined the roles of Rac small G proteins in SSC homing. Rac is often activated downstream of the integrin receptor and mediates HSC homing (Cancelas et al., 2006). We hypothesized that Rac may also be involved in SSC adhesion to the basement membrane, but our analyses showed that Rac1 was involved in a different step of homing: i. e. transmigration of SSCs through the BTB.

Results

Expression of Rac genes in SSCs and primary spermatogonia

Using magnetic-activated cell sorting (MACS), we collected spermatogonia from the testes of 8-day-old pups by taking advantage of EpCAM, a marker of SSCs (Oatley and Brintser, 2008). Within the Rac subfamily, real-time PCR analyses showed that Rac1 was expressed predominantly in spermatogonia. We then examined the expression of Rac genes in germline stem (GS) cells, cultured spermatogonia with enriched SSC activity (Kanatsu-Shinohara et al., 2003). GS cells depend on glial cell line-derived neurotrophic factor (GDNF) and epidermal growth factor (EGF)/basic fibroblast growth factor (bFGF) for proliferation in vitro. They produce germ cell colonies following transplantation into seminiferous tubules. The addition of self-renewal factors inhibited Rac1 expression. While the combination of EGF and bFGF showed a comparable effect to GDNF, the addition of all cytokines reduced the Rac1 levels to 50%.

Deletion of the Rac1 gene inhibits SSC homing after germ cell transplantation

To understand the role of Rac1 in SSC homing, we induced Rac1 gene deletion in SSCs using mice carrying a Rac1 gene flanked by loxP sites (Rac1 floxed mice) generated by homologous recombination (Glogauer et al., 2003). Exposure of cultured SSCs to adenovirus expressing Cre (AxCANCre) deletes target genes, which can reinitiate spermatogenesis after germ cell transplantation (Takehashi et al., 2007). The Rac1 mutant mouse strain was crossed with the ROSA26 reporter mouse strain (R26R) to visualize the pattern of proliferation and differentiation of mutant SSCs (Soriano, 1999). Heterozygous R26R mice were used as controls.

Single-cell suspensions of testis cells from 8-12-day-old pups were exposed to adenovirus AxCANCre overnight in vitro. Southern blotting analyses showed that $60.0 \pm 3.2\%$ ($n = 3$) of the floxed allele was deleted from the Rac1 gene locus at the time of transplantation. To quantify the SSC number, $\sim 1.2 \times 10^5$ testis cells were microinjected into the seminiferous tubules of WBB6F1-W/W^v (W) mice, which lack endogenous spermatogenesis and serve as recipients for donor SSCs (Brinster and Zimmermann, 1994). The recipient testes were stained for β -galactosidase activity with X-gal 3 months after transplantation.

The recipient testes showed significant reduction of blue germ cell colonies, while transplantation of control cells resulted in extensive colonization (Figure 1). The number of colonies generated from the control and mutant cells were 29.4 ± 1.7 ($n = 10$) and 3.6 ± 0.6 ($n = 12$) per 10^5 transplanted cells, respectively. Moreover, the blue staining in the recipient testes that received mutant cells showed

weaker blue staining, suggesting poorer spermatogenesis recovery. The result indicates that deletion of the Rac1 gene inhibited SSC colonization.

Analysis of Rac1 function using GS cells

GS cells expressing a dominant-active (RacV12; DA-Rac) or a dominant-negative Rac1 (RacN17; DN-Rac) construct were produced by stably transfecting GS cells established from a transgenic mouse expressing enhanced green fluorescent protein (EGFP). Flow cytometric analyses indicated that both DA- and DN-Rac cells show normal levels of β 1- and α 6-integrins, which are considered to be involved in SSC homing. Reverse transcription-polymerase chain reaction (RT-PCR) analyses also confirmed the normal spermatogonia phenotype of both DA- and DN-Rac cells.

On the other hand, DN-Rac cells showed increased adhesion to laminin. While $58.4 \pm 4.9\%$ of the DN-Rac cells could attach to laminin-coated plates, 43.6 ± 4.1 and $47.6 \pm 3.8\%$ of control and DA-Rac cells adhered after 30 min incubation ($n=12$). In addition to the increased adhesion, DN-Rac cells proliferated more actively than control and DA-Rac cells. While both control and DA-Rac GS cells expanded 6.4 ± 0.3 and 6.6 ± 0.9 -fold, respectively, during 6 days, DN-Rac cells expanded 11.9 ± 0.9 fold during the same period ($n=6$).

To examine the effect of Rac activity on SSC self-renewal *in vivo*, we used a serial transplantation technique. Approximately 4×10^3 cells expressing the EGFP gene were microinjected into the seminiferous tubules of W mice (primary recipients). Two months after transplantation, the number of colonies in the testes was determined under UV illumination. DN-Rac cells produced significantly fewer colonies, but we found no significant difference between DA-Rac and WT cells. DA-Rac, DN-Rac and WT cells produced 231.3 ± 25.0 , 129.2 ± 16.8 , and 275.0 ± 35.4 colonies per 105 transplanted cells, respectively ($n = 12$ for DA- and DN-Rac cells; $n = 9$ for control cells). Colonies in each recipient testis were dissociated into single cells and suspended in 15-16 μ l of injection medium, and approximately 4 μ l of the single cell suspension was microinjected into two secondary W recipient testes.

DN-Rac cells produced significantly fewer secondary colonies than control and DA-Rac cells. Assuming that each colony is produced by one SSC and that seeding efficiency is 10% (Nagano et al, 1999), the multiplication of colony numbers (total regenerated colony number $\times 10$ / primary colony number used for serial transplantation) were 26.4 ± 0.3 ($n = 9$) and 23.3 ± 0.3 ($n = 12$) for control and DA-Rac cells, respectively. However, DN-Rac cells produced significantly fewer secondary colonies, and the average number of colonies per primary colony was 14.2 ± 0.3 ($n = 12$). The difference between DN-Rac and control or DA-Rac cells was significant. The doubling times of the SSCs during the 2-month period were 12.7, 13.2, and 15.7 days for control, DA-Rac and DN-Rac SSCs, respectively. These results suggested that the inhibition of Rac induced more differentiating divisions of SSCs.

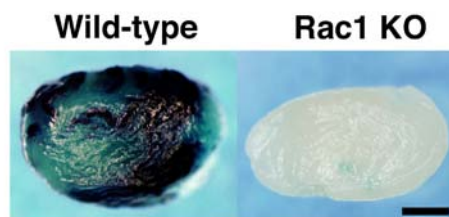


Figure 1. Reduced colonizing ability of Rac1 mutant cells. Testes from Rac1 conditional mutant mice were dissociated and exposed to AxCANCre *in vitro* for overnight. Cre-mediated deletion removed the target genes, and the cells were transplanted into recipient pup or adult testes to evaluate SSC activity. Macroscopic appearances of the recipient testes are shown. Blue tubules indicate donor cell colonization. Note the reduced colonization levels in adult recipients that received Rac1 mutant cells. Bar = 1 mm.

Transplantation into immature testes rescues defective colonization of Rac1 KO SSCs

SSC homing is thought to occur in several steps: attachment to Sertoli cells, passage through the tight junctions between Sertoli cells, and migration to the germline niche on the basement membrane (Nagano et al., 1999). To determine whether decreased SSC homing was caused by defective migration of SSCs through the tight junctions between Sertoli cells, we next used immature 5-10-day-old recipient testes that lack tight junctions. Approximately 1.2×10^5 Rac1 KO or control cells after overnight incubation with AxCANCre in vitro. Analyses at 3 months after transplantation revealed significant colonization of SSCs lacking the Rac1 gene. In total, 440/783 (61.4%) tubules showed spermatogenesis with control cells, and 488/1083 (47.1%) tubules showed spermatogenesis with mutant cells (n=11). Both histological analyses and RT-PCR analyses confirmed normal differentiation of Rac1 mutant cells. These results showed that Rac1 deficiency did not influence SSC homing in the pup testes.

Decreased expression of tight junction-associated proteins in Rac mutant cells

We hypothesized that homing defects were caused by abnormal expression of tight junction-associated adhesion molecules in SSCs. Thus, we next examined the expression of occludin and claudins, components of tight junction, in GS cells and W testis. Surprisingly, RT-PCR analyses showed that GS cells expressed all of these molecules except claudin 5. Using real-time PCR, we then quantitatively assessed expression levels of genes commonly expressed in GS cells and W testis. Although we did not find significant changes in occludin, claudins 1, 2, 10b, 11, 12, 19, 20, or 22 expression, claudins 3, 4, 6, 7, 8, 10a, 15, and 23 were down-regulated in DN-Rac cells. Western blotting analyses confirmed the reduced expression of claudins 3, 7, and 8. Claudin 10 expression, however, did not change significantly. These results indicate that Rac1 regulates expression of tight junction-associated molecules potentially involved in the SSC transmigration through the BTB.

Discussion & Conclusion

In the spermatogenic system, Rac1 is predominantly expressed in spermatogonia, and this is the second molecule demonstrated to be involved in SSC homing. Unlike β 1-integrin, which mediates attachment of SSCs to the basement membrane, our results suggest that Rac1 operates in a different step of SSC homing by regulating the transmigration of SSCs through the BTB. To successfully cross the BTB, SSCs have to bypass or block the tight junctions between Sertoli cells, which is comprised of claudins or occludin. Not surprisingly, this process is inefficient, because <10% of the transplanted SSCs can reinitiate spermatogenesis after transplantation into the adult testes (Oatley and Brinster, 2008). On the other hand, the transplantation efficiency increased by about 10-20-fold when SSCs were transplanted into pup testes without a BTB, indicating that this is the most important step of SSC homing (Shinohara et al., 2001). In this study, the involvement of Rac1 in transmigration was examined using pup and adult recipients for transplantation. While β 1-integrin-deficient SSCs disappeared within 3 weeks after transplantation in either pup or adult testes (Kanatsu-Shinohara et al., 2008), Rac1-deficient SSCs could colonize pup, but not adult, seminiferous tubules, indicating that condition of the host testes is key in Rac-mediated SSC homing.

As Rac is involved in the regulation of cytoskeletal rearrangements (Burrige and Wennerberg, 2004), an explanation for the homing failure may be that Rac-deficiency prevents formation of membrane ruffles or lamellipodia, where activated Rac is concentrated. The lack of this spatial regulation of Rac1 may have compromised directed movement towards the niche or did not allow necessary morphological changes required for transmigration. Alternatively, or additionally, Rac deficiency compromised the transmigration of SSCs by deregulating tight junction protein expression. Our results showed that expression levels of claudins was significantly reduced in DN-Rac cells, suggesting that decreased levels of these proteins contributed to low homing efficiency in the adult testis (Figure 2).

We initially expected that Rac would reinforce integrin-mediated signaling, but Rac1-deficient SSCs and DN-Rac cells were able to bind to the basement membrane and laminin-coated plates. In addition to SSC homing, our study also suggested that Rac is involved in the regulation of stem cell division and differentiation. Inhibition of Rac by a dominant-negative construct significantly increased the number of GS cell divisions. Likewise, serial transplantation of DN-Rac cells also showed that SSCs in the germ cell colonies exhibit decreased self-renewal *in vivo*. The results of these experiments suggest that inhibition of Rac1 activity has a negative effect on SSC self-renewal and promotes spermatogenic differentiation.

β 1-integrin and Rac1 operate at distinct steps of homing and also play important roles in HSC homing to the bone marrow niche. Further comparison between the two self-renewing systems will reveal the common molecular machinery of stem cell homing and will provide insight into the mechanism and regulation of stem cell-niche interaction.

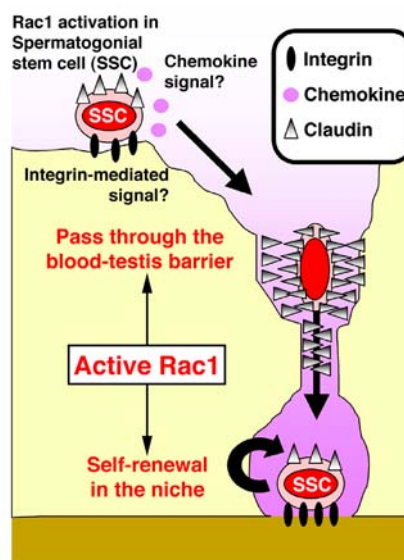


Figure 2. Model for SSC homing. Rac in SSCs is activated either by chemokines or adhesion to Sertoli cells. SSCs then transmigrate through the BTB by modulating the expression of tight junction-associated proteins before they settle on the basement membrane via β 1-integrin. The down-regulation of tight junction-associated proteins by Rac inactivation interfered with the SSC transmigration. In contrast, SSCs can directly settle on the basement membrane of the seminiferous tubules in the pup testes without a BTB.

References

- 1) Brinster, R. L. and Zimmermann, J. W. (1994). Spermatogenesis following male germ-cell transplantation. *Proc. Natl. Acad. Sci. USA* **91**, 11298-11302.
- 2) Burrige, K., and Wennerberg, K. (2004). Rho and Rac take center stage. *Cell* **116**, 167-179.
- 3) Cancelas, J. A., Jansen, M., and Williams, D. A. (2006). The role of chemokine activation of Rac GTPases in hematopoietic stem cell marrow homing, retention, and peripheral mobilization. *Exp. Hematol.* **34**, 976-985.
- 4) Chiarini-Garcia, H., Hornick, J. R., Griswold, M. D., and Russell, L. D. (2001). Distribution of type A spermatogonia in the mouse is not random. *Biol. Reprod.* **65**, 1179-1185.

- 5) Glogauer, M., Marchal, C. C., Zhu, F., Worku, A., Clausen, B. E., Foerster, I., Marks, P., Downey, G. P., and Kwiatkowski, D. J. (2003). Rac1 deletion in mouse neutrophils has selective effects on neutrophil functions. *J. Immunol.* **170**, 5652-5657.
- 6) Kanatsu-Shinohara, M., Ogonuki, N., Inoue, K., Miki, H., Ogura, A., Toyokuni, S., and Shinohara, T. (2003) Long-term proliferation in culture and germline transmission of mouse male germline stem cells. *Biol. Reprod.* **69**, 612-616.
- 7) Kanatsu-Shinohara, M., Takehashi, M., Takashima, S., Lee, J., Morimoto, H., Chuma, S., Raducanu, A., Nakatsuji, N., Fässler, R., and Shinohara, T. (2008). Homing of mouse spermatogonial stem cells to germline niche depends on β 1-integrin. *Cell Stem Cell* **3**, 533-542.
- 8) Nagano, M., Avarbock, M. R., and Brinster, R. L. (1999). Pattern and kinetics of mouse donor spermatogonial stem cell colonization in recipient testes. *Biol. Reprod.* **60**, 1429-1436.
- 9) Oatley, J.M., and Brinster, R.L. (2008). Regulation of spermatogonial stem cell self-renewal in mammals. *Annu. Rev. Cell Dev. Biol.* **24**, 263-286.
- 10) Shinohara, T., Orwig, K. E., Avarbock, M. R., and Brinster, R. L. (2001). Remodeling of the postnatal mouse testis is accompanied by dramatic changes in stem cell number and niche accessibility. *Proc. Natl. Acad. Sci. USA* **98**, 6186-6191.
- 11) Soriano, P. (1999). Generalized lacZ expression with the ROSA26 cre reporter strain. *Nat. Genet.* **21**, 70-71.
- 12) Takehashi, M., Kanatsu-Shinohara, M., Inoue, K., Ogonuki, N., Miki, H., Toyokuni, S., Ogura, A., and Shinohara, T. (2007). Adenovirus-mediated gene delivery into mouse spermatogonial stem cells. *Proc. Natl. Acad. Sci. USA* **104**, 2596-2601.

Development of New Asymmetric Carbene Ligands toward Contributions to Medicinal Chemistry

Kazuhiro Yoshida

Chiba University

kyoshida@faculty.chiba-u.jp

Abstract

The preparation of new chiral bicyclic imidazoles and their transformation into bisimidazolium salts are reported. The utility of the salts as precursors for chiral *N*-heterocyclic carbenes was demonstrated by the synthesis of a C-N-C pincer Ni-complex, the structure of which was characterized by single-crystal X-ray analysis.

Keywords: Carbene, Asymmetric Catalyst, Bidentate Ligand

Introduction

Chiral *N*-heterocyclic carbenes (NHCs) have recently received growing attention in the fields of coordination chemistry and asymmetric catalysis.^[1] In this study, we developed new chiral bicyclic imidazoles **1** and the transformation of **1** into chiral bisimidazolium salts **2** (Figure 1). As **2** are prepared with the intent of applying them to metal-catalyzed asymmetric reactions, the synthesis of a new chiral Ni-complex is also developed.

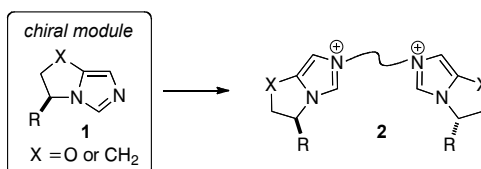
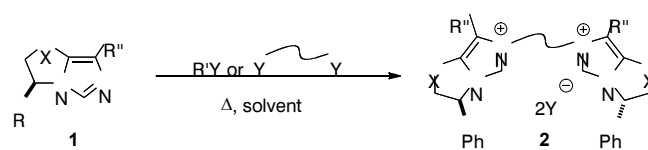


Figure 1. Modular Synthesis of Chiral Bicyclic Imidazolium Salts **2**.

Results

The results of the synthesis of bisimidazolium salts **2** are summarized in Table 1. When the reaction of **1a** with 1,3-dibromopropane was performed at 70 °C in acetonitrile, the desired bisimidazolium salt **2a** was obtained in good yield, as expected (entry 1). Moreover, the reaction of **1a** with α,α' -dibromo-*o*-xylene gave corresponding imidazolium salt **2b** (entry 2). Pyrrolidine-fused imidazolium salts were likewise prepared. The reaction of **1b** with dibromomethane, 1,2-dibromoethane, and 1,3-dibromopropane gave methylene, ethylene, and propylene bridged bisimidazolium salts **2c-2e**, respectively (entries 3-5). The last example is the formation of bisimidazolium salt **2f** that has a pyridyl moiety in the cross-linker (entry 6). The reaction of **1b** with 2,6-bis(bromomethyl)pyridine proceeded well to give desired product **2f** in 97% yield.

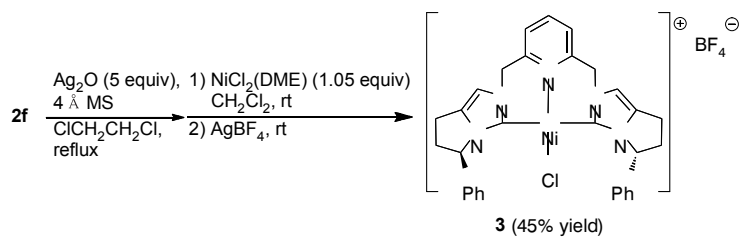


entry	reagents	product	conditions	yield (%) ^b
1	(<i>R</i>)- 1a Br (2.2:1)	2a	CH ₃ CN, 70 °C, 5 days	82
2	(<i>R</i>)- 1a Br (2.2:1)	2b	CH ₃ CN, 70 °C, 40 h	99
3	(<i>R</i>)- 1b CH ₂ Br ₂ (1:5)	2c	CH ₃ CN, 70 °C, 5 days	93
4	(<i>S</i>)- 1b Br (2.1:1)	2d	1) CH ₃ CN, 70 °C, 2 days 80 °C, 3 days 2) KPF ₆	>99
5	(<i>S</i>)- 1b Br (2.1:1)	2e	1) CH ₃ CN, 70 °C, 2 days 80 °C, 3 days 2) KPF ₆	>99
6	(<i>R</i>)- 1b Br (2.4:1)	2f	1) MeOH, 75 °C, 48 h	97

^a All reactions were carried out in CH₃CN or MeOH at 70-80 °C. ^b Isolated yields.

Table 1. Synthesis of Chiral Imidazolium Salts **2** from Imidazoles **1**.^a

The synthesized imidazolium salts can be utilized as precursors for chiral NHCs. For example, we tried to synthesize C-N-C pincer Ni-complex^[2] **3** from **2f** (Scheme 1). The transformation was performed by reacting NiCl₂(DME) with a silver complex that was prepared from **2f** and Ag₂O, followed by counter anion exchange with AgBF₄.^[3] As a result, chiral complex **3** was obtained in 45% yield. Similar to the general agreement for NHC complexes, **3** was found to be quite stable in air. Its purification was possible even by open silica gel column chromatography.



Scheme 1. Synthesis of C-N-C Pincer Ni-Complex **3** from **2f**.

A single crystal suitable for X-ray single-crystal structure determination was obtained by slow diffusion of pentane into a solution of **3** in CH_2Cl_2 . The structure of **3** displays an expected C_2 -symmetric chiral environment with square-planar coordination geometry (Figure 2).

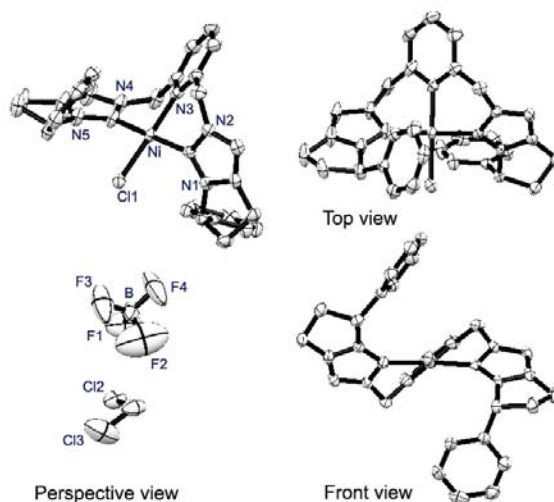


Figure 2. Crystal Structure of **3**: Hydrogen atoms are omitted for clarity (perspective view). Hydrogen atoms, CH_2Cl_2 , and BF_4^- anion are omitted for clarity (top and front views).

Discussion & Conclusion

In conclusion, we have prepared new chiral bicyclic imidazoles **1** and applied them to the modular synthesis of bisimidazolium salts **2**. Obviously, this approach can provide a wide variety of imidazolium salts beyond the range we have demonstrated here. Our ongoing study is focusing on various asymmetric reactions using these salts, and the results will be reported in due course.

References

- 1) For recent reviews, see: (a) *N-Heterocyclic Carbenes in Synthesis*; Nolan, S. P., Ed.; Wiley-VCH; Weinheim, 2006. (b) *N-Heterocyclic Carbenes in Transition Metal Catalysis*; Glorius, F., Ed.; Springer; Berlin, 2007. (c) Enders, D.; Niemeier, O.; Henseler, A. *Chem. Rev.* 2007, **107**, 5606-5655. (d) Díez-González, S.; Marion, N.; Nolan, S. P. *Chem. Rev.* 2009, **109**, 3612-3676.
- 2) (a) Pugh, D.; Danopoulos, A. A. *Coord. Chem. Rev.* 2007, **251**, 610-641. (b) Poyatos, M.; Mata, J. A.; Peris, E. *Chem. Rev.* 2009, **109**, 3677-3707.
- (3) Inamoto, K.; Kuroda, J.; Kwon, E.; Hiroya, K.; Doi, T. *J. Organomet. Chem.* 2009, **694**, 389-396.

Role of tissue plasminogen activator for hematopoietic-cell driven neoangiogenesis

Beate Heissig

Institute of Medical Science University of Tokyo

heissig@ims.u-tokyo.ac.jp

Abstract

Ischemia of the heart, brain and limbs is a leading cause of morbidity and mortality worldwide. Treatment with tissue type plasminogen activator (tPA) can dissolve blood clots and can ameliorate the clinical outcome in ischemic diseases. But the underlying mechanism by which tPA improves ischemic tissue regeneration is not well understood. Bone marrow (BM)-derived myeloid cells facilitate angiogenesis during tissue regeneration. Here we report that a serpin-resistant form of tPA by activating the extracellular proteases matrix metalloproteinase-9 and plasmin mobilizes CD45+CD11b+ pro-angiogenic, myeloid cells, a process dependent on vascular endothelial growth factor-A (VEGF-A) and Kit ligand signaling.¹ tPA improves the incorporation of CD11b+ cells into ischemic tissues, and increases expression of neoangiogenesis-related genes including VEGF-A. Remarkably, transplantation of BM-derived tPA-mobilized CD11b+ cells and VEGFR-1+ cells, but not carrier-mobilized cells or CD11b- cells, accelerates neovascularization and ischemic tissue regeneration. Inhibition of VEGF-signaling suppresses tPA-induced neovascularization in a model of hindlimb ischemia. Thus, tPA mobilizes CD11b+ cells from the BM and increases systemic and local (cellular) VEGF-A, which can locally promote angiogenesis during ischemic recovery. tPA might be useful to induce therapeutic revascularization in the growing field of regenerative medicine.

Keywords: 1-3 Cell Biology, 2-12 Hematology, 2-5 Cardiovascular/Metabolic/Endocrine

Introduction

The fibrinolytic system includes a broad spectrum of proteolytic enzymes with physiological and pathophysiological functions in tissue remodeling, tumor invasion, reproduction and angiogenesis. The serine protease plasmin is responsible for the degradation of fibrin into soluble degradation products (fibrinolysis). Plasmin is generated through cleavage of the proenzyme plasminogen (Plg) by the urokinase plasminogen activator (uPA) or tPA. Plasmin and plasminogen activators are also implicated in tissue proliferation and cellular adhesion, as they can proteolytically degrade the extracellular matrix (ECM) and regulate the activation of both growth factors and matrix metalloproteinases (MMPs) (for review²). PAs and plasmin generation in specific microenvironments in the bone marrow (BM) may be one of the factors orchestrating hematopoiesis.^{3,4} Plg activation promotes the release of Kit ligand from BM stromal cells.^{4,5} A number of cell model studies have demonstrated that MMP activation, notably activation of stromelysin-I, MMP-3 and MMP-9 can occur at the cell surface through the uPA/uPAR/plasminogen cascade for plasmin generation.⁶ Endothelial cells are the major source of tPA in

the blood circulation. tPA is released following injury or by brain endothelial cells upon monocyte interaction.⁷ Recent studies emphasized a role for BM-derived CD45⁺ myeloid hematopoietic cells at ongoing angiogenic sites.⁸ Myeloid cells may locally secrete angiogenic factors or MMP-9, which may in turn increase vascular endothelial growth factor (VEGF-A) bioavailability.⁹

Results

We could show that tissue type plasminogen activator (tPA) mobilizes CD11b⁺ cells into the circulation, a process dependent on plasmin and MMP-9-mediated release of Kit ligand and VEGF-A

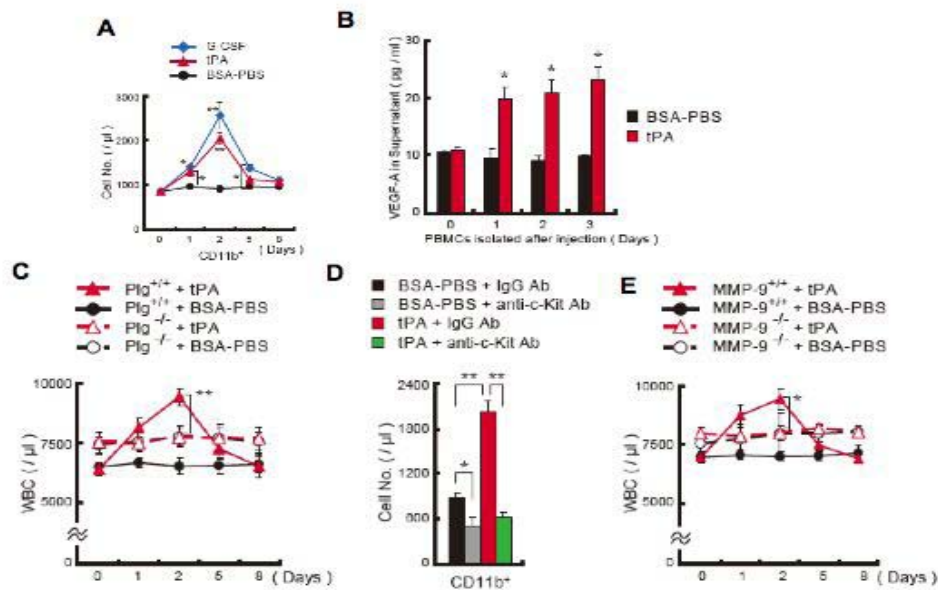


Figure 1. tPA mobilizes hematopoietic myelomonocytic cells into the circulation, a process dependent on plasmin and MMP-9-mediated growth factor release. (A) FACS analysis of CD45⁺CD11b⁺ and CD45⁺CD11b⁻ cells in peripheral blood of tPA-treated, G-CSF-treated or BSA-PBS-treated mice (n = 3 per group). (B) PBMCs were isolated at the indicated time points from tPA treated and untreated C57BL/6 mice. Cells were cultured under serum-free conditions for 24 hours. Supernatants were analyzed for VEGF-A by ELISA (n = 6). (C) Plg^{+/+} and Plg^{-/-} mice received tPA i.p., or BSA-PBS, from day 0-2. WBC counts were assessed (n = 5 per group; **P < 0.001; comparing Plg^{-/-} to Plg^{+/+} group). (D) C57BL/6 mice were injected with tPA and anti-c-Kit or control antibodies. The frequency of circulating CD45⁺CD11b⁺ cells was measured on day 2 (n = 3 per group). (E) WBC counts were determined in MMP-9^{+/+} and MMP-9^{-/-} mice after tPA administration (n = 4).

(Figure 1). The absolute number of cells mobilized after tPA treatment was lower than after treatment with the cell mobilizing cytokine granulocyte colony stimulating factor (G-CSF) (Figure 1). These mobilized CD45⁺CD11b⁺ cells isolated from tPA-treated, but not BSA-PBS-treated mice showed higher expression of the angiogenesis-associated genes VEGF-A, CD184, GM-CSF, CC chemokine receptor 2 (CCR2; a monocyte chemotactic protein-1 receptor), and neuropilin-1, VEGF receptor-1 and c-Kit (data not shown). PBMCs isolated from tPA-treated animals at the indicated time points released VEGF-A into culture supernatants (Figure 1B). Similarly, a drug impairing tPA-mediated plasmin activation (Figure 1L) or genetic ablation of Plg (Figure 1C) blocked the tPA-induced WBC (data not shown) and CD11b⁺ cell increase. tPA administration can promote myeloid cell expansion via MMP-9-mediated release of KitL from stromal/niche cells.¹⁰ Indeed, antibodies against c-Kit blocked tPA-mediated CD11b⁺ cell mobilization (Figure 1D) and tPA-mediated cell

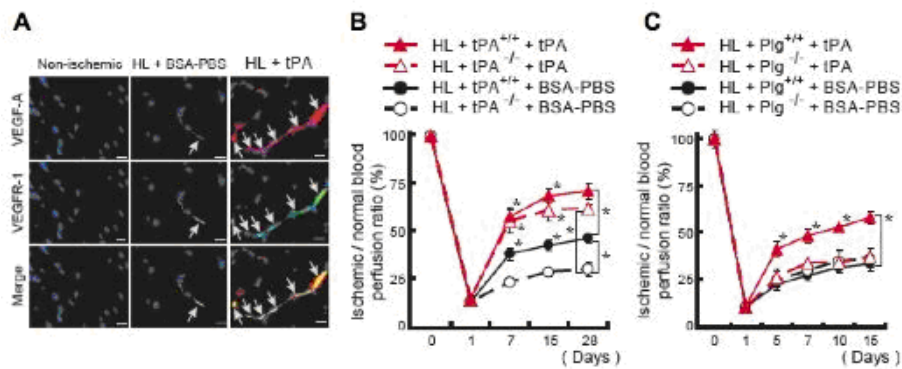


Figure 2. tPA administration accelerates revascularization in a hindlimb ischemia model. (A-C) tPA, or vehicle, was injected i.p. daily from day 0-2 into tPA^{+/+} and tPA^{-/-} mice after hindlimb (HL) ischemia induction. (A) Immunohistochemical staining of VEGFR-1 and VEGF-A of ischemic muscle tissues derived from vehicle-treated, tPA-treated and non-treated HL ischemic mice. Arrows indicate VEGFR-1+VEGF-A+ cells (Bar = 20 μ m). (B-C) tPA, or vehicle, was injected i.p. daily into tPA (B) or Plg (C) wild-type and deficient mice after induction of HL ischemia. Functional perfusion measurements of the collateral region were performed (n = 3 per group). A significant difference between tPA^{+/+} and tPA^{-/-} mice treated with BSA-PBS (*) is shown. If not otherwise mentioned, asterisks denote significant differences between BSA-PBS and tPA-treated groups. Single asterisks, P < 0.05; double asterisks, P < 0.001; values represent the mean \pm SEM.

mobilization did not occur in MMP-9 deficient mice (Figure 1E). These data indicate that c-Kit signaling is required for tPA-mediated cell mobilization.

We then could demonstrate that tPA administration accelerated ischemic revascularization (data not shown). We exploited a hindlimb (HL) ischemic model to show that tPA was required for CD11b⁺ myeloid cell mobilization, neoangiogenesis and ischemic muscle tissue regeneration. tPA augmented

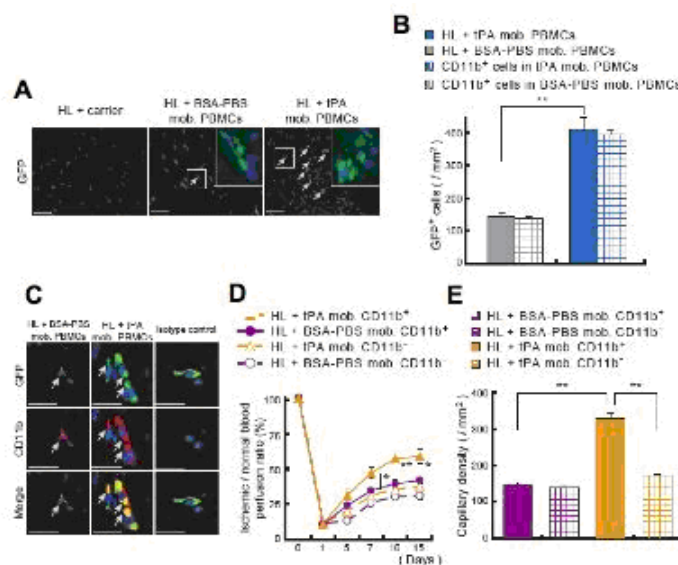


Figure 3. Transplantation of tPA-treated CD11b⁺ and VEGFR-1⁺ myeloid cells improve neoangiogenesis. (A-C) tPA or BSA-PBS mobilized PBMCs from GFP mice or carrier (no cells) were injected i.v. into HL-ischemia-induced recipients. (A-B) Within ischemic muscle tissues GFP-positive donor cells (arrows) were quantified. Inserts depict a magnified view (Magnification x630). (B) Quantification of the number of GFP⁺ cells and GFP⁺ cells coexpressing CD11b in ischemic tissues (n = 8 per group). (C) CD11b (Mac-1) staining of lower limb ischemic tissue from mice receiving carrier injections, from mice transplanted with PBMCs or from BSA-PBS-treated or tPA-treated donor GFP mice. Arrows indicate transplanted GFP⁺CD11b⁺ cells in ischemic tissues (Bar = 20 μ m). (D-E) PB-derived CD11b⁺ or CD11b⁻ cells isolated from tPA or BSA-PBS-treated donors were transplanted into HL ischemia induced recipients for 3 days (n = 4 per group). (D) Blood flow was determined. (E) Capillary density was evaluated.

the number of ischemic muscle-residing VEGF-A⁺ cells coexpressing VEGFR-1 (Figure 2A) in HL ischemia-induced mice compared to controls. tPA improved blood flow recovery and increased capillary density (data not shown) in tPA^{-/-} mice (Figure 2B), but was ineffective in Plg^{-/-} (Figure 23) or MMP-9^{-/-} mice (data not shown).

To determine the pro-angiogenic potential of tPA-mobilized cells we isolated PBMCs from GFP donor mice receiving tPA or vehicle and transplanted them daily into HL-ischemic recipients. Mice transplanted with tPA-mobilized PBMCs showed faster blood flow recovery, smaller areas of fatty degeneration (data not shown) compared to mice injected with BSA-PBS-stimulated PBMCs. Nearly all donor-derived GFP⁺ cells coexpressed CD11b (Figure 3A,B,C) and were detectable in ischemic muscle tissues of mice injected with tPA-mobilized PBMCs, but not in tissues of mice injected with control cells.

To examine if CD11b⁺ cells, known to enhance both normal and malignant neoangiogenesis³³ were the effector cells for tPA-driven neoangiogenesis we transplanted equal numbers of tPA-mobilized CD11b⁺ cells into HL recipient mice. tPA-mobilized, but not BSA-PBS-mobilized CD11b⁺ cells accelerated ischemic reperfusion (Figure 3D) and increased capillary density in ischemic tissues of HL-ischemic recipients (Figure 3E).

VEGF-A administration partially rescued impaired angiogenesis observed in Plg^{-/-} HL-ischemic

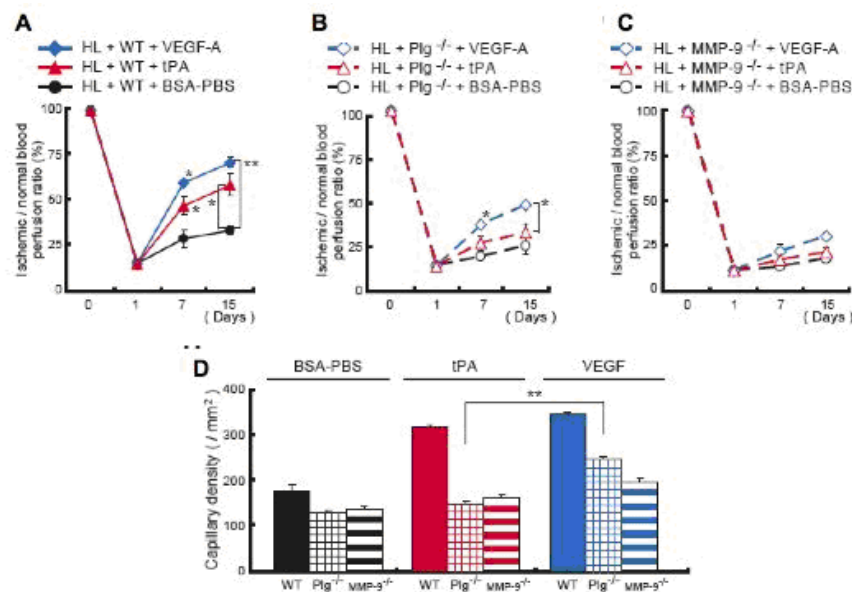


Figure 4. Administration of rec. VEGF-A partially rescues the angiogenic defect observed in Plg and MMP-9 deficient mice. HL-induced wildtype control (A), Plg^{-/-} mice (B) and MMP-9^{-/-} mice (C,D) were injected i.p. daily with tPA, mVEGF-A or BSA-PBS from day 0 until day 2. (A-C) Blood flow recovery was determined by LDPI in the ischemic limbs (n = 3; *P < 0.05). (D) Capillary density was evaluated on CD31-stained sections 15 days following ligation (n = 3; **P < 0.001). Asterisks indicate a significant difference between the indicated groups. Error bars represent ±SEM.

mice, as reported,³⁴ but did not in MMP-9^{-/-} mice (Figure 4A-D).

But is VEGF-A signaling required for tPA-mediated tissue neoangiogenesis? Blockade of VEGF signaling with antibodies against murine VEGF-A (data not shown), or VEGF receptors (data not shown) inhibited tPA-mediated ischemic tissue recovery and neoangiogenesis as well as myeloid cell

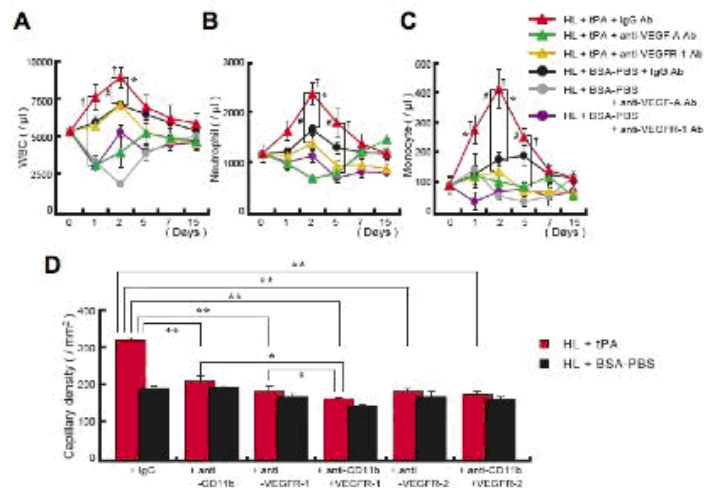


Figure 5. Inhibition of VEGF signaling prevented tPA-mediated ischemic tissue recovery. (A-C) Blood cell counts were determined at the indicated time points after hindlimb ischemia induction. (A) WBC, (B) neutrophils, and (C) monocytes ($*P < 0.05$; $\dagger P < 0.05$; $*$ is a comparison of the tPA plus IgG-treated HL group with the BSA-PBS plus IgG-treated group. \dagger is a comparison of the tPA plus IgG-treated HL group with the tPA plus anti-VEGFR-1 group). Error bars represent \pm SEM. (D) HL-induced C57BL/6 mice treated with tPA, or BSA-PBS and antibodies against CD11b were cotreated with antibodies against VEGFR-1 or VEGFR-2. Capillary density was evaluated ($n = 3$ per group). If not otherwise indicated, a single asterisk ($P < 0.05$) and double asterisk ($P < 0.001$) or a cross ($P < 0.05$) indicate a significant difference between groups. Values represent the mean \pm SEM.

mobilization via VEGFR-1 (Figure 5A-C) in an HL ischemic model. Similarly, tPA did not improve neovascularization in myeloid cell-depleted mice (Figure 5D). Coinjection of anti-VEGFR-1 antibodies into myeloid cell-depleted mice further reduced neovascularization both in BSA-PBS and tPA-treated mice. These data indicate that CD11b⁺ hematopoietic cells are the major “angiogenic effector cells” for tPA-mediated cell-driven neovascularization. However, it is possible that some non-CD11b/VEGFR-1⁺ cells (e.g. endothelial cells) might contribute to the tPA-induced angiogenic response.

Discussion & Conclusion

In the present study, we demonstrate that plasmin activation through administration of serpin-resistant mutant tPA alone was sufficient to mobilize BM-derived hematopoietic, angiopotent cells into the circulation. Our findings support a mechanism whereby tPA-generated plasmin mobilizes myeloid cells through the release of VEGF-A and KitL, processes that are dependent on MMP-9 activation, and possibly on that of other MMPs. We recently demonstrated that tPA alone had no effect on myeloid precursor cell expansion in vitro, but increased BM cell numbers in vivo/in the presence of stromal cells a process partially dependent on c-Kit/KitL signaling.⁵ Here, we report that the tPA-mediated increase in BM cells (myeloid cells) also requires VEGF-A signaling, as neutralizing antibodies against VEGF-A prevented tPA-mediated BM cell (including CD11b⁺) cell expansion (data not shown). In addition, the c-Kit/KitL signaling pathway is also implicated in cell migration/mobilization.¹¹ Here, we demonstrate that tPA administration increases circulating proangiogenic CD45⁺CD11b⁺ cells coexpressing both VEGFR-1 and c-Kit, a process which could be blocked using antibodies against VEGF-A and c-Kit. Interestingly, intraventricular leukocytosis has been observed in rats with intraventricular hemorrhage/

hematoma that were treated with high doses of tPA.¹² Streptokinase administration in patients with acute myocardial infarction caused a marked increase in circulating white blood cells.¹³

The angiogenic effect of tPA was seen as early as 5 to 7 days after surgery. These data suggest that the kinetics of angiogenic-cell mobilization by tPA may mirror that observed for hematopoietic cell mobilization peaking on day 2. Here, we demonstrate that the angiogenic effect of tPA can be adoptively transferred by blood mononuclear cells. Of interest, tPA administration increased not only the absolute number of these angiopotent cells, but more importantly tPA-stimulated cells showed qualitatively improved angiogenic performance/potential when compared to PBS treated controls in an hindlimb ischemic murine model. This is in contrast to the reported proangiogenic effects of other mobilizing agents such as G-CSF, which cause an increase in the basal numbers of circulating mononuclear cells rather than inducing the mobilization of a unique angiogenic-cell population. Macrophage migration during inflammation has been shown to depend on CD11b/Mac-1 recognition of a binary complex consisting of fibrin within the provisional matrix and tPA.¹⁴ Cao et al elegantly demonstrated that subsequent neutralization of tPA by its inhibitor PAI-1 enhanced binding of the integrin-protease-inhibitor complex to the endocytic receptor lipoprotein receptor-related protein, triggering a switch from cell adhesion to cell detachment. Our combined data show that a serpin-resistant form of tPA induces leukocyte mobilization and promotes neoangiogenesis. Our findings have implications for regenerative medicine: Administration of tPA alone or in combination with other growth factors might be a novel strategy to increase the efficiency of hematopoietic, angiopotent cell harvests for cell-based therapy of ischemic diseases. These data set forth the novel concept that plasmin activation, apart from controlling coagulation, controls myeloid cell-driven neoangiogenesis during tissue regeneration.

References

This study is published as full article in Ohki et al. *Blood* 2010;¹

- 1) Ohki M, Ohki Y, Ishihara M, et al. Tissue type plasminogen activator regulates myeloid-cell dependent neoangiogenesis during tissue regeneration. *Blood*.
- 2) Zorio E, Gilabert-Estelles J, Espana F, Ramon LA, Cosin R, Estelles A. Fibrinolysis: the key to new pathogenetic mechanisms. *Curr Med Chem*. 2008;**15**:923-929.
- 3) Hannoeks MJ, Oliver L, Gabilove JL, Wilson EL. Regulation of proteolytic activity in human bone marrow stromal cells by basic fibroblast growth factor, interleukin-1, and transforming growth factor beta. *Blood*. 1992;**79**:1178-1184.
- 4) Heissig B, Ohki M, Ishihara M, et al. Contribution of the fibrinolytic pathway to hematopoietic regeneration. *J Cell Physiol*. 2009;**221**:521-525.
- 5) Heissig B, Lund LR, Akiyama H, et al. The Plasminogen Fibrinolytic Pathway Is Required for Hematopoietic Regeneration. *Cell Stem Cell*. 2007;**1**:658-670.
- 6) Murphy G, Atkinson S, Ward R, Gavrilovic J, Reynolds JJ. The Role of Plasminogen Activators in the Regulation of Connective Tissue Metalloproteinases. *Annals of the New York Academy of Sciences*. 1992;**667**:1-12.

- 7) Reijerkerk A, Kooij G, van der Pol SMA, et al. Tissue-Type Plasminogen Activator Is a Regulator of Monocyte Diapedesis through the Brain Endothelial Barrier. *The Journal of Immunology*. 2008;**181**:3567-3574.
- 8) Rafii S, Lyden D, Benezra R, Hattori K, Heissig B. Vascular and haematopoietic stem cells: novel targets for anti-angiogenesis therapy? *Nat Rev Cancer*. 2002;**2**:826-835.
- 9) Bergers G, Brekken R, McMahon G, et al. Matrix metalloproteinase-9 triggers the angiogenic switch during carcinogenesis. *Nat Cell Biol*. 2000;**2**:737-744.
- 10) Heissig B, Lund LR, Akiyama H, et al. The plasminogen fibrinolytic pathway is required for hematopoietic regeneration. *Cell Stem Cell*. 2007;**1**:658-670.
- 11) Heissig B, Hattori K, Dias S, et al. Recruitment of stem and progenitor cells from the bone marrow niche requires MMP-9 mediated release of kit-ligand. *Cell*. 2002;**109**:625-637.
- 12) Wang YC, Lin CW, Shen CC, Lai SC, Kuo JS. Tissue plasminogen activator for the treatment of intraventricular hematoma: the dose-effect relationship. *J Neurol Sci*. 2002;**202**:35-41.
- 13) Adams SA, Froese SP, Green BK, et al. Treatment of acute myocardial infarction with streptokinase does not appear to modulate circulating neutrophil function. *Clin Cardiol*. 1995;**18**:459-463.
- 14) Cao C, Lawrence DA, Li Y, et al. Endocytic receptor LRP together with tPA and PAI-1 coordinates Mac-1-dependent macrophage migration. *Embo J*. 2006;**25**:1860-1870 Epub 2006 Apr 1866.

Identification and characterization of novel prion-like cytoplasmic genetic factors

Motomasa Tanaka
RIKEN Brain Science Institute
motomasa@brain.riken.jp

Abstract

Prions are epigenetic elements that are caused by protein conformational switches, functional proteins to misfolded, self-propagating, β -sheet-rich infectious amyloid proteins. All of the yeast prion proteins identified so far contain intrinsic domains with high glutamine and asparagines content (Q/N-rich domain) and it remains unclear whether the prion phenomenon in yeast is general to a diverse set of proteins without a Q/N-rich domain. Here we found Sug5 is a novel yeast prion protein without a Q/N-rich domain. Sug5 forms fibrillar aggregates in vitro and we could induce a prion state [SUG+] by introducing sug5 aggregates into yeast. The [SUG+] state is dominant and dependent on Hsp104 levels as observed for most yeast prion proteins identified. These results demonstrate that sug5 is a novel yeast prion protein and suggest that the prion phenomena are general in the biological world.

Keywords: Prion, Amyloid, Aggregation

Introduction

Prions are epigenetic elements that are caused by protein conformational switches from functional proteins to misfolded and β -sheet-rich infectious amyloid forms. In *S. cerevisiae*, several yeast prion proteins have been reported. All of the yeast prion proteins identified so far contain intrinsic domains including high glutamine and asparagines contents (Q/N-rich domain), which thought to be critical for the aggregate formation and its propagation (1-3). On the other hands, a mammalian prion protein and a protein from filamentous fungi, *P.anserine*, a HET-s protein lack such a Q/N-rich sequence while they also have an ability to form infectious amyloid forms of the proteins.

Nonetheless, no yeast prion proteins are identified that lack Q/N-rich domains and it remains unclear whether the prion phenomenon in yeast is general to a diverse set of proteins without a Q/N-rich domain. In this study, we sought to identify a non-Q/N-rich yeast prion protein to address whether the prion phenomena can be general.

Results

Using a novel genetic screening method with a yeast prion [PSI+] system, we identified several proteins as candidates for novel yeast prion proteins without a Q/N-rich domain. Among them, we focused on sug5 in the following experiments.

First we investigated whether the sug5 protein highly purified from bacteria possesses features of amyloid. We examined morphology of the aggregates by transmitted electron microscopy and the

binding to amyloid specific dyes, thioflavin-T and Congo-Red. The sug5 aggregates formed fiber-like structure (Figure 1) and bound well to the amyloid specific dyes. These results show that sug5 forms amyloid fibrils in vitro as other yeast prion proteins do.

Next, we investigated whether endogenous sug5p also forms amyloid in vivo and a prion-based phenotype is induced by its amyloid form. Sug5 is tRNA isopentenyl transferase and catalyzes the transfer of an isopentenyl group to A37 in the anticodon loop (4). Even single mutant of SUG5 gene causes a slight sensitivity to the pyrimidine analog 5-fluorouracil (5FU), and a double mutant of SUG5 and TRM1, which encodes tRNA methyltransferase and is responsible for m22G26 modification, shows more severe sensitivity to the 5FU. Therefore, we constructed a $\Delta trm1$ yeast strain and introduced sug5 amyloids into the $\Delta trm1$ yeast cells by a method of “protein infection” (5).

Colonies of the infectants were assayed for their sensitivity to 5FU. A fraction of the colonies showed 5FU sensitivity as a $\Delta sug5\Delta trm1$ double mutant does. However, these colonies were able to grow on 5FU plate after the treatment with 3mM guanidine hydrochloride. This treatment eliminates all known yeast prions. We then refer to this prion state of sug5 as [SUG+], using standard prion nomenclature. We next examined effects of Hsp104p, a member of AAA+ATPase chaperones, on the [SUG+] prion state. Disruption and overexpression of HSP104 eliminates the [SUG+] state. Thus, these data suggested that [SUG+] is propagated by an Hsp104p-dependent manner. Furthermore, we found that the [SUG+] state transmits in a dominant manner upon mating with a WT yeast strain.

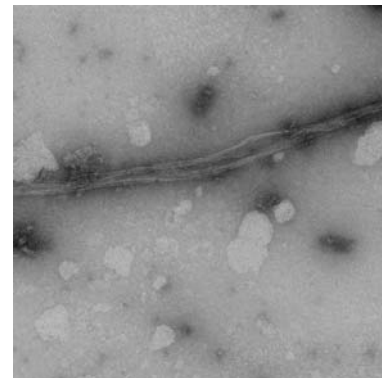


Figure 1: Fibrillar structure of sug5 aggregates

Discussion & Conclusion

The protein infection experiment shows that sug5 amyloids are infectious and the conversion of endogenous sug5p to an aggregated form makes the [SUG+] yeast sensitive to 5FU. These results show that sug5 amyloids are cytoplasmic genetic factors. In addition, the prion state of [SUG+] yeast was dependent on levels of Hsp104 as observed for most yeast prion proteins identified. Furthermore, the diploid strain formed by mating between a [SUG+] yeast and a WT strain shows the [SUG+] phenotype, indicating that [SUG+] is dominant.

These results demonstrate that sug5 is a novel yeast prion protein which lacks an aggregation-prone Q/N-rich domain and suggest that the prion phenomena are general in the biological world.

References

- 1) Du Z, Park KW, Yu H, Fan Q, Li L. SWI Newly identified prion linked to the chromatin-reSUGeling factor Swi1 in *Saccharomyces cerevisiae*. *Nat Genet.* **40**(4):460-465 (2008).
- 2) Patel BK, Gavin-Smyth J, Liebman SW. The yeast global transcriptional co-repressor protein Cyc8 can propagate as a prion. *Nat Cell Biol.* **11**(3):344-349 (2009).

- 3) Alberti S, Halfmann R, King O, Kapila A, Lindquist S. A systematic survey identifies prions and illuminates sequence features of prionogenic proteins. *Cell* 3;**137**(1):146-158 (2009).
- 4) Benko AL, Vaduva G, Martin NC, Hopper AK. Competition between a sterol biosynthetic enzyme and tRNA SUGification in addition to changes in the protein synthesis machinery causes altered nonsense suppression. *Proc Natl Acad Sci U S A.* 4;**97**(1):61-66 (2000).
- 5) Tanaka M, Collins SR, Toyama BH, Weissman JS. The physical basis of how prion conformations determine strain phenotypes. *Nature* 3;**442**(7102):585-589 (2006).

Epigenetic profiling in germ and somatic cells for establishment of induced Germline Stem Cells

Kimiko Inoue

Bioresource Center, RIKEN

inoue@rtc.riken.jp

Abstract

The final goal of this study is establishment of induced germline stem cells (iGS cells) by introducing epigenetic and transcriptional status of germ cells into somatic cells. As the first step, I developed a transcriptional profiling system for small amount of RNA extracted from mouse oocytes and preimplantation embryos.

Keywords: Germ cells, Microarray, Preimplantation embryos

Introduction

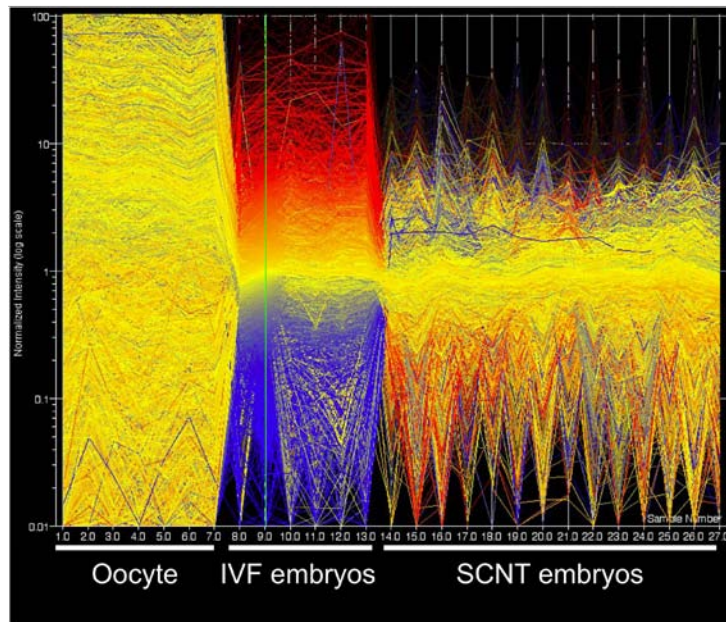
Because germ cells are very special cells that transmit genetic information into next generation, effective use of these cells is very valuable for medical, biological and agricultural purposes.

Recently, induced pluripotent stem cells (iPS cells) were established by introducing three to four transcriptional factors into somatic cells (1). iPS cells have pluripotency and can differentiate into various types of somatic cells in the body. However, because germ cells have very specific epigenetic status (Histone modification, DNA methylation and transcriptional profile), it is still impossible to generate entire germline cells from iPS cells. In this study, I attempt to establish iGS cells by introducing the germ cell-specific epigenetic and transcriptional status into somatic cells. As the first step for this purpose, I developed a transcriptional profiling system with small amount of RNA using mouse unfertilized oocytes and preimplantation embryos.

Results

Total RNAs from 10 mouse unfertilized oocytes, 2-cell stage in vitro fertilization (IVF) or somatic cell nuclear transferred (SCNT) embryos were isolated with TRIzol (Invitrogen) treatment. The amount of RNA included in single oocyte and 2-cell embryo are estimated 0.35 ng and 0.24 ng, respectively (2). Amplified RNAs were labeled with Cy3 and hybridized into 44K Whole Mouse Genome Oligo DNA Microarray (Agilent). By Principle Component Analysis, oocytes, IVF and SCNT embryos were clearly separated into different group, indicating technical reliability in this system. The transcriptional pattern of IVF embryos was clearly different from that of unfertilized oocytes, showing dramatic change in their transcriptional profile after maternal-zygotic transition. In SCNT embryos, transcriptional patterns among each sample were apparently different and indicated incomplete zygotic gene activation in SCNT embryos (Figure).

I am now investigating whether regulation of 117 candidate genes that are differently expressed between IVF and SCNT embryos can improve incomplete reprogramming in SCNT embryos.



Discussion & Conclusion

In this study, I developed a novel system for transcriptional profiling with small amount of RNA using preimplantation mouse embryos. The transcriptional profiling system described here showed clearly different gene expression patterns among unfertilized oocytes, IVF and SCNT embryos, indicating this system is technically reliable. Because the number of primordial germ cells in a mouse fetus at 8.5-10.5 dpc is around 150-1000 (3), it is difficult to collect enough numbers of cells for transcriptional or epigenetic genome analysis. Thus, the transcriptional profiling system I developed here is applicable and reliable method for further investigation for establishment of iGS cells.

References

- 1) Takahashi K, Yamanaka S. Induction of pluripotent stem cells from mouse embryonic and adult fibroblast cultures by defined factors. *Cell* 2006;**126**(4):663-76.
- 2) Piko L, Clegg KB. Quantitative changes in total RNA, total poly(A), and ribosomes in early mouse embryos. *Dev Biol* 1982;**89**(2):362-78.
- 3) Tam PP, Snow MH. Proliferation and migration of primordial germ cells during compensatory growth in mouse embryos. *J Embryol Exp Morphol* 1981;**64**:133-47.

The role of semaphorin in organogenesis during development: Semaphorin 4A navigates intracellular trafficking of retinoids for photoreceptor survival

Toshihiko Toyofuku

Research Institute for Microbial Diseases, Osaka University

toyofuku@ragtime.biken.osaka-u.ac.jp

Abstract

Sema4A is a transmembrane protein belonging to the semaphorin family, many members of which have been identified as axon guidance cues during neuronal development. We here show that Sema4A plays indispensable roles in retinoid cycle in retinal pigment cells for photoreceptor survival. Sema4A-deficient mice exhibit massive apoptosis of photoreceptors in the neonatal stage due to the failure of regenerating retinoids. In retinoid cycle, the intracellular transport of retinoid-binding proteins is accomplished by the association with Sema4A, the apical sorting of which depends on the Rab11/FIP2-mediated apical endosomal trafficking machinery. Collectively, these findings not only demonstrate a crucial role of Sema4A in intracellular transport of retinal binding proteins for photoreceptor survival but also present a novel functional aspect of semaphorins as an regulator for endosomal trafficking

Keywords: Semaphorin, Retinoid cycle, Photoreceptor,

Introduction

Blindness often results from the death of photoreceptors, which respond directly to light and mediate the first step in vision. The homeostasis of photoreceptors is functionally and mechanically supported by retinal pigment cells. Retinal pigment cells perform specialized and essential functions for photoreceptors, that is, retinoid cycle and daily phagocytosis of the distal end of photoreceptor outer segment. In particular, retinoid cycle by retinal pigment cells is shown to be essential for photoreceptor survival, in which they take up and regenerate retinoids, and then transport them back to the outer segment of photoreceptors. However, it remains unclear how retinoids are trafficked to be recycled in retinal pigment cells

Sema4A is a transmembrane-type semaphorin, of which family members have been identified as axonal guidance cues during neuronal development. It has been reported that insertion of gene-trap vector into intron 11 of mouse Sema4A gene results in loss of retinal photoreceptors through the search for molecules responsible for retinal degeneration. Subsequently, mutations in human Sema4A gene have been found in patients with retinal degeneration. We have previously established Sema4A-deficient (Sema4A^{-/-}) mice and demonstrated that Sema4A regulates T-cell mediated immunity and angiogenesis. Sema4A^{-/-} mice exhibited the similar changes in retinal photoreceptors to those reported in mice with the gene-trap vector into the Sema4A gene; the normal retinal development

at P0, but disruption of outer segment of photoreceptors at P14, followed by complete loss of photoreceptor until P28. These findings confirm the indispensable roles of Sema4A in photoreceptor survival.

Results

To examine whether light exposure enhances the photoreceptor death in Sema4A^{-/-} retina, in which dark-adapted mice were exposed to white fluorescent light. Under the illumination, Sema4A^{-/-} retina exhibited the dramatic increase of apoptotic cells in the outer nuclear layer with the distorted rosette-like appearance and then recovered to the basal levels. Of note, even in the dark adapted state, Sema4A^{-/-} retina displayed more apoptotic cells than Sema4A^{+/+} retina. Collectively, these results indicate the inappropriate hyper-activation of photoreceptors in Sema4A^{-/-} retina, which can induce massive apoptosis of photoreceptors by the illumination.

To determine how Sema4A is involved in retinoid cycle, we analyzed retinoid levels in mouse retina by HPLC. Either Sema4A^{+/+} or Sema4A^{-/-} retina showed low but comparable levels of 11-cis-retinal. These results indicated that retinoid cycle, crucial for photoreceptor survival after eye opening, is severely impaired in Sema4A^{-/-} retina.

Based on the defects of 11-cis retinal in Sema4A^{-/-} retina and the expression of Sema4A in retinal pigment cells, we hypothesized that Sema4A is involved in the retinoid cycle in retinal pigment cells. Co-immunoprecipitation experiments showed that Sema4A was associated with either CRALBP or CRBP1 through its extracellular region in the transfected cells. We next examined the intracellular trafficking of Sema4A, CRALBP and CRBP1 by chasing chromophore-tagged proteins in the living cells. When Sema4A-SNAP and CRALBP-CLIP or CRBP1-CLIP were co-expressed in Sema4A^{+/+} retinal pigment cells, either CRALBP-CLIP or CRBP1-CLIP, both of which was co-localized with Sema4A-SNAP in the endoplasmic reticulum, exhibited the synchronous spreading to the cell periphery with Sema4A-SNAP. These results indicated that Sema4A plays an important role in regulation of the intracellular trafficking of retinoid-binding proteins.

The retinoid cycle takes place in the narrow compartments between microvilli of retinal pigment cells and outer segment of photoreceptors. We then addressed the intricate sorting machinery by which Sema4A is polarized to the apical cell periphery to deliver retinoid-binding proteins. Members of the Rab GTPase family have been emerged as important regulators of endosomal trafficking governing specific membrane traffic steps. In particular, Rab11 has been shown to play an essential role in apical endosomal trafficking in polarized epithelial cells in combination with the Rab11-binding protein, FIP2. Co-immunoprecipitation experiments showed that Sema4A bound to the complex of Rab11 and FIP2 through its cytoplasmic region. Filter-grown retinal pigment cells from Sema4A^{+/+} retina showed the apical distribution of Sema4A, which was disrupted by the microtubule-depolymerizing nocodazole but not by the microtubule stabilizing taxol, indicating that the apical distribution of Sema4A requires the microtubule-dependent mechanism. To investigate the role of Rab11 on the apical transport of Sema4A-containing vesicle, the filter-grown retinal pigment

cells were transfected with Sema4A-GFP and either with Rab11, dominant negative Rab11(S25N) or constitutively active Rab11(Q70L). Rab11(S25N) blocked the apical distribution of Sema4A-GFP. These findings indicate that the intracellular apical sorting of Sema4A is regulated by the Rab11/FIP2-mediated endosomal trafficking machinery.

Discussion & Conclusion

We here present evidence that the intracellular transport of retinoid-binding proteins, essential for retinoid cycle, is mediated by Sema4A, the apical sorting of which depends on the Rab11/FIP2-mediated endosomal trafficking. These findings propose the novel aspect of semaphorin function in that Sema4A functions as an intracellular navigator for specific molecules. This concept is surprising because semaphorins have been regarded as a guidance molecule in the extracellular space.

Regeneration of retinoids by retinal pigment cells is essential for the homeostasis of photoreceptors. This is high-lightened by conditions abolishing retinoid supply in many retinal degenerative diseases. Our findings showed the importance of Sema4A on retinoid recycling. Therefore, it would be of value to determine the mechanisms of how mutations in human Sema4A identified in patients are involved in retinoid metabolism. Thus, our results will provide a novel functional aspect of semaphorins as an endosome trafficking molecule but also a therapeutic target for retinal degenerative diseases.

The prevention of postoperative intestinal adhesion by hepatocyte growth factor (HGF)

Tomohiro Yoshimoto

Laboratory of Allergic Diseases. Institute for Advanced Medical Sciences.

Hyogo College of Medicine

tomo@hyo-med.ac.jp

Abstract

Intestinal adhesions are bands of fibrous tissue, which connects the loops of intestine to each other, or to other abdominal organs or wall. Fibrous tissue formation is regulated by the balance between plasminogen activator inhibitor type 1 (PAI-1) and tissue type plasminogen activator (tPA), which reciprocally regulate fibrin deposition. Several components including cytokines, chemokines, cell adhesion molecules, and neuropeptide substance P are reported to participate in adhesion formation. We have developed a unique experimental mouse model of intestinal adhesion by cecal cauterization. Mice developed severe intestinal adhesion following this treatment. Adhesion development depends upon an IFN- γ system. Natural killer T cell (NKT)^{-/-} mice poorly developed adhesion; while they developed severe adhesion after reconstitution with NKT cells from wild-type mice, suggesting NKT cell IFN- γ production is indispensable. Wild-type mice increased the ratio of PAI-1/tPA following cecal cauterization, while *Ifn γ ^{-/-}* mice failed to do so, suggesting IFN- γ plays a critical role in differential regulation of PAI-1 and tPA. Hepatocyte growth factor, a potent mitogenic factor for hepatocytes, strongly inhibited intestinal adhesion by diminishing IFN- γ production, providing a novel way for prevention of postoperative adhesions.

Keywords: postoperative adhesions, IFN- γ , NKT, PAI-1, hepatocyte growth factor

Introduction

Abdominal adhesion formation occurs in 67 to 93% of abdominal surgeries^{1,2}. Adhesion also develops following abdominal bacterial infections such as peritonitis³. Recent study indicates that Th1 cells are critical for the development of adhesion in mouse model of intraabdominal sepsis⁴. Nevertheless, only limited studies investigated the molecular process involved in intestinal adhesions. In addition, there are no appropriate treatment or preventive way for intestinal adhesions. Here we have established a unique experimental mouse model for elucidation of molecular mechanism underlying organ adhesions⁵.

Results

- 1) We could induce intestinal adhesion by cecal cauterization with coagulation mode of bipolar forceps. Wild-type mice formed thick adhesion with planter attachment (Score 4) or developed very thick vascularized adhesion (Score 5) (Figure 1).

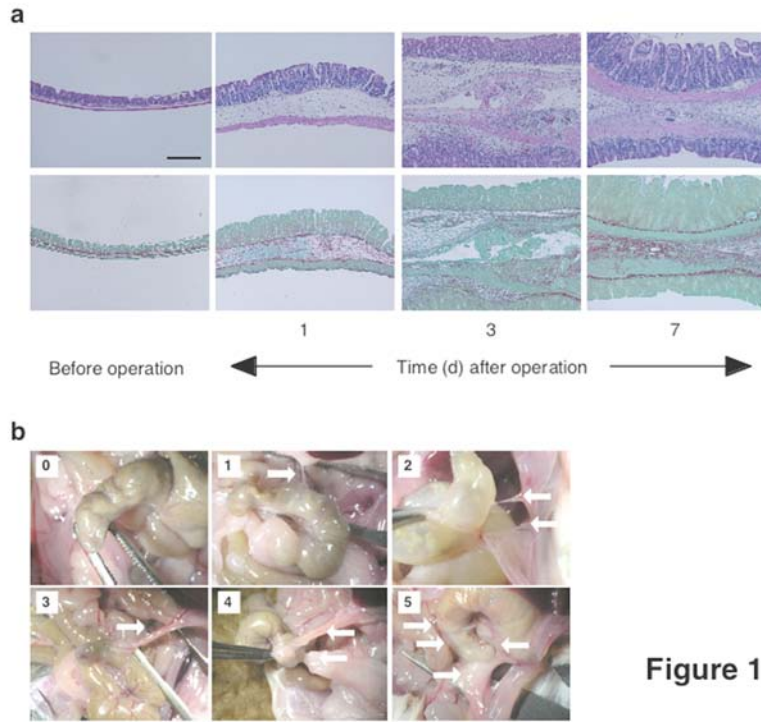


Figure 1

2) NKT knockout ($NKT^{-/-}$) mice developed lower grade (Score 1~2) intestinal adhesion and fibrotic changes, however, when they were reconstituted with unfractionated $CD4^{+}T$ cells from wild-type mice but not from $Ifng^{-/-}$ mice, they gained the capacity to develop severe intestinal adhesion and severe fibrotic changes, indicating that NKT cells contributed to intestinal adhesion formation by production of $IFN-\gamma$ in our adhesion model (Figure 2). Indeed, we found marked and rapid increase in the number of $Ly49^{+}CD4^{+}T$ (NKT) cells at 3 hours after operation in the intestine.

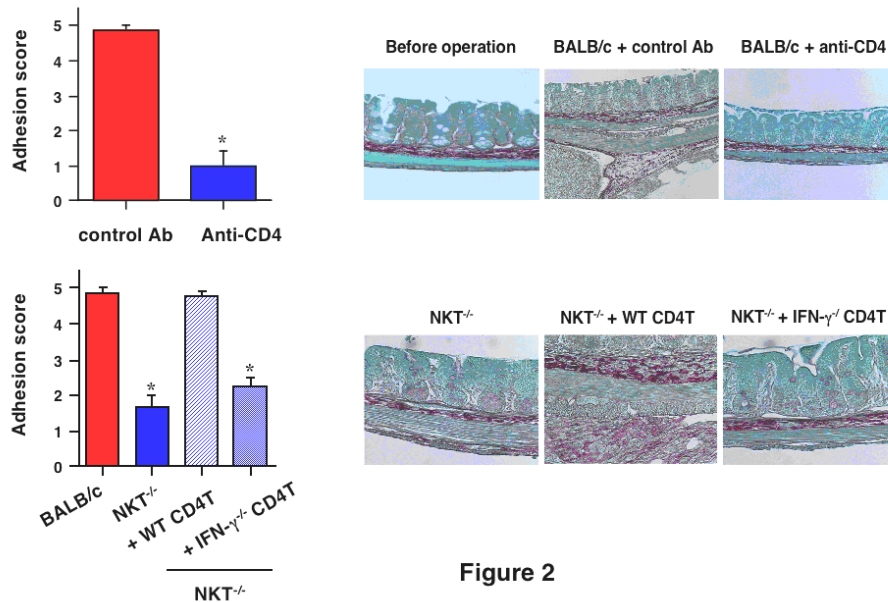


Figure 2

3) Wild type mice increased and decreased PAI-1-and tPA, respectively, in their ceca (mRNA levels) at day 1, while $Ifng^{-/-}$ mice failed to do so, indicating that $IFN-\gamma$ is a causative factor in postsurgical adhesion formation (Figure 3).

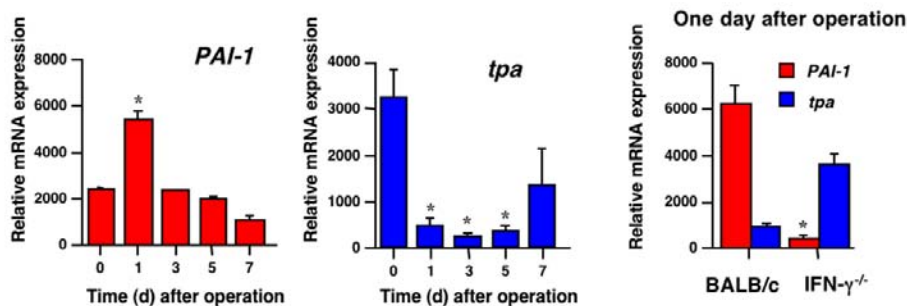


Figure 3

- 4) We found that single injection of HGF (20 μ g/body) subcutaneously one day before operation significantly reduced intestinal adhesion (score 0 or 1). Furthermore, HGF treatment suppressed mRNAs for IFN- γ and PAI-1 (Figure 4), suggesting HGF inhibits PAI-1 via inhibition of IFN- γ production.

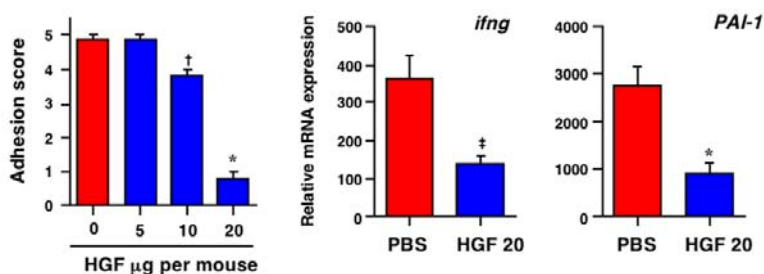


Figure 4

- 5) In addition to the mouse model of intestinal adhesion formation induced by cecal cauterization with bipolar forceps, we found that partial hepatectomy bipolar forceps induced severe intestinal adhesion formation (Score 5).
- 6) The mechanisms of the intestinal adhesion formation induced by partial hepatectomy were similar to those of intestinal adhesion formation induced by cecal cauterization. And single injection of HGF (20 μ g/body) subcutaneously one day before operation significantly reduced intestinal adhesion (score 0 or 1).

Discussion & Conclusion

We have developed a new experimental intestinal adhesion model. We can use bipolar forceps, which we routinely use in human surgery, mimicking human intestinal adhesion. We can control duration and intensity of cauterization by changing the mode, allowing us to treat the animals with identical invasive maneuver in terms of quantity and quality. Procedure is simple and very straightforward and obtained results are very reproducible.

Here, we demonstrated IFN- γ is important for induction of PAI-1, because both *Ifng*^{-/-} mice did not increase PAI-1-mRNA. Thus, IFN- γ is very important for induction of PAI-1 mRNA, intestinal adhesion formation.

Recombinant human HGF is already available for patients with fatal liver disease; these results

presented here strongly indicate that HGF treatment can be a novel strategy for prevention of postsurgical adhesion formation.

References

- 1) Ellis, H. The clinical significance of adhesions: focus on intestinal obstruction. *Eur J Surg Suppl*, 5-9 (1997).
- 2) Ellis, H. *et al.* Adhesion-related hospital readmissions after abdominal and pelvic surgery: a retrospective cohort study. *Lancet* **353**, 1476-1480 (1999).
- 3) Ghellai, A. M. *et al.* Role of transforming growth factor beta-1 in peritonitis-induced adhesions. *J Gastrointest Surg* **4**, 316-323 (2000).
- 4) Chung, D. R. *et al.* CD4⁺ T cells regulate surgical and postinfectious adhesion formation. *J Exp Med* **195**, 1471-1478 (2002).
- 5) Kosaka, H. *et al.* Interferon- γ is a therapeutic target molecule for prevention of postoperative adhesion formation. *Nature Med.* **14**, 437-41 (2008).

Life and death Signalings in fly photoreceptors

Akiko Kono Satoh

Graduate School of Science, Nagoya University
aksatoh@bio.nagoya-u.ac.jp

Keywords: Photoreceptor, Arrestin, Translocation

Introduction

Arrestin is a multi-functional protein first identified as terminating GPCR signaling, but now known to have several roles, including GPCR endocytosis and signaling via Src kinase, MAP kinase and other signaling pathways. There is also growing awareness that endocytic transport can play a direct role in signaling. Two kinds of visual arrestin in *Drosophila* photoreceptors have important roles for cell death and survival signaling via endocytosis. Identification of cell death and survival signaling pathway is not only great interest for cell biology, but also useful to the design of rational therapies for retinal disease. We first investigated these signaling pathways, but during researches, we got some interesting results to uncover the mechanism of Arrestin translocation, so we focused on the analysis and paper writing of this phenomenon, and currently this paper is in revision for a top journal, *Neuron*.

Upon illumination visual arrestin translocates from the photoreceptor cell body to rhodopsin and membrane-rich photosensory compartments - vertebrate outer segments or invertebrate rhabdomeres - where it quenches ongoing phototransduction. However, despite intensive study many aspects remain controversially debated, with two deeply conflicting models: translocation by motor and translocation by diffusion, dominating discussion. Further, whether signal transduction plays a role in translocation is contentious, whilst the functional significance is poorly understood.

Results

Our study, which combines genetics, in vivo imaging of GFP-tagged arrestin, electrophysiology and confocal immunohistochemistry, makes novel and definitive contributions in respect of all these controversially debated topics.

- 1) Our real-time in-vivo measurements of GFP-tagged arrestin set a new benchmark for the quantitation of translocation, providing unprecedented temporal resolution and by far the most accurate data on the relationship between translocation and rhodopsin isomerizations.
- 2) Translocation is remarkably rapid with forward and reverse time constants of ~ 7 and ~ 2 seconds respectively.
- 3) Our results support a diffusion model by showing that translocation is reversibly driven by stoichiometric binding to activated rhodopsin

- 4) We show that whilst not being absolutely required, phototransduction profoundly accelerates arrestin translocation, implicating a novel regulatory role for PLC-mediated Ca^{2+} influx. 5) We show that the time course of translocation is directly reflected in electrophysiological responses, and that following translocation, response termination is accelerated. To our knowledge these results represents the first direct functional correlates of arrestin translocation.
- 6) Finally our results essentially disprove the current model that NINAC, (myosin III), powers Arr2 transport (Lee et al., 2003; Lee and Montell, 2004; Strissel).

Discussion & Conclusion

Our results indicate that diffusion drives and phototransduction speeds Arr2 translocation in *Drosophila* photoreceptors. These results make major and definitive contributions to this important topic, which is one of the most intensively studied areas in photoreceptor biology.

References

- 1) Lee, S.J., and Montell, C. (2004). Light-dependent translocation of visual arrestin regulated by the NINAC myosin III. *Neuron* **43**, 95-103.
- 2) Lee, S.J., Xu, H., Kang, L.W., Amzel, L.M., and Montell, C. (2003). Light adaptation through phosphoinositide-regulated translocation of *Drosophila* visual arrestin. *Neuron* **39**, 121-132.
- 3) Strissel, K.J., Sokolov, M., Trieu, L.H., and Arshavsky, V.Y. (2006). Arrestin translocation is induced at a critical threshold of visual signaling and is superstoichiometric to bleached rhodopsin. *J. Neurosci.* **26**, 1146-1153.

Crosstalk between arginine methylation of BAD and its phosphorylation by Akt

Hiroaki Daitoku

Graduate School of Life and Environmental Sciences, University of Tsukuba
hiroakid@tara.tsukuba.ac.jp

Abstract

Arginine methylation of BAD counteracts its phosphorylation and inactivation by AKT.

Keywords: PRMT1, arginine methylation, AKT, phosphorylation, BAD, apoptosis

Introduction

The BCL-2 family members are critical regulators of the intrinsic apoptotic pathway. BAD, a BH3-only subfamily of the BCL-2 proteins, initiates apoptosis by inhibiting anti-apoptotic BCL-2 and BCL-X_L. BAD is negatively regulated by AKT-induced phosphorylation and following 14-3-3-mediated cytoplasmic sequestration. We previously reported that protein arginine methyltransferase PRMT1 methylates FOXO transcription factors at an RxR motif within an AKT consensus sequence (RxRxxS/T) and this methylation blocks AKT-dependent phosphorylation of FOXO (Ref).

Results

We focused on the notion that the potential methylation site for PRMT1, an RxR motif, overlaps the consensus AKT phosphorylation sequence (RxRxxS/T), which is broadly found in almost all AKT substrates. We, therefore, investigated whether PRMT1 also methylates and regulates another AKT substrate BAD as well as FOXO proteins. We found that PRMT1 bound to and methylated BAD protein at Arg94 and Arg96 within the AKT consensus sequence (Figure 1). Peptide phosphorylation assay showed that arginine methylation of BAD at Arg94 and Arg96 directly blocked AKT-

Fig. 1

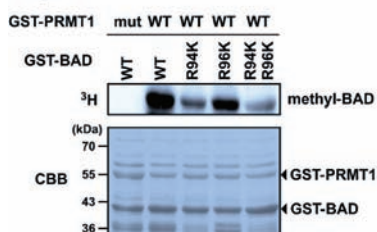
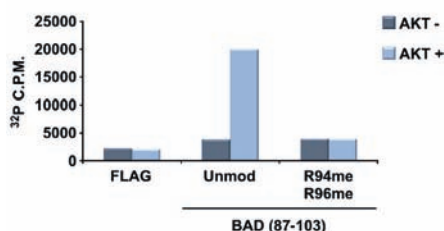


Fig. 2



mediated phosphorylation at Ser99 *in vitro* (Figure 2). Overexpression of PRMT1 decreased BAD phosphorylation and disrupted its interaction with 14-3-3 proteins (Figure 3A and B). Furthermore, knockdown of PRMT1 reduced the extent of BAD methylation, which in turn led to an increase in

Fig. 3

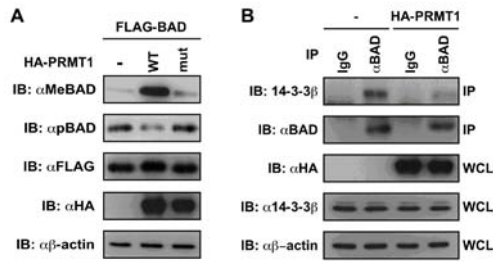
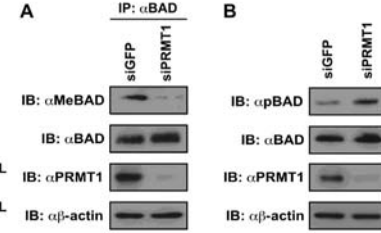


Fig. 4



its phosphorylation and subsequent binding of 14-3-3 (Figure 4 A and B). Consequently, silencing of PRMT1 enhanced dissociation of BAD from mitochondria. Finally, we found that BAD-induced apoptosis was abrogated upon depletion of PRMT1.

Discussion & Conclusion

Our finding suggest that PRMT1-mediated arginine methylation of BAD directs cell fate towards apoptosis by counteracting AKT-mediated phosphorylation, and also proposed that the functional crosstalk between arginine methylation and phosphorylation could be expended to other AKT substrates, which regulates cell-cycle progression, glucose metabolism, and stress resistance.

References

- 1) Yamagata, K. *et al. Mol. Cell* **32**, 221-231 (2008)

Enantioselective synthesis of α -aminophosphonic acid by the process chemistry-oriented method

Kaori Ando
Gifu University
ando@gifu-u.ac.jp

Abstract

A new one-pot synthesis of α -aminophosphonates from aldehydes, amines, and triethyl phosphite using magnesium organosulfate catalysts was studied.

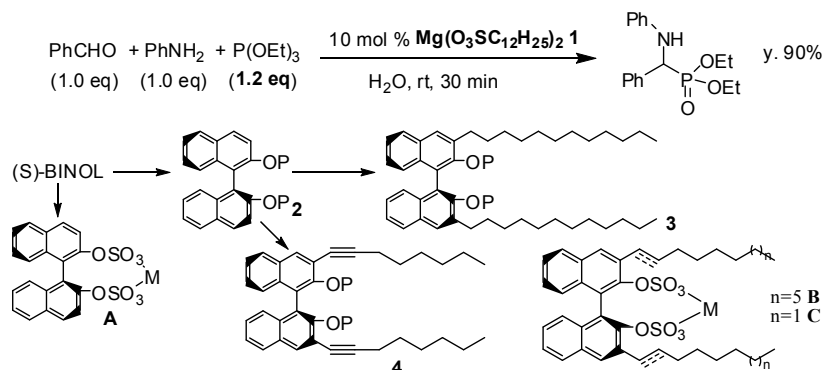
Keywords: α -aminophosphate, reaction in water, asymmetric catalyst

Introduction

Since α -aminophosphonate are considered to be structural analogues of the corresponding α -amino acids¹ and transition-state mimics of peptide hydrolysis,² the development of their efficient and practical synthesis is highly desirable. Use of aqueous media is very attractive because water is cheap and safe. In this work, we studied the one-pot synthesis of α -aminophosphonates from aldehydes, amines, and triethyl phosphite using magnesium organosulfate catalysts in water.

Results

The catalysts were prepared from the reaction of sodium dodecane sulfate with MgCl_2 , CaCl_2 , BaCl_2 , AlCl_3 , and CeCl_3 . When the one-pot synthesis of α -aminophosphonates from aldehydes, amines, and $\text{P}(\text{OEt})_3$ using 0.1 equiv of these catalysts in water was performed, the magnesium dodecane sulfate **1** gave the highest yields. Although the same reaction catalyzed by $\text{Sc}(\text{O}_3\text{SOC}_{12}\text{H}_{25})_3$ required 4 equiv of $\text{P}(\text{OEt})_3$,³ the reaction using only 1.2 to 1.5 equiv of $\text{P}(\text{OEt})_3$ gave high yields for the reaction of several types aromatic aldehydes and aromatic amines. For the reaction of aliphatic aldehydes and/or aliphatic amines, using 1.5 equiv of $(\text{PhO})_2\text{P}(\text{O})\text{H}$, catalyst **1**, and 0.1 equiv of Et_3N gave good yields of α -aminophosphonates. After establishing the reaction condition, we started the preparation of chiral catalysts for the asymmetric version of the above one-pot synthesis of α -aminophosphonates. First, the catalyst **A** was prepared from (S)-1,1'-Bi-2-naphthol. Since the catalyst **A** has only low catalytic activity and the reaction gave only low stereoselectivity, we decided to prepare a new catalyst having a long alkyl chain. Thus, (S)-1,1'-Bi-2-naphthol was first protected with Me or MOM group. These compounds **2** were treated with 3 equiv of n-BuLi in the presence of TMEDA in ether to generate the dilithiated compound. The alkylation with dodecyl iodide was slow and gave mainly mono alkylated compound together with a low yield of **3**. Since the reactivity of dodecyl iodide was low, we changed our synthetic plan. The Me protected **2** was treated with 3 equiv of n-BuLi in the same way to generate the dilithiated compound, which reacted with Bromine or iodine to afford the dibromide or the diiodide. Unfortunately, the dibromide with 1-octyne in the presence of $\text{PdCl}_2(\text{PPh}_3)_2$ did not



reacted. However, the iodide gave **4** in the above reaction condition in a moderate yield. We are now trying to prepare the catalyst **C**.

Discussion & Conclusion

In summary, we established the reaction condition for the one-pot synthesis of α -aminophosphonates from aldehydes, amines, and triethyl phosphite using magnesium organosulfate catalysts. We also tried to do the asymmetric version of the above reaction using the catalyst **A** derived from (S)-1,1'-Bi-2-naphthol. However, the yield was about 50% and the stereoselectivity was low. Therefore, we started to prepare new chiral catalysts **B** and **C**. Right now, the compounds **3** and **4** were in hand and we are planning to prepare the catalyst **B** and **C**. The asymmetric one-pot reaction of aldehydes, amines, and triethyl phosphite using these catalysts will be tried soon.

References

- 1) Allen, M. C.; Fuhrer, W.; Tuck, B.; Wade, R.; Wood, J. M. *J. Med. Chem.* 1989, **32**, 1652.
- 2) Hirshmann, R.; Smith, A. B. III; Taylor, C. M.; Benkovic, P. A.; Taylor, S. D.; Yager, K. M.; Sprengler, P. A.; Venkovic, S. J. *Science* 1994, **265**, 234.
- 3) Manabe, K.; Kobayashi, S. *Chem. Commun.* 2000, 669.

Impact of GILC1 downregulation on the generation and progression of lung cancer

Motoshi Suzuki

Nagoya University Graduate School of Medicine, Molecular Carcinogenesis
msuzuki@med.nagoya-u.ac.jp

Abstract

We studied the relationship between genomic instability and causative genes. Three genes were focused, GILC1, PSMD2, and POLA1.

Keywords: DNA damage, genomic instability, lung cancer

Introduction

Lung cancer has become the leading cause of cancer death in many industrialized countries, due to its highly proliferative and metastatic potential, as well as frequent recurrence after chemotherapy.

In lung cancer, it is conceivable that smoking plays a major role in induction of DNA damage that may be detected by checkpoint responses, though the intrinsic driving force behind this related genomic erosion has yet to be identified. In the current studies, we have analyzed the relationship between genomic instability and putative driving genes. We also focused on DNA replication and DNA repair pathways because initiation of carcinogenesis requires DNA replication.

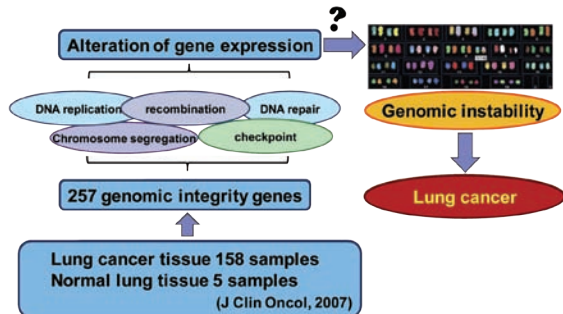
Results

Genomic instability is thought to contribute to the pathogenesis of lung cancer. To elucidate the underlying mechanisms, we screened for genes involved in DNA metabolism that had altered expressions using our previous profiling data set consisting of 149 cases of NSCLC, 9 cases of SCLC, and 5 normal lung mixture specimens.

- 1) We found that GILC1 expression was distinctly reduced in an SCLC-specific manner. GILC1 overexpression reduced the intensity of gammaH2AX. GILC1 reduction also induced checkpoint activation as well as chromosome aberrations.
- 2) PSMD2 has been screened from the same cohort. We found that patients with higher PSMD2 expression had poorer prognosis and a small fraction of lung cancer specimens carried increased copies of PSMD2. Consistently, knockdown of PSMD2 decreased proteasome activity, and induced growth inhibition and apoptosis in lung cancer cell lines.
- 3) Recent studies have revealed that the base selection step of DNA polymerases (pol) plays a role in prevention of DNA replication errors. We investigated whether base selection is required for the DNA replication fidelity of pol alpha and genomic stability in human cells. We introduced a Leu864 to Phe substitution (L864F) into human pol alpha (POLA1) and performed an in vitro forward mutation assay. Our results showed that the overall mutation rate was increased by 180-

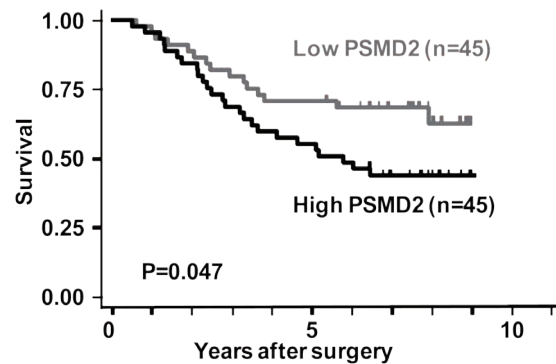
fold as compared to that of the wild type. Using the HPRT gene as a reporter, the spontaneous mutation rate of pola1L864F cells was determined to be 2.4-fold greater than that of wild-type cells.

Discussion & Conclusion



- 1) Regulation of genomic integrity by cell cycle and DNA transaction genes
- 2) Our results suggest that PSMD2 may be a good molecular target candidate and that other co-regulated proteasome pathway genes and/or their common regulator(s) might also be potential targets.

1) Our data imply that GILC1 downregulation may play a role in lung cancer pathology.



2) High PSMD2 expression was correlated to poor prognosis in lung cancer patients.



3) Base selectivity of DNA polymerase alpha is required for genomic integrity.

3) Our results indicate that the base selection step in human pol alpha functions to prevent DNA replication errors and maintain genomic integrity in HCT116.

References

- 1) submitted
- 2) Matsuyama Y, Suzuki M, Arima C, Huang QM, Tomida S, Takeuchi T, Sugiyama R, Itoh Y, Yatabe Y, Goto H, Takahashi T. Proteasomal Noncatalytic Subunit PSMD2 as a Potential Therapeutic Target in Association With Various Clinicopathologic Features in Lung Adenocarcinomas. *Mol Carcinogen*, in press
- 3) Tanaka S, Cao K, Niimi A, Limsirichaikul S, Miao HQ, Nakamura N, Murate T, Hasegawa Y, Takahashi T, Suzuki M. Functions of base selection step in human DNA polymerase alpha. *DNA Repair (Amst)*. in press

Molecular basis for regulation of glucosinolate biosynthesis: Cancer preventive sulfur-containing compounds

Akiko Maruyama-Nakashita
Fukui Prefectural University Faculty of Bioscience
amaru@agr.kyushu-u.ac.jp

Abstract

Glucosinolates are known as the beneficial compounds for human health with the anticarcinogenic, antioxidative, and antimicrobial activities. Among the many glucosinolate moieties, methionine-derived aliphatic glucosinolates are known as the cancer-preventing compounds. Many enzymes involved in glucosinolate biosynthesis have been isolated, however, the regulatory mechanism of glucosinolate metabolism is poorly understood. On the other hand, glucosinolate metabolism is greatly influenced by sulfur nutrition. Plants activate sulfate acquisition and degradation of glucosinolates under sulfur deficient (–S) condition. Under –S condition, SLIM1 transcription factor controls gene expression and metabolic changes in sulfate acquisition but also the repressions of glucosinolates synthetic genes. These observations suggested the existence of repression factors of glucosinolate biosynthesis downstream of SLIM1. In this study, we took the reverse genetic approach focusing on functionally unidentified proteins controlled by SLIM1, in order to identify the repression factor of aliphatic glucosinolate biosynthesis.

Keywords: Glucosinolate, Repressor, Sulfur, Arabidopsis

Introduction

Glucosinolates, one of the sulfur-containing secondary compounds mainly produced in Brassica plants, are known as the anticarcinogenic, antioxidative, and antimicrobial compounds (1-3). Glucosinolates are classified by their precursor amino acids and the types of modification of the side chain. The precursor amino acids Phe, Tyr and Trp are synthesized into aromatic glucosinolates, and Met is synthesized into aliphatic glucosinolates. Among these, aliphatic glucosinolates are known as the cancer-preventing compounds (3). Because of the useful activities of glucosinolates, the synthetic pathway has been extensively studied and many enzymes involved in glucosinolates biosynthesis were identified (1, 2). However, the regulatory mechanism of glucosinolates metabolism is poorly understood.

On the other hand, glucosinolates metabolism is greatly influenced by sulfur nutrition (4-6). Plants activate sulfate acquisition and degradation of glucosinolates under sulfur deficient (–S) condition. We previously identified the SLIM1 transcription factor, which controlled gene expression and metabolic changes in response to –S condition (7). The repression of glucosinolate synthetic genes under –S condition was observed in wild type plants, however, which was diminished in *slim1* mutant. This

result suggested the existence of repression factors of glucosinolate biosynthesis downstream of SLIM1, which is activated in response to –S condition.

In this study, we took the reverse genetic approach to reveal the function of unknown genes regulated by –S and SLIM1. Gene expression and metabolites analysis of the knockout and overexpressed plants will identify the novel repression factor of aliphatic glucosinolate biosynthesis in *Arabidopsis thaliana*.

Results

From the data of microarray analysis comparing wild type plants and *slim1* mutant grown under sulfur sufficient (+S) and deficient (–S) condition (7), we selected candidate genes that were upregulated by –S condition and regulated by SLIM1. Among them, there were 3 unknown genes named X, Y, Z. Then we isolated their T-DNA knockout mutants.

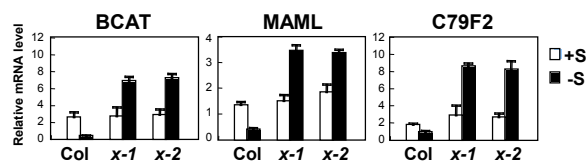
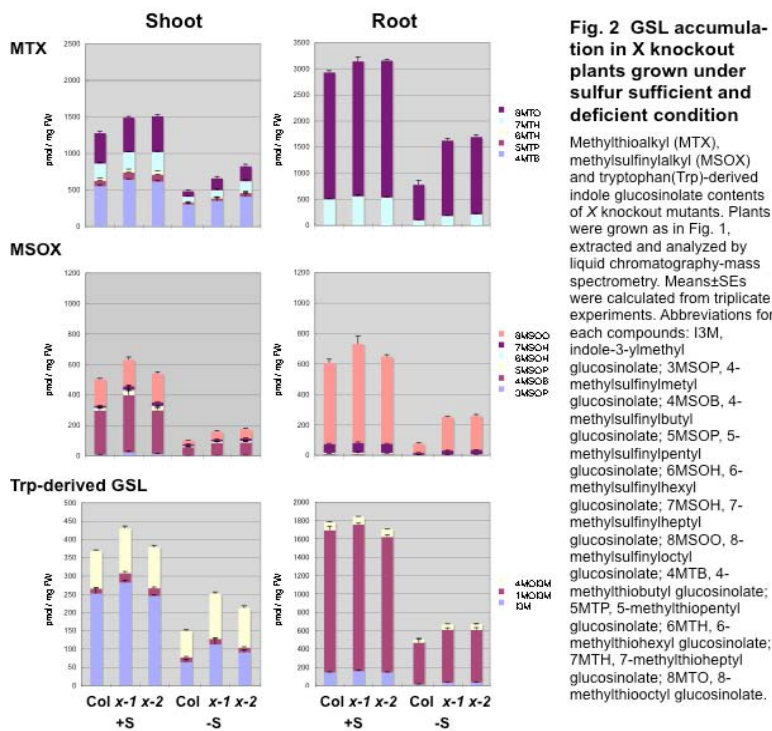


Fig. 1 Expression of mGSL synthetic genes in X knockout plants
Plants were grown for 10 days under –S (15 μ M sulfate) or +S (1500 μ M sulfate) conditions. Real-time RT-PCR was carried out using SYBR Green Perfect Real Time kit (Takara) and GeneAmp 5700 Sequence Detection System (Applied Biosystems). The mRNA contents were calculated using ubiquitin as an internal standard. Expression of branched-chain amino acid aminotransferase (BCAT), Methyl(thio)alkylmalate synthase (MAML) and cytochrome P450 CYP79F2 (C79F2) were analyzed using their gene-specific primers (7).



Transcript levels of –S and SLIM1 regulated genes in these mutants were analyzed by real-time RT-PCR. The –S-upregulated genes, *SULTR1;2*, *SULTR4;2*, *Thioglucosidase*, were not significantly changed in all knockout mutants compared to wild type plants (Col). Surprisingly, the –S-downregulated glucosinolates synthetic genes, branched-chain amino acid aminotransferase (BCAT), methyl(thio)alkylmalate synthases (MAM1 and MAML) and cytochrome P450 CYP79F2 (CYP79F2), were upregulated by –S in 2 knockout lines of X, X-1 and X-2 (Fig. 1). To define whether

the depletion of X affects glucosinolate accumulation, we analyzed the glucosinolate levels in Col, *X-1* and *X-2* grown under +S and –S conditions, by using liquid chromatography-mass spectrometry (Fig. 2). Both under +S and –S conditions, glucosinolate levels were increased in knockout lines of X compared to Col, and the levels were more strongly increased under –S condition than +S condition in the mutants. These results strongly suggested that X functioned as a repression factor of glucosinolate biosynthesis.

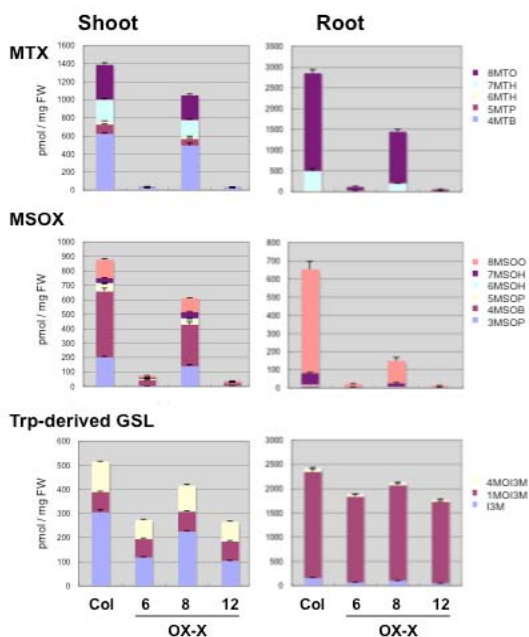


Fig. 4 GSL accumulation in X over-expressing plants. MTX, MSOX and Trp-derived glucosinolate contents of X over-expressing plants. Plants were grown as in Fig. 3, extracted and analyzed by liquid chromatography-mass spectrometry. Means±SEs were calculated from triplicate experiments. Abbreviations for each compounds were described in Fig.3.

regulated by –S and SLIM1. As there is no obvious domain or motif in X, the function had been completely unknown. The results obtained in this study indicate that SLIM1 induces the transcription of X under –S condition and X represses the glucosinolate biosynthesis through the downstream signal transduction pathway. Recently, PMG1 and PMG2 were reported as the transcription factors which positively regulate glucosinolate biosynthesis in *Arabidopsis thaliana* (8). As the transcript levels of *PMG1* and *PMG2* were higher in *slim1* mutant than wild type plants, X should function in transcriptional repression of these transcription factors. The mechanism of how X represses the transcription remains as the problem to be solved.

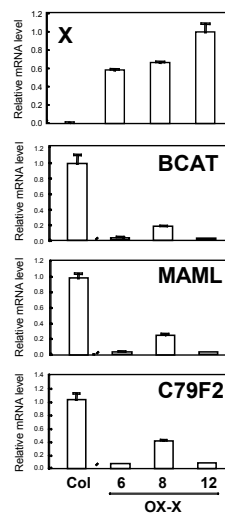


Fig. 3 Expression of X and mGSL synthetic genes in X over-expressing plants

Plants were grown for 10 days under +S (1500 μM sulfate) condition. Real-time RT-PCR was carried out as described in Fig. 1.

To further confirm repression activity of X, we generated X over-expressing plants. As expected from the results obtained by X knockout plants, transcript levels of glucosinolate synthetic genes were substantially lowered by overexpression of X (Fig. 3). Glucosinolate levels were lowered in these lines correlatively with the expressions of glucosinolates synthetic genes (Fig. 4). Overexpression of X influenced more strongly on Met-derived glucosinolates levels rather than the Trp-derived glucosinolates.

Discussion & Conclusion

In this study, we discovered the repression factor X of aliphatic glucosinolate biosynthesis by the reverse genetic approach searching for unknown genes

References

- 1) Grubb C. and Abel S. (2006) Glucosinolate metabolism and its control. *Trends Plant Sci.* **11**, 89-100.
- 2) Halkier B.A. and Gershenzon J. (2006) Biology and biochemistry of glucosinolates. *Annu. Rev. Plant Biol.* **57**, 303-333.
- 3) Talalay P. and Fahey J.W. (2001) Phytochemicals from cruciferous plants protect against cancer by modulating carcinogen metabolism. *J. Nutr.* **131**, 3027S–3033S.
- 4) Hirai M.Y., Yano M., Goodenowe D.B., Kanaya S., Kimura T., Awazuhara M., Arita M., Fujiwara T. and Saito K. (2004) Integration of transcriptomics and metabolomics for understanding of global responses to nutritional stresses in *Arabidopsis thaliana*. *Proc. Natl. Acad. Sci. USA.* **101**, 10205-10210.
- 5) Maruyama-Nakashita A., Inoue E., Watanabe-Takahashi A., Yamaya T. and Takahashi H. (2003) Transcriptome profiling of sulfur-responsive genes in *Arabidopsis* reveals global effect on sulfur nutrition on multiple metabolic pathways. *Plant Physiol.* **132**, 597-605.
- 6) Nikiforova V., Freitag J., Kempa S., Adamik M., Hesse H. and Hoefgen R. (2003) Transcriptome analysis of sulfur depletion in *Arabidopsis thaliana*: interlacing of biosynthetic pathways provides response specificity. *Plant J.* **33**, 633-650.
- 7) Maruyama-Nakashita A., Nakamura Y., Tohge T., Saito K. and Takahashi H. (2006) Central transcriptional regulator of plant sulfur response and metabolism. *The Plant Cell* **18**, 3235-3251.
- 8) Hirai M.Y., Sugiyama K., Sawada Y., Tohge T., Obayashi T., Suzuki A., Araki R., Sakurai N., Suzuki H., Aoki K., Goda H., Nishizawa O.I., Shibata D. and Saito K. (2007) Onics-based identification of *Arabidopsis* Myb transcription factors regulating aliphatic glucosinolate biosynthesis. *Proc. Natl. Acad. Sci. USA.* **104**, 6478-6483.

Synthetic Study and Structural Study of Super-carbon-chain Compounds Produced by the Marine Plankton

Hiroyoshi Takamura

Division of Chemistry and Biochemistry,
Graduate School of Natural Science and Technology, Okayama University
takamura@cc.okayama-u.ac.jp

Abstract

We have synthesized the C14—C24, C23—C34, C33—C42, C79—C96, and C1'—C25' fragments of symbiodinolide including the various stereoisomers. These stereoselective syntheses have established the absolute configuration of each fragment of symbiodinolide.

Keywords: Natural Product, Organic Synthesis, Structural Determination

Introduction

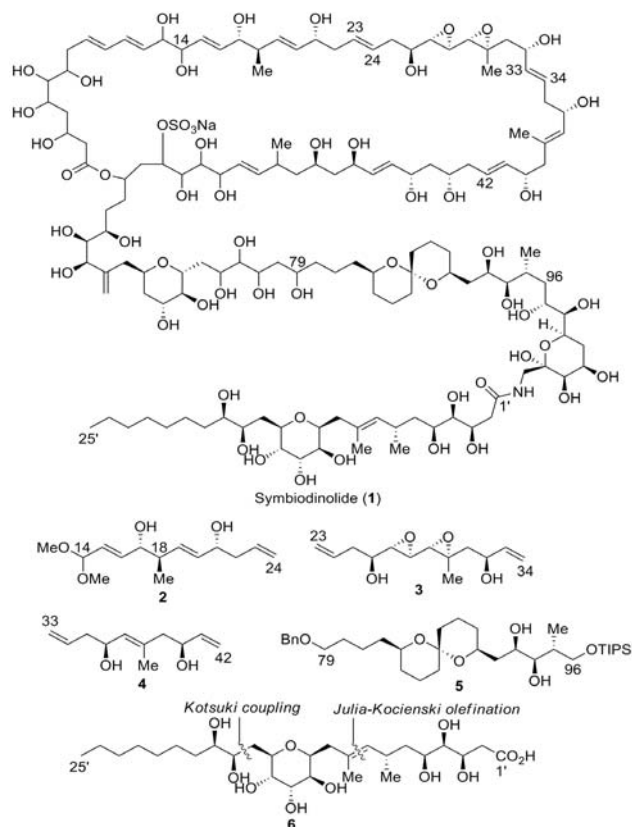
Symbiodinolide (**1**), a novel super-carbon-chain compound, has been isolated from the marine dinoflagellate *Symbiodinium* sp., which exhibits a Ca²⁺ channel-opening activity and COX-1 inhibitory effect.¹ The planar structure and partial stereochemistry of **1** were elucidated by spectroscopic analysis. In this report, we will describe our synthetic efforts on symbiodinolide aiming at the complete structural determination of this molecule.

Results

With regard to the C14—C24 fragment, the diol **2** with the 18*R* chiral center and the 18*S* isomer were synthesized, respectively. The spectroscopic data of the synthetic **2** were identical to those of the degraded C14—C24 fragment obtained from **1**, which has confirmed that the absolute configuration of this fragment is that shown in **2**.² All four possible stereoisomers on the diepoxide moiety of the C23—C34 fragment were synthesized, which has concluded that the absolute configuration of this fragment is that described in **3**.³ The C33—C42 fragment *syn* diol **4** and the *anti* diol which was the diastereomer of **4** were synthesized, which has resulted in the structural determination of this fragment.⁴ The C79—C96 fragment **5** was synthesized via the acid-catalyzed spiroacetalization as a key step.⁵ The synthesis of the C1'—C25' fragment **6** was achieved via Kotsuki coupling and Julia-Kocienski olefination in the introduction of the side chains, which has established the absolute configuration of this fragment.⁶

Discussion & Conclusion

In conclusion, the C14—C24, C23—C34, C33—C42, C79—C96, and C1'—C25' fragments of symbiodinolide have been synthesized, respectively. Comparison of spectroscopic data of the synthetic products with those of the degraded product of symbiodinolide has resulted in the structural elucidation of each fragment.



References

- 1) Kita, M.; Ohishi, N.; Konishi, K.; Kondo, M.; Koyama, T.; Kitamura, M.; Yamada, K.; Uemura, D. *Tetrahedron* 2007, **63**, 6241.
- 2) Takamura, H.; Kadonaga, Y.; Kadota, I.; Uemura, D. *Tetrahedron Lett.* 2010, **51**, 2603.
- 3) Murata, T.; Sano, M.; Takamura, H.; Kadota, I.; Uemura, D. *J. Org. Chem.* 2009, **74**, 4797.
- 4) (a) Takamura, H.; Kadonaga, Y.; Yamano, Y.; Han, C.; Aoyama, Y.; Kadota, I.; Uemura, D. *Tetrahedron Lett.* **2009**, *50*, 863. (b) Takamura, H.; Kadonaga, Y.; Yamano, Y.; Han, C.; Kadota, I.; Uemura, D. *Tetrahedron* 2009, **65**, 7449.
- 5) Takamura, H.; Ando, J.; Abe, T.; Murata, T.; Kadota, I.; Uemura, D. *Tetrahedron Lett.* **2008**, *49*, 4626.
- 6) Takamura, H.; Murata, T.; Asai, T.; Kadota, I.; Uemura, D. *J. Org. Chem.* 2009, **74**, 6658.

Live-imaging studies on the biogenesis of thylakoid membranes in plastids

Wataru Sakamoto

Institute of Plant Science and Resources, Okayama University
saka@rib.okayama-u.ac.jp

Abstract

Chloroplasts in higher plants derive from color-less proplastids in shoot meristems and perform photosynthesis, which is one of the most important biological functions on the earth to sustain our atmospheric environment. To understand chloroplast biogenesis, particularly the early events leading to thylakoid formation, we performed ultrastructural and live-imaging analysis of plastids in model plant *Arabidopsis thaliana*.

Keywords: Chloroplast, *Arabidopsis thaliana*, thylakoid formation, Live-imaging

Introduction

The thylakoid network is central and essential to photosynthesis. Thus, structure-function aspects of the photosynthetic machinery have been studied extensively over decades (1). Our understanding of processes involved in gene expression and chloroplast biogenesis has also been greatly progressed in recent years. In sharp contrast, our understanding of the processes involved in the initial stages of thylakoid formation is very limited. Thylakoids are believed to derive from budding of inner envelope vesicles, but nothing is known about this process at the molecular level. It is well established that cells in the shoot apical meristem (SAM) contain proplastids, devoid almost totally of internal membrane structures, whereas cells in advanced leaf primordia contain cells with fully developed thylakoids. In this study, we attempted to characterize the initial steps leading to the formation of the fully developed thylakoid network mainly using by live-imaging analysis.

Results

We carried out two independent experiments to examine how thylakoid membranes are formed during chloroplast biogenesis.

1) Electron microscopic observation of aberrant plastids in variegated leaf sectors of *Arabidopsis var2* mutant

Our previous study demonstrated that cells in the variegated sectors of *var2* leaves contain abnormal plastids that perhaps result from arrested chloroplast development (2, 3). These plastids contain remarkable globular vacuolated membrane structures (termed PVB, Figure 1). PVB was

characterized in detail by transmission electron microscopy to test if it represents intermediates of thylakoid formation (4). To do so, we observed first true leaves at various developmental stages and the results showed that PVBs are rarely detectable at the early stage of variegation formation. Instead, abnormal plastids in white sectors contain prolamellar body-like structures (PLBs) that are frequently seen in etioplasts (Figure 2). These results suggested that unlike our initial assumption, PVBs detected in plastids of white sectors derive from PLB and not from inner envelope (4).

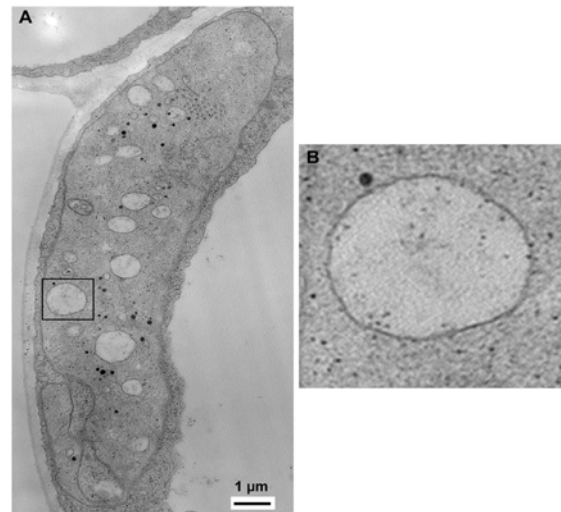


Figure 1 (A) Electron micrograph of a plastid in 30-day-old *var2* mature leaves. A PVB squared in (A) is enlarged and shown in (B).

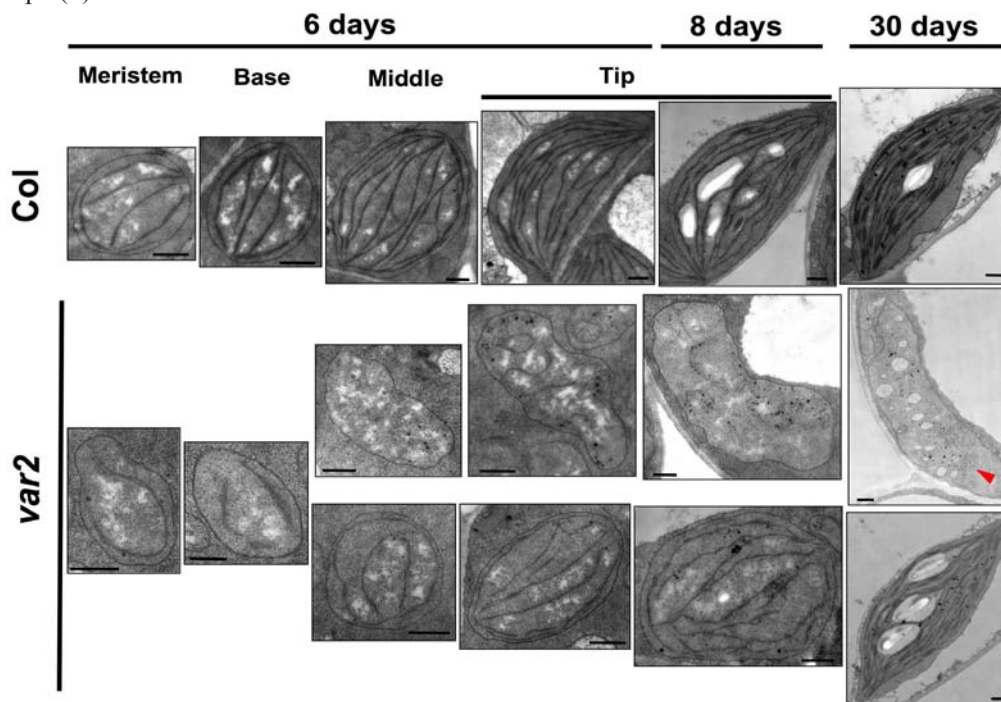


Figure 2 Summarized plastid ultrastructures during leaf development in Col and *var2* leaves. Representative images of plastids in 6-day-old (meristem, base, middle, tip parts of FTL) and 8-day-old (tip part of FTL) plants are shown. In *var2*, two types of plastids representing abnormal plastids and chloroplasts that likely form green sectors afterwards (after 6 days, middle part) are indicated as separate rows.

2) Live-imaging analysis of chloroplasts using green fluorescent protein and Vipp1

We attempted to visualize chloroplasts and thylakoid formation via inner envelope, using green fluorescent protein (GFP) as a reporter for our live-imaging analysis. Vipp1 has been reported to be located in inner envelope and play a role in thylakoid formation (5, 6). Therefore, we generated a transgenic *Arabidopsis* plant in which Vipp1-GFP fusion protein was over-expressed. Our live-imaging analysis demonstrated that Vipp1-GFP forms a large complex as previously

suggested (Figure 3). However, Vipp1-GFP appeared to be located outside of outer envelope. More interestingly, we frequently observed the GFP signals moving along the side of chloroplasts, perhaps representing Brownian motion. Although our data showed that Vipp1-GFP is not an appropriate reporter to visualize inner envelope and the initial stage of thylakoid formation, we instead raised a possibility that the function of Vipp1 in chloroplasts is ill-defined.

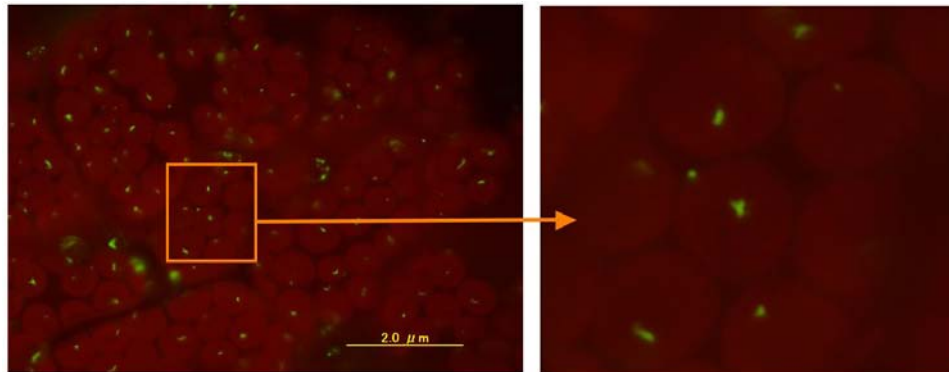


Figure 3 Live-imaging analysis of Vipp1 visualized by Vipp1-GFP. Mesophylls of an Arabidopsis transgenic plant that expresses Vipp1-GFP was observed under fluorescence microscopy with B-excitation filter set. Red colors represent chloroplasts (due to chlorophyll autofluorescence) and green dots represent Vipp1-GFP signals.

Discussion & Conclusion

We originally hypothesized that PVB detected in *var2* mature leaves derive directly from inner envelope. Live-imaging analysis of PVB using the reporter such as Vipp1-GFP was supposed to allow us to observe the formation of thylakoids. However, our electron microscopic observation showed that PVBs derive from PLB, that is characteristic to etiolated tissues. Membrane structures like PLB are often seen in a mutant defective in chloroplast development. Although our data demonstrate arrested plastid development in *var2* white sectors, initial event of thylakoid formation from inner envelope was hardly detectable by using these materials. Nevertheless, we are in the process of generating *var2* plants expressing Vipp1-GFP, and it will be a good material to further study thylakoid development.

Our results obtained from Vipp1-GFP unexpectedly showed that Vipp1 is located outside chloroplast. Further study on the localization of Vipp1-GFP is in progress (trypsin and thermolysin digest of purified chloroplasts) and suggests that Vipp1 forms a large complex at the outside of outer envelope and the inter-membrane space of inner and outer envelopes. It also suggests that a majority of Vipp1-GFP are in the cytosol. Because we used CaMV 35S promoter to overexpress Vipp1-GFP, the possibility remains that the observed GFP signals do not represent native GFP location. To address this possibility, we generated transgenic plants expressing Vipp1-GFP under *Vipp1* own promoter. We also introduced Vipp1-GFP into *vipp1* mutant, to examine if Vipp1-GFP overexpression rescues the *vipp1* mutant phenotype. These experiments are underway and will reveal the novel function of Vipp1 protein in chloroplast development.

Part of the results obtained from this project have been published as an original article (4) and presented in the annual meeting of Japan Society of Plant Physiologists (March 21, 2010, Kumamoto).

References

- 1) Sakamoto, W., Miyagishima, S., and Jarvis, P. (2008) Chloroplast biogenesis: Plastid division, inheritance, regulation, protein import and proteome. The Arabidopsis Book, <http://www.aspb.org/publications/arabidopsis/>.
- 2) Takechi, K., Sodmergen, Murata, M., Motoyoshi, F., and Sakamoto, W. (2000) The *YELLOW VARIEGATED (VAR2)* locus encodes a homologue of FtsH, an ATP-dependent protease in Arabidopsis. *Plant and Cell Physiol.*, **41**: 1334-1346.
- 3) 坂本 亘 (2002) ミトコンドリアと葉緑体の制御機構—斑入り突然変異と原因遺伝子の解析から—。蛋白質核酸酵素. **47** (8): 1115-1120 .
- 4) Sakamoto, W., Uno, Y., Zhang, Q., Miura, E., Kato, Y., and Sodmergen (2009) Arrested differentiation of proplastids into chloroplasts in variegated leaves characterized by plastid ultrastructure and nucleoid morphologies. *Plant Cell Physiol.*, **50**: 2069-2083.
- 5) Kroll, D., Meierhoff, K., Bechtold, N., Kinoshita, M., Westphal, S., and Vothknecht, U. (2000) *VIPPI*, a nuclear gene of *Arabidopsis thaliana* essential for thylakoid membrane formation. *Proc. Natl. Acad. Sci. USA*, **98**: 4238-4242.
- 6) Aseeva, E., Ossenbuhl, F., Eichancker, L.A., Wanner, G., Soll, J., and Vothknecht, U. (2004) Complex formation of Vipp1 depends on its alpha-helical PspA-like domain. *J. Biol. Chem.* **279**: 35535-35541.

Roles of GABAergic local circuits in the amygdala for emotional memory

Hideki Miwa

Gunma University Graduate School of Medicine

hmiwa@med.gunma-u.ac.jp

Abstract

Characterization of GABAergic neurons in the amygdala was performed, using VGAT-Venus transgenic mice.

Keywords: Emotion/Amygdala/GABAergic neuron

Introduction

The amygdala performs a primary role in emotional behavior and learning. GABAergic neurotransmission in the amygdala is thought to be important for expression and memory of emotion, and associated with psychiatric disorder, including anxiety disorder. In contrast to glutamatergic neurons, GABAergic neurons are morphologically, connectionally, electrically and chemically heterogeneous. However, little is known how each subclass of GABAergic neurons serves its functions for amygdala circuits.

Results

1. Immunohistochemical characterization of calcium-binding protein (parvalbumin, calretinin, and calbindin-D28k)-containing GABAergic neurons in the amygdala was performed, using vesicular GABA transporter (VGAT)-Venus transgenic mice, in which GABAergic neurons are labeled with Venus fluorescent protein. As a result, 90 of 333 (27%) of parvalbumin-positive, 146 of 318 (45%) of calbindin-positive, and 69 of 339 (20%) of calretinin-positive were Venus-positive in the lateral nucleus of the amygdala.
2. To investigate the physiological functions of parvalbumin (PV)-positive GABAergic neurons in the amygdala, we generated PV positive neuron-selective VGAT knockout mice in which Cre recombinase was expressed under a parvalbumin promoter and a loxP-flanked VGAT was eliminated. These PV positive neuron-selective VGAT-knockout mice were born and were indistinguishable from control (VGAT flox/flox) mice. However, by postnatal day 10, the growth rate of the knockout mice had slowed significantly and showed motor deficits and were prone to apparent seizures, and all the mutants had died by the second week.

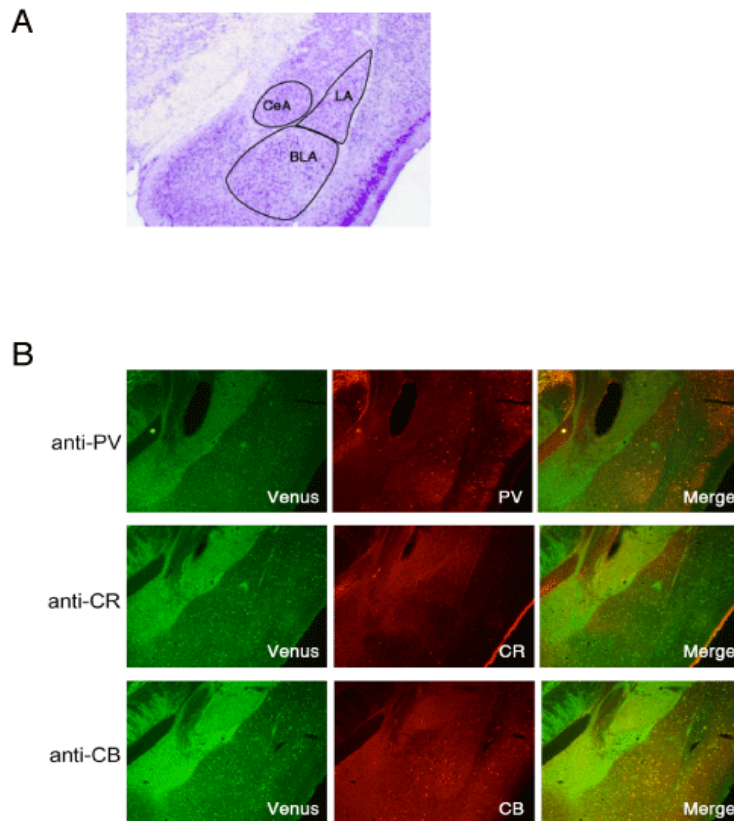


Fig. Immunohistochemical characterization of GABAergic neurons in the amygdala using VGAT-Venus transgenic mice. (A) Nissl-staining of the amygdala. LA, lateral nucleus; BLA, basolateral nucleus; CeA, central nucleus. (B) Immunohistochemical characterization of calcium-binding protein (parvalbumin, calretinin, and calbindin-D28k)-containing GABAergic neurons in the amygdala.

Discussion & Conclusion

1. Each subclass of calcium-binding protein containing GABAergic neurons in the amygdala might have unique properties for regulating amygdaloid functions.
2. PV-positive GABAergic neurons are critical for development of the CNS. I could not reveal roles of PV-positive GABAergic neurons in the amygdala because of the postnatal lethality of PV positive neuron-selective VGAT knockout mice, different approaches will be required.

Dissecting the mechanisms for inhibitory effects of ACE2 on aberrant activation of innate-immune system.

Keiji Kuba

Akita University Graduate School of Medicine

kuba@med.akita-u.ac.jp

Abstract

Newly emerging infectious respiratory diseases have threatened human beings in 21st century, such as severe acute respiratory syndrome (SARS), H5N1 influenza, and 2009 H1N1 influenza pandemic. In this project, to tackle acute respiratory distress syndrome (ARDS) caused by the severe respiratory infectious diseases, we investigated the role of ACE2 and renin-angiotensin system in activation of innate immune system. Our *in vivo* mouse ARDS model and *in vitro* cell culture experiments revealed the significance of hematopoietic cell renin-angiotensin system in aberrant innate-immune system in ARDS and acute lung injury. The results will be expanded to further dissect underlying molecular mechanisms and develop as potential therapeutic applications.

Keywords: ACE2, angiotensin, innate immune system

Introduction

A newly emerging infectious respiratory disease has threatened human beings in 21st century. In 2003, severe acute respiratory syndrome (SARS) spread rapidly from China throughout Asia to Canada. Most patients who died of SARS developed acute respiratory distress syndrome (ARDS)—the most severe form of acute lung injury (ALI). ARDS was also the cause of death in millions of people during the Spanish Influenza pandemic. Recently, swine H1N1 influenza and H5N1 avian influenza virus infections have spread through the world. Although latest swine flu pandemic was ceased, the reported death rates of H5N1 avian influenza infections in humans are ~50%, still prompting the fear that H5N1 might cause a worldwide pandemic. Certainly, vaccine development based on immunology is important to protect from those virus infections, but once infected with virus and developing respiratory diseases the patients cannot be treated with vaccines. The patients essentially need treatments in intensive care unit to control ARDS. We have recently elucidated ACE2 protects from ALI and is an essential SARS receptor. Based on our findings, we hypothesized ACE2 may negatively regulate innate-immune responses, and in this project we investigated whether and how renin-angiotensin system influences innate-immune system.

Results

We asked whether ACE2 gene deficiency affects the replication of influenza virus *in vivo*. When ACE2 knockout mice are infected with H1N1 influenza, the replication rates of virus were almost

the same as those in wild type mice. However, in ACE2 KO mice some of the cytokine productions were significantly increased, implicating enhanced Angiotensin II signaling in ACE2 KO mice may upregulate innate immune responses. Next we investigated the role of Angiotensin II type 1 (AT1) receptor in inflammatory cells *in vitro* by analyzing macrophages isolated from AT1 receptor knockout mice or wild type mice. Unexpectedly, AT1 receptor knockout macrophages showed reduced cytokine production upon stimulation with Toll-like receptor (TLR) ligands. In addition, when we treat human macrophage THP1 cell lines with AT1 receptor blocker, we observed similar reduction of cytokine responses to TLR ligand stimulation. To further dissect mechanisms, we analyzed NF- κ B signaling activation and found marked reduction of I κ B phosphorylation. Furthermore, AT1 receptor blocker was identified to activate Peroxisome proliferator-activated receptor- γ (PPAR γ), and PPAR γ antagonists, GW9662 and T0070907, reversed the inhibitory effects of AT1 receptor blocker on TLR ligands-induced cytokine productions.

Discussion & Conclusion

Although this needs to be further confirmed, the data suggest that enhancement of innate immune signaling in ACE2 KO mice involves the activation of AT1 receptor in macrophages. Controlling renin-angiotensin system in macrophages might be useful for treating ARDS in emerging lung infectious diseases.

References

- 1) An J, Nakajima T, Kuba K, Kimura A. Losartan inhibits LPS-induced inflammatory signaling through a PPAR γ -dependent mechanism in human THP-1 macrophages. *Hypertens Res.* 2010 May 27.
- 2) Neely GG, Kuba K, et al. A global *in vivo* Drosophila RNAi screen identifies NOT3 as a conserved regulator of heart function. *Cell.* **141**(1):142-153, 2010.
- 3) Haubner BJ, Neely GG, Voelkl JG, Damilano F, Kuba K, Imai Y, Komnenovic V, Mayr A, Pachinger O, Hirsch E, Penninger JM, Metzler B.: PI3K γ protects from myocardial ischemia and reperfusion injury through a kinase-independent pathway. *PLoS One.* **5**(2):e9350, 2010.
- 4) Imai Y, Kuba K, Ohto-Nakanishi T, Penninger JM.: Angiotensin-converting enzyme 2 (ACE2) in disease pathogenesis. *Circ J.* **74**(3):405-10, 2010.
- 5) Isobe K, Kuba K, Maejima Y, Suzuki J, Kubota S, Isobe M.: Inhibition of endostatin/collagen XVIII deteriorates left ventricular remodeling and heart failure in rat myocardial infarction model. *Circ J.* **74**(1):109-19, 2010.
- 6) Singer D, Camargo SM, Huggel K, Romeo E, Danilczyk U, Kuba K, Chesnov S, Caron MG, Penninger JM, Verrey F: Orphan Transporter SLC6A18 Is Renal Neutral Amino Acid Transporter B0AT3. *J Biol Chem.* 2009 Jul 24;**284**(30):19953-60.
- 7) Kishi Y, Kuba K, Nakamura T, Wen J, Suzuki Y, Mizuno S, Nukiwa T, Matsumoto K, Nakamura T.: Systemic NK4 gene therapy inhibits tumor growth and metastasis of melanoma and lung carcinoma in syngeneic mouse tumor models. *Cancer Sci.* 2009 Jul;**100**(7):1351-8.

- 8) Oudit GY, Imai Y, Kuba K, Scholey JW, Penninger JM: The role of ACE2 in pulmonary diseases--relevance for the nephrologist. *Nephrol Dial Transplant*. 2009 May;**24**(5):1362-5.
- 9) Camargo SM, Singer D, Makrides V, Huggel K, Pos KM, Wagner CA, Kuba K, Danilczyk U, Skovby F, Kleta R, Penninger JM, Verrey F: Tissue-specific amino acid transporter partners ACE2 and Collectrin differentially interact with Hartnup mutations. *Gastroenterology*. 2009 Mar;**136**(3):872-82.

Analysis of molecular function and dynamics of nuclear pore complex protein Rae1 and tumorigenesis

Richard W. Wong

Frontier Science Organization, Kanazawa University

rwong@staff.kanazawa-u.ac.jp

Abstract

Nuclear pore complexes are massive multiprotein channels responsible for traffic between the nucleus and cytoplasm, and are composed of approximately 30 proteins, termed nucleoporins (Nup). Our recent studies indicated that one of the nucleoporin Rae1 (RNA export factor 1) plays critical roles in maintaining the spindle bipolarity during cell division. In this study, we tried to generate Rae1 transgenic mice and Rae1 stable expressed tumor cell lines to analyze how Rae1 contributes tumorigenesis *in vivo* and *in vitro*.

Keywords: Nuclear pore complex, Rae1, tumorigenesis, aneuploidy

Introduction

The nuclear envelope forms a physical selective barrier between the nucleus and cytoplasm, and controls protein, RNA and ribonucleoprotein transportations in eukaryotic cells. Nucleocytoplasmic transport is exclusively mediated by nuclear pore complexes (NPCs), which are large proteinaceous channels that span the nuclear envelope. Vertebrate NPCs are composed of about 30 proteins, termed nucleoporins (Nups), which are present in multiple copies. Despite differences in the overall sizes in different species, the basic architecture of NPCs is well conserved among species. NPCs/Nups localization is very dynamics. In higher eukaryotes, NPCs are disassembled during cell division. We found that nucleoporins (Rae1 and Tpr) play critical roles in maintaining the spindle bipolarity during mitosis [1-3]. Recently, we found Nup88 plays a role in proper chromosome segregation [4,5]. On the other hand, during interphase, pore proteins or nucleoporins (designated Nup followed by their predicted molecular weight) are modular in that a limited number of structural motifs (coiled-coils, α -solenoids and β -propellers) are used repeatedly to build the symmetrical NPC channels on the nuclear membrane. Approximately one-third of nucleoporins contain a domain of phenylalanine-glycine (FG) motifs interspersed with spacer sequences. These repeat domains are natively unstructured and serve as interaction sites for transport receptors (karyopherins) that escort cargos through the pore.

In the past few years, several components of NPCs have been revealed to play important roles during mitosis. In particular, we demonstrated that a nucleoporin, RNA export factor 1 (Rae1), interacted with NuMA and cohesin subunit SMC1 during mitosis, and played crucial roles in proper spindle formation [1,2,7,8]. In this study, we tried to generate Rae1 transgenic mice and Rae1 stable expressed tumor cell lines to analyze how Rae1 contributes tumorigenesis *in vivo* and *in vitro*.

Results

Generation of GFP-Rae1 transgenic mice

We addressed the physiological role of Rae1 through transgenic mice approach. We constructed a plasmid which contained *GFP* (*green fluorescent protein*)-tagged human *Rae1* gene down-stream of CMV promoter. Mouse ES cells were transfected the plasmid and implanted into mother mice. Genotype analysis was performed by genomic PCR with GFP specific primer to confirm generation of GFP-Rae1 transgenic mice. Western blotting of gels loaded with equal amounts of screened mice main tissues. GFP-Rae1 was detected in testis dominantly (Fig. 1).

Analysis of GFP-Rae1 transgenic mice

GFP-Rae1 transgenic mice's tissues had been fixed in formalin, conventionally processed, and embedded in paraffin. The sections were stained with hematoxylin-eosin staining or immunostaining.

Establishment of DsRed-Rae1 stable expressed cell lines

To confirm the functional dynamics of Rae1 through cell cycle, we established DsRed-tagged Rae1 stable expressed cell lines. Human *Rae1* gene was subcloned into a DsRed vector. The plasmid was transfected into a breast cancer cell line MDA-MB-231 and selected with G418 medium. To identify DsRed-Rae1 stable expressed cells, we performed confocal microscopy analysis. An established cell line was stained with Red on the nuclear ring which localized on Rae1 (Fig. 2).

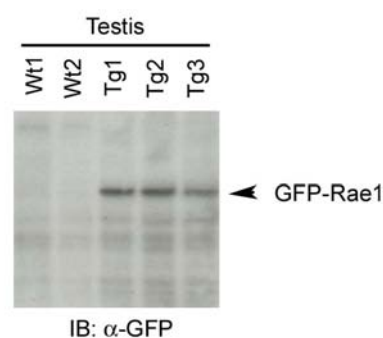


Figure 1

DsRed-Rae1 stable transtected- MDA-MB-231 cells

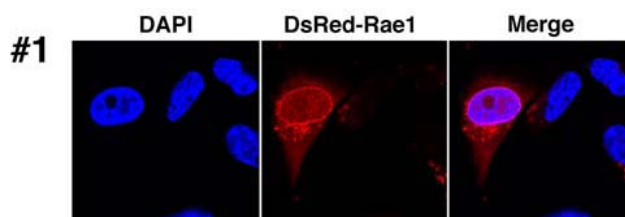


Figure 2

Discussion & Conclusion

Gain or loss of whole chromosomes is often observed in cell from cancer patients and is thought to be caused by aberrant chromosome segregation during mitosis. Errors in chromosome segregation are the main source of aneuploidy and a driving force in tumor development. We have demonstrated that alterations in the expression of Rae1 by modulating its concentration using RNAi and overexpression strategies enhanced multinucleated cells and multipolar spindle formation, leading to aneuploidy and

enhanced genomic instability [1-3]. In this study, we tried to analyze how Rae1 contributes tumorigenesis *in vivo* by generating Rae1 transgenic mice. We are analyzing Rae1 transgenic mice tissue sections. An established Rae1 stable expressed tumor cell line is performing immunoprecipitation assay to detect novel binding-partners of Rae1 *in vitro*. These detailed histochemical and biochemical characterization of the Rae1 function that will considerably advance our understanding of tumorigenesis relating Rae1 dynamics *in vivo*.

References

- 1) Wong RW. (2010) Interaction between Rae1 and Cohesin subunit SMC1 is required for proper spindle formation. *Cell Cycle*. **9**: 198-200. (IF 4.1)
- 2) Wong RW. (2010) An update on cohesin function as a “molecular glue” on chromosomes and spindles. *Cell Cycle*. (accepted). (IF 4.1)
- 3) Nakano H, Funasaka T, Hashizume C, Wong RW. (2010) Nucleoporin Tpr associates with dynein complex preventing chromosome lagging formation during mitosis. *J Biol Chem*. **285**(14): 10841-10849. (IF 5.5)
- 4) Hashizume C, Nakano H, Wong RW. (2010) Characterization of the role of the tumor marker Nup88 in mitosis. *Mol. Cancer*. (accepted). (IF 5.3)
- 5) Napetschnig J, Kassube SA, Debler EW, Wong RW, Blobel G, Hoelz A. (2009) Structural and functional analysis of the interaction between the nucleoporin Nup214 and the DEAD-box helicase Ddx19. *Proc Natl Acad Sci U S A*. **106**(9):3089-94.
- 6) Wong RW, Blobel G (2008) Cohesin subunit SMC1 associates with mitotic microtubules at the spindle pole. *Proc. Natl. Acad. Sci. USA* **105**(40):15441-15445.
- 7) Wong, RW, Blobel G, Coutavas E (2006) Rae1 interaction with NuMA is required for bipolar spindle formation *Proc Natl Acad Sci U S A*. **103**(52): 19783-19787.

Analysis of HNF transcription network in pancreatic β -cells

Kazuya Yamagata

Department of Medical Biochemistry, Faculty of Life Sciences, Kumamoto University

k-yamaga@kumamoto-u.ac.jp

Abstract

Mutations in the genes encoding hepatocyte nuclear factor (HNF)-1 α , and HNF-4 α cause maturity onset diabetes of the young (MODY) that is characterized by impairment of glucose-stimulated insulin secretion by pancreatic β -cells. To gain insights into the molecular mechanism of HNF diabetes, we compared gene expression patterns in pancreatic islets between control and β -cell specific HNF-4 α KO mice. We found about 300 down-regulated genes in KO islets. By scanning the mouse genome for HNF4 binding motif, we found possible three HNF-4 α direct target genes in pancreatic β -cells.

Collectrin is a novel target gene of HNF-1 α in pancreatic β -cells and controls insulin exocytosis. We found that glucose, in a dose-dependent manner, increased collectrin expression in MIN6 cells. Collectrin might be involved in glucose-stimulated insulin secretion.

Keywords: Diabetes mellitus, transcription factor, insulin

Introduction

Mutations in the genes encoding hepatocyte nuclear factor (HNF)-1 α , and HNF-4 α cause maturity onset diabetes of the young (MODY) that is characterized by impairment of glucose-stimulated insulin secretion by pancreatic β -cells. In addition, recent genetic studies have shown that single nucleotide polymorphisms in the promoter region of the HNF-4 α gene are associated with type 2 diabetes. These results indicate that HNFs are involved in the molecular pathogenesis of MODY as well as common type 2 diabetes. To gain insights into the molecular mechanism of HNF diabetes, we compared gene expression patterns in pancreatic islets between control and β -cell specific HNF-4 α KO mice.

Collectrin is a novel target gene of HNF-1 α in pancreatic β -cells and controls insulin exocytosis. Although glucose is known to stimulate the expression of genes of the insulin secretory pathway, there is no information whether glucose regulates collectrin expression. We investigated in the study the expression of collectrin in a mouse β -cell line (MIN6).

Results

HNF-4 α target gene analysis

We isolated pancreatic islets from wild type and β -cell specific HNF-4 α KO (β HNF-4 α KO) mice for RNA isolation. DNA microarrays were used to identify differentially expressed genes in β HNF-4 α KO islets. We found that about 300 genes were down-regulated in KO islets. Furthermore, we scanned

the mouse genome for HNF4 binding motif in the down-regulated genes. This analysis revealed three possible direct HNF-4 α target genes in pancreatic β -cells.

Collectrin expression analysis

Recently, we identified that collectrin is a novel target gene of HNF-1 α in pancreatic β -cells and controls insulin exocytosis. We hypothesized that the expression of collectrin is regulated by glucose. MIN6 cells were incubated for 24 hours under different glucose concentrations, and then examined for collectrin protein expression levels. As shown in Fig. 1, glucose significantly increased collectrin expression. Incubation of collectrin with pyruvate also increased collectrin expression (Fig. 2).

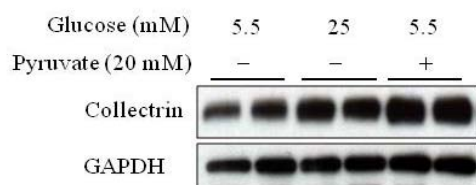


Figure 2. Effects of pyruvate on the expression of collectrin protein. MIN6 cells were cultured at 5.5 or 25 mM glucose concentrations for 24 hours in the presence or absence of 20 mM pyruvate.

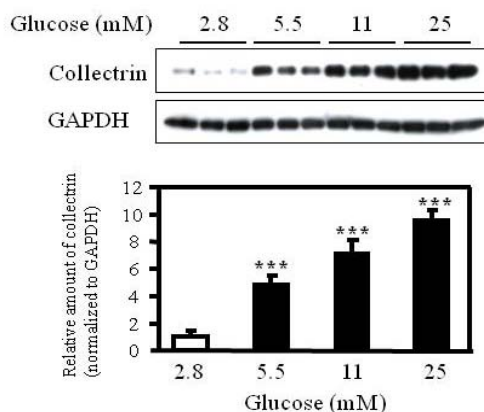


Figure 1. Effects of glucose on collectrin protein expression. MIN6 cells were cultured in the presence of 2.8, 5.5, 11, or 25 mM glucose for 24 hours. Collectrin protein levels were normalized to GAPDH levels. The results are from three independent samples. Data are mean \pm SD. ***p<0.005.

Discussion & Conclusion

Although previous studies have identified HNF-4 α target genes in liver, the information about target genes in β -cells was lacking. In the present study, we found possible HNF-4 α target genes in pancreatic β -cells. Further studies about these three genes might lead to a better understanding of MODY1 as well as type 2 diabetes.

We also found that both glucose and pyruvate increase collectrin expression in MIN6 cells. Further studies are needed to clarify the molecular mechanism of collectin expression. Since collectrin controls insulin exocytosis, better understanding of collectrin expression might be therapeutically beneficial in diabetic patients with impaired insulin secretion.

References

- 1) Saisho K, Fukuhara A, Yasuda T, Sato Y, Fukui K, Iwahashi H, Imagawa A, Hatta M, Shimomura I, Yamagata K: Glucose enhances collectrin protein expression in insulin-producing MIN6 β cells. *Biochem. Biophys. Res. Commun.* **389**: 133-137, 2009

Study on mechanosensitive calcium channels as mechano-sensors in plants

Hidetoshi Iida

Tokyo Gakugei University, Faculty of Education, Department of Biology

iida@u-gakugei.ac.jp

Abstract

The three dimensional structure of a putative mechanosensitive channel, MCA2, of *Arabidopsis thaliana* was determined by single particle analysis of its images from cryo-electron microscopy. In addition, possible physiological roles of MCA1 and MCA2 were investigated especially for sensitivity to mechanical stress and excessive ions in growth medium. We found that MCA1, but not MCA2, is involved in mechanosensing and/or mechanotransduction. Plants lacking both proteins are hypersensitive to excess Mg^{2+} .

Keywords: Mechanosensitive Ca^{2+} channel, MS channel, Ca^{2+} , ion stress, Mg^{2+} sensitivity

Introduction

Mechanosensitive (MS) Ca^{2+} channels transduce physical stresses, such as touch, gravity, and osmotic shock, at the cell membrane into an electrochemical or Ca^{2+} signal, and are thus thought to act as mechano-sensors. To date, bacterial and animal MS channels have been studied intensively and characterized considerably at the molecular level. By contrast, the molecular nature of plant MS channels is poorly understood, although their physiological roles have long been implicated in thigmotropism and gravitropism. Recently, we found genes for potential MS channels in the model plant *Arabidopsis thaliana*, named *MCA1* and its paralogue *MCA2* (Nakagawa *et al.*, *PNAS* **104**:3639-3644, 2007). *MCA1* shows 73% full-length identity to *MCA2* in amino acid sequence. *MCA1* cDNA was first isolated from an *Arabidopsis* cDNA library by functional complementation of a yeast *mid1* mutant defective in a putative MS channel component. *MCA1* and *MCA2* can enhance Ca^{2+} influx in yeast cells. Mechanical stress appears to activate *MCA1*: First, hypotonic shock increases $[Ca^{2+}]_{cyt}$ higher in *MCA1*-overexpressing (*MCA1ox*) seedlings than in control seedlings. Second, *MCA1ox* roots accumulate Ca^{2+} about 1.7-fold greater than wild-type roots. Third, *MCA1* expressed in CHO cells increases $[Ca^{2+}]_{cyt}$ in response to membrane stretch. Finally, primary roots of *mca1*-null seedlings fail to penetrate the harder, lower agar medium of two-phase agar medium from the softer, upper agar medium, suggesting that *MCA1* is responsible for touch sensing. These findings imply that *MCA1* and *MCA2* act as mechanosensitive Ca^{2+} channels.

A goal of our research is to determine the three-dimensional structure and physiological roles of *MCA1* and *MCA2*.

Results

1. Structural analysis

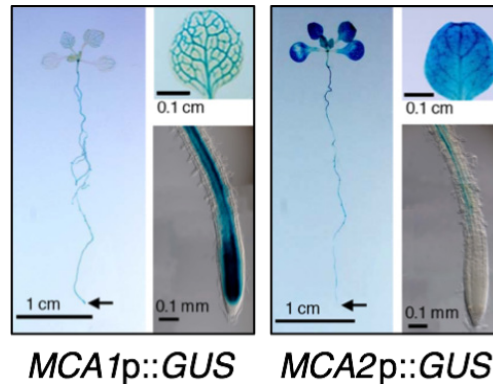
We first expressed individually MCA1 and MCA2 in yeast cells to try obtaining a sufficient amount of the proteins for structural analyses and found that they both appeared to form a homo-dimer and homo-tetramer in crude extracts of the yeast. However, we noticed that the amounts of MCA1 and MCA2 were still insufficient for the determination of the three-dimensional structure. Then, we expressed both proteins in insect Sf9 cells using a baculovirus expression system and successfully purified MCA2 by affinity column chromatography in collaboration with Prof. Kuniaki Nagayama and Dr. Hideki Shigematsu at the Okazaki Institute for Integrative Bioscience. By cryo-electron microscopy followed by single particle analysis, the three-dimensional structure of MCA2 was reconstructed and predicted to have two components, a transmembrane region and a cytoplasmic region. This structural feature seems to resemble that of the bacterial mechano-sensitive channel MscS. A manuscript describing these findings is in preparation.

2. Physiological role

Since high concentrations of ions in the soil are stressful for plants, we investigated the effect of several ions added to the medium on the growth of the *mca1* and *mca2* single mutants and the *mca1 mca2* double mutant. We found that a high concentration of Mg^{2+} (30 mM) inhibited the growth of the *mca1 mca2* double mutant, while it did not affect the growth of the *mca1* and *mca2* single mutants. Supplementation of 10 mM $CaCl_2$ to the Mg^{2+} -containing medium rescued the double mutation from Mg^{2+} -induced growth defect. Since it is known that Ca^{2+} and Mg^{2+} compete for the same sites of absorption on the plant plasma membrane, we measured the levels of Ca and Mg in the root and shoot of wild-type and *mca1*-null *mca2*-null plants grown for 24-26 days on MS medium with or without 30 mM $MgSO_4$. In control MS medium containing no supplemented $MgSO_4$, the Ca and Mg contents of the double mutant did not differ significantly from those of the wild type in both roots and shoots. When 30 mM $MgSO_4$ was included in MS medium, the Ca content was decreased by approximately 50% in roots and 60% in shoots, whereas the Mg content was increased approximately fivefold in roots and sevenfold in shoots. Notably, however, the degrees of the increase and decrease in both Ca and Mg contents were not significantly different between the *mca1 mca2* and wild-type plants. When 10 mM $CaCl_2$ was added to the MS/Mg medium, the Ca content was recovered nearly to the control level in roots and increased more than the control level in shoots, whereas the Mg content hardly changed. Again, the Ca content was not different between the *mca1*-null *mca2*-null and wild-type plants. These results indicate that while Mg^{2+} added to MS medium indeed lowers Ca^{2+} accumulation in plants, this effect influences equally both wild-type and *mca1*-null *mca2*-null plants.

Histochemical observation (see Figure presented below) showed that *MCA1* promoter:: β -glucuronidase (*GUS*) and *MCA2*p::*GUS* fusion reporter genes were universally expressed in the primary root of 10-day old seedlings with some exceptions: *MCA1*p::*GUS* was expressed in the cap and the elongation zone of the primary root, but *MCA2*p::*GUS* was not. In the shoot, *MCA2*p::*GUS* was expressed in mesophyll cells, but *MCA1*p::*GUS* was not.

Our previous study has shown that the primary root of the *mca1* mutant is unable to enter the lower, harder medium from the upper, softer medium in the two-phase agar medium (Nakagawa *et al.*, 2007). In the present study, on the other hand, the primary root of the *mca2* mutant was shown to enter the lower, harder medium, like the wild-type primary root. This phenotypic difference is likely due to a difference in a spatial expression of *MCA1p::GUS* and *MCA2p::GUS* in the cap and the elongation zone of the primary root, as described above.



MCA1p::GUS ***MCA2p::GUS***
Spatial patterns of *MCA1* and *MCA2* transcription as revealed by *GUS* staining. Ten-day old *MCA1p::GUS* and *MCA2p::GUS* plants were shown. A whole plant (An arrow indicates the extreme end of the primary root), a leaf (not a cotyledon), and the tip of a primary root are shown.

Discussion & Conclusion

Single particle analysis of the images of MCA2 obtained by cryo-electron microscopy have shown that a three-dimensional model of this protein comprises a transmembrane region and a cytoplasmic region. This structural feature is similar to that of the bacterial mechano-sensitive channel MscS.

Physiological study has suggested that MCA1, but not MCA2, is involved in sensing and/or transducing a mechanical stimulation in the tip of the primary root. Deletion of both MCA1 and MCA2 results in hypersensitivity to excess Mg^{2+} in growth medium. Mg^{2+} may affect the intracellular concentration of Ca^{2+} that is to be used as a signal, not a nutrient because the Ca content (not concentration) has been shown to be the same between the *mca1 mca2* mutant and wild type.

References

- 1) Yamanaka, T.*, Nakagawa, Y.*, Mori, K.*, Nakano, M., Imamura, T., Kataoka, H., Terashima, A., Iida, K., Kojima, I., Katagiri, T., Shinozaki, K., and Iida, H. (2010) MCA1 and MCA2 that mediate Ca^{2+} uptake have distinct and overlapping roles in Arabidopsis. *Plant Physiol.* **152**:1284-1296.

*These authors contributed equally to this work.

- 2) Teng, J., Iida, K., Ito, M., Izumi-Nakaseko, H., Kojima, I., Adachi-Akahane, S.*, and Iida, H.* (2010) Role of glycine residues highly conserved in the S2-S3 linkers of domains I and II of voltage-gated calcium channel $\alpha 1$ subunits. *Biochim. Biophys. Acta-Biomembr.* **1798**:966-974.

*Co-corresponding author

Role of endoplasmic reticulum stress-induced phosphorylation of translation initiation factor 2 α in metabolic regulation

Seiichi Oyadomari

Division of Molecular Biology, Institute for Genome Research, The University of Tokushima

oyadomar@genome.tokushima-u.ac.jp

Abstract

The endoplasmic reticulum (ER) is a multifunctional organelle responsible for protein folding, lipid biosynthesis and calcium storage. Perturbations of the ER function lead to stress-response mechanisms called the ER stress response, which ameliorate the accumulation of unfolded proteins in the ER. Dysfunctional ER stress response is involved in many diseases such as neurodegenerative diseases, ischemia, cancer and diabetes. The role of the ER stress response to maintain the ER homeostasis under the ER stress condition has been extensively studied over years. Recent studies suggest that the ER stress response regulates a physiological process besides cellular adaptation. We have focused on PERK-eIF2 α signaling branch of the ER stress response in liver, a key organ for intermediary metabolism. The hepatic PERK-eIF2 α signaling modulates glucose and lipid metabolism in a biphasic manner. The eIF2 α phosphorylation regulates translation of key hepatic transcription factor, which is accounted for modulation of intermediary metabolism in response to nutrient excess. Further analysis of gene expression profile of PERK-eIF2 α signaling reveals that the eIF2 α phosphorylation signaling affects the expression of circadian factor. We postulate that the ER stress response could serve to link physiologic perception of the environment to the circadian oscillatory apparatus.

Keywords: endoplasmic reticulum, eIF2 α , metabolism, circadian clock

Introduction

The endoplasmic reticulum (ER) serves many central functions, including synthesis and folding of membrane and secretory proteins. The unfolded protein response (UPR) is an intricate signaling pathway that adjusts the ER's capacity and tunes up cellular physiology in response to accumulation of unfolded proteins in the ER (ER stress). The UPR signaling is mediated from the ER to the cytosol and nucleus by three proximal effectors, IRE1, ATF6 and PERK [1]. The three UPR pathways have been implicated in the transcriptional regulation of genes important in metabolism. IRE1 processed mature XBP1 regulates the transcription of genes involved in fatty acid and cholesterol biosynthesis in liver [2]. ATF6 reduces hepatic gluconeogenic gene expression by regulated interaction with CRT2 [3]. We showed that PERK mediated eIF2 α phosphorylation also regulates the expression of hepatic lipogenic genes through activating C/EBP and PPAR γ [4]. However, the role of the UPR in the regulation of metabolism is not yet fully understood.

Results

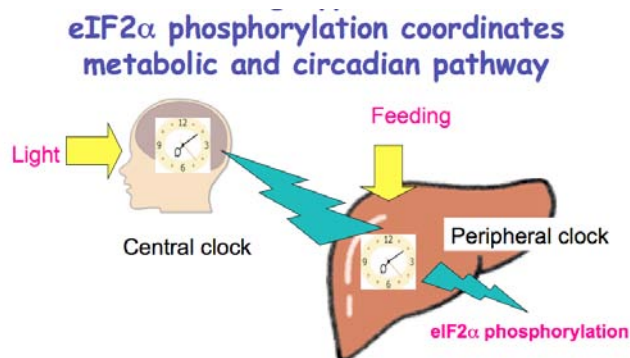
The enforced expression of a translation initiation 2α (eIF2 α)-specific phosphatase, GADD34, was used to selectively compromise signaling in the eIF2(α P)-dependent arm of the ER unfolded protein response in liver of transgenic mice. The transgene resulted in lower liver glycogen levels and susceptibility to fasting hypoglycemia in lean mice and glucose tolerance and diminished hepato-steatosis in animals fed a high fat diet. Attenuated eIF2(α P) correlated with lower expression of the adipogenic nuclear receptor PPAR γ and its upstream regulators, the transcription factors C/EBP α and C/EBP β , in transgenic mouse liver, whereas eIF2 α phosphorylation promoted C/EBP translation in cultured cells and primary hepatocytes.

Further analysis of gene expression profile of PERK-eIF2 α signaling reveals that the eIF2 α phosphorylation signaling affects the expression of circadian factor. We found that phosphorylation of eIF2 α oscillates the hepatic circadian clock.

Discussion & Conclusion

The circadian clock coordinates diverse physiological and metabolic process. The clock oscillators in both central and peripheral tissues drive circadian rhythmicity. Accumulating evidence suggests that peripheral clock is entrained by food intake and that the cell-autonomous entrainment of peripheral clock is intimately linked to metabolic homeostasis [5]. The mechanism of circadian rhythmicity is composed of an autoregulatory feedback loop that contains both positive and negative transcriptional elements. It has been suggested that circadian and metabolic pathway converge at transcriptional level. Recent studies provide some insights into the molecular mechanism how metabolic signals couple with circadian clock function.

ER is an important organelle that responds to various nutrient signals, such as those induced by glucose, lipid and amino acids metabolism. Interestingly, recent paper showed that circadian clock controls hepatic lipid metabolism by 12 hour period rhythmic activation of IRE1 pathway [6]. However, it is not known whether the UPR pathway alters the circadian clock. Here, we show that signaling in eIF2 α phosphorylation dependent UPR pathway is initiated by food intake in liver. Selective activation of PERK modulates the level of the core clock gene Per2 mRNA expression. We propose that phosphorylation of eIF2 α transduces nutrient signals to circadian clock in peripheral tissues (Figure).



References

- 1) Oyadomari S, Mori M (2004) Roles of CHOP/GADD153 in endoplasmic reticulum stress. *Cell Death Differ* **11**: 381-389.
- 2) Lee AH, Scapa EF, Cohen DE, Glimcher LH (2008) Regulation of hepatic lipogenesis by the transcription factor XBP1. *Science* **320**: 1492-1496.
- 3) Wang Y, Vera L, Fischer WH, Montminy M (2009) The CREB coactivator CRTC2 links hepatic ER stress and fasting gluconeogenesis. *Nature* **460**: 534-537.
- 4) Oyadomari S, Harding HP, Zhang Y, Oyadomari M, Ron D (2008) Dephosphorylation of translation initiation factor 2alpha enhances glucose tolerance and attenuates hepatosteatosis in mice. *Cell Metab* **7**: 520-532.
- 5) Green CB, Takahashi JS, Bass J (2008) The meter of metabolism. *Cell* **134**: 728-742.
- 6) Cretenet G, Le Clech M, Gachon F (2010) Circadian clock-coordinated 12 Hr period rhythmic activation of the IRE1alpha pathway controls lipid metabolism in mouse liver. *Cell Metab* **11**: 47-57.

Transcription factor networks for maintenance and regeneration of the thymic epithelial stem cells

Ryo Goitsuka

Tokyo University of Science

ryogoi@rs.noda.tus.ac.jp

Abstract

In the present study, we demonstrate that a transcription factor that is expressed in thymic epithelial cells (TEC) upon regeneration is required for the maintenance of TEC progenitor cells in the postnatal thymus by using *EGFP* reporter and temporally inducible TEC-specific conditional knock-out (CKO) mice.

Keywords: Transcription factor, thymic epithelial cells, stem cells, regeneration

Introduction

In the postnatal thymus, the cortical and medullary architecture of TEC microenvironment displays dynamic alterations in response to the various physiological and pathological stimuli. The existence of TEC stem/progenitor cells that function to maintain the homeostasis of the postnatal thymic microenvironment has long been a matter of debate. Thus, in the present study, we intended to analyze the phenotype and function of TECs expressing a transcription factor (designated as X).

Results

We identified the heterogeneity of postnatal TECs in terms of X expression levels, which becomes evident at 4 weeks after birth, when the size of the thymus reaches peak and the architecture of the medulla and cortex compartments is fully established. These TEC populations of distinct transcription factor expression levels, displayed different TEC maturation profiles; X^{high} cells is enriched in the most immature TECs of a $\text{CD40}^- \text{MHCII}^- \text{CD80}^- \text{CD86}^-$ phenotype, while X^{low} and X cells are enriched in mature TECs of a $\text{CD40}^+ \text{MHCII}^+ \text{CD80}^+ \text{CD86}^+$ phenotype. Since these surface markers are expressed in both medullary TECs and cortical TECs at different levels among their maturation stages, the absence of these maturation markers on X^{high} TECs. In addition, X^{high} TECs, but not X^{low} and X^- cells, has the ability to generate mature X cells, and formed thymus-like epithelial tissues when transplanted in the renal capsule of nude mice. Furthermore, we demonstrated that postnatal loss of X in K14^+ TEC compartment causes complete disappearance of the thymus by 12 weeks post induction of X deletion. We finally examined the differences in gene expression associated with epithelial cell stemness between TECs of distinct X expression levels by using quantitative PCR. Most of transcription factors involved in the embryonic thymus organogenesis were almost equally expressed in all of the three TEC populations, whereas some were 5-fold more expressed in X^{high} cells than in other cells. Furthermore,

X^{high} population was found to express significantly higher levels of several transcription factors that are involved in epithelial cell stemness than did X^{low} and X^- populations. To further investigate the target genes regulated by X in TECs, we compared gene expression profiles of TECs from X -CKO and controls at 1wk post X deletion. Among the genes highly expressed in X^{high} TECs, some were significantly down-regulated more than 2-fold in TECs upon X deletion.

Discussion & Conclusion

In conclusion, this study defines a potential postnatal TEC stem/progenitor cell population by using X as a functional molecular marker associated with “epithelial cell stemness”. Further dissection of the postnatal TEC stem/progenitor cell population in combination of other stem cell markers with our system described here will be helpful to understand molecular control of thymic homeostasis, and therefore potential therapeutic targets to maintain postnatal T cell production.

Research for regulation mechanism of lymphocyte activation by CARMA1

Hikomitsu Hara
Saga University
harah@cc.saga-u.ac.jp

Abstract

Essential role of SH3-GUK interaction of Carma1 in antigen receptor-mediated NF- κ B activation.

Keywords: Antigen receptor, NF- κ B, Carma1

Introduction

The CARD-Maguk family protein Carma1 is an essential signaling adaptor in antigen receptor-induced NF- κ B activation and thus essential for T and B lymphocyte activation. Reports have suggested a crucial role for the Carma1-mediated NF- κ B activation signaling in survival of ABC-type DLBCLs.

Results

We performed a yeast two-hybrid screening for factors that bind to the Guk domain of Carma1, and have screened the SH3 domain of Carma1 as a binding partner of the Guk domain. We found that the intramolecular SH3-Guk interaction dominates the intermolecular SH3-Guk interaction. By using a NF- κ B reporter system in Jurkat cells, we found that mutations abrogating the SH3-GUK interaction (ie, deletion of SH3 or GUK domain, or a point mutation (denotes X) in SH3 domain) impaired TCR or PKC-induced NF- κ B activation, suggesting a positive regulatory role of the SH3-Guk interaction in the NF- κ B signaling. To clarify the physiological role of the SH3-Guk interactions we generated knock-in mice bearing the point mutation X (KI-X). The KI-X mice have phenotypes that resemble those of Carma1-null knock out mice (ie, defective TCR/BCR-induced T/ B cell activation owing to defective NF- κ B activation, reduced serum immunoglobulins, reduced B-1 and MZ B cells, and regulatory T cells). These results demonstrated a physiologically relevant role of the SH3-Guk interaction in Carma1-mediated NF- κ B activation.

Discussion & Conclusion

We have found that the SH3-Guk interaction of Carma1 is an essential regulation in the antigen-receptor-induced NF- κ B activation. This regulation would be a molecular target of drugs for diseases in which the Carma1-mediated NF- κ B activation has a crucial role in its development and progression, such as ABC-type DLBCLs.

References

- 1) Hara H, Iizasa E, Nakaya M, Yoshida H: L-CBM signaling in lymphocyte development and function. *Journal of Blood Medicine*. 2010, **1**, *in press*.
- 2) Hara H and Saito T: CARD9 vs. CARMA1 in innate and adaptive immunity. *Trends in immunol*. 2009, **30**(5): 234-242.

Development of G-quadruplex motifs search in genome by the use of G-q ligands

Kazuo Nagasawa

Department of Biotechnology and Life Science, Faculty of Technology
Tokyo University of Agriculture and Technology
knaga@cc.tuat.ac.jp

Abstract

A BODIPY-labeled macrocyclic heptaoxazole, L1BOD-7OTD, was developed as a fluorescent ligand for G-quadruplexes. The results of the study show that L1BOD-7OTD both selectively induces the formation of intramolecular G-quadruplexes from some G-quadruplex forming oligonucleotides (GFOs). In addition, the labelled macrocyclic heptaoxazole strongly binds to and stabilizes intramolecular G-quadruplexes. Moreover, this substance can be used to directly visualize the G-quadruplexes in the form of green fluorescence.

Keywords: G-quadruplexes, telomestatin, BODIPY

Introduction

Since G-quadruplexes have a variety of biological functions and are expected to be useful as bioengineering tools, they hold great importance.¹ As a result, the selection of new structures of this type in genes and artificial synthetic nucleotides is significant. Studies guided by these goals would be greatly aided by the availability of methods to visualize G-quadruplexes. Herein, we describe the results of an effort that has led to the development of fluorescent labeled L1BOD-7OTD (**1**) and its application to the visualization of nucleotide sequences that form G-quadruplex structures.

Results

L1BOD-7OTD (**1**) was synthesized starting with previously reported L1H1-7OTD (Fig. 1).^{2,3} **1** has BODIPY moiety in its side chain and displays green fluorescence with wavelengths for its excitation and emission maxima of 502 and 512 nm, respectively.

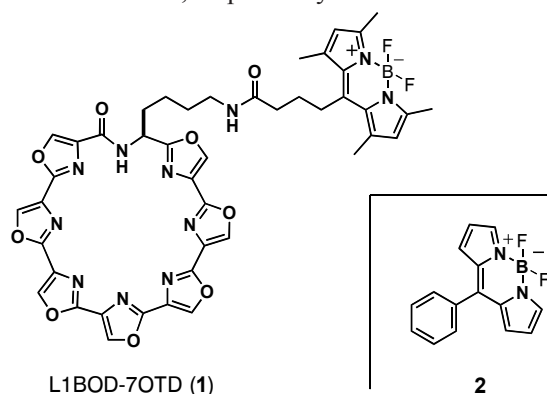


Figure 1. Molecular structure of fluorescent labeled L1BOD-7OTD (**1**) and control compound **2**.

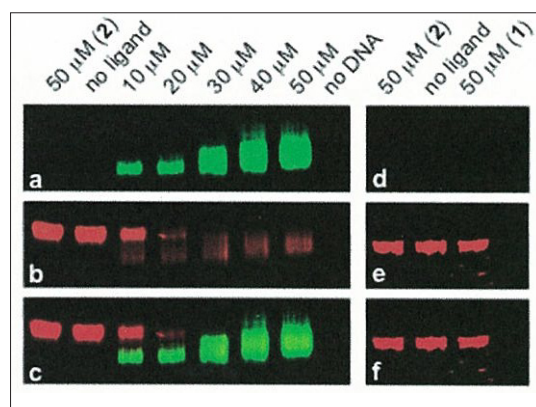


Figure 2. Visualization of the telo24 G-quadruplex by LIBOD-7OTD (**1**). Gel electrophoresis (12% native polyacrylamide, in 1 x TBE buffer, 4°C) of 10 mM oligonucleotides (a-c: telo24, d-f: double-stranded (ds)-telo24) in the presence of various concentrations of **1** (no salt added). a, d) All bands were detected using the 526 nm short pass filter. The gel was stained with b) Stains-all® and e) ethidium bromide then all bands were detected using the 580-640 nm band pass filter. c, f) Merged images of a and b or d and e. Compound **2** was used as a control for the BODIPY moiety of **1**. telo24 = (TTAGGG)₄

The presence of selective interactions between **1** and the telomeric DNA sequence, which is one of the G-quadruplex forming oligonucleotide; GFO, as well as visualization of the telomeric G-quadruplex structure were examined by using an electrophoresis mobility shift assay (EMSA). In the presence of **1**, a green band associated with the telo24 - LIBOD-7OTD complex is observed with an intensity that varies in a dose dependent manner (Fig. 2a). The presence of oligonucleotide in this band was determined by treatment of the gel with Stains-all® which enables visualization of uncomplexed telo24 as a red band (Fig. 2b). The results show that the amount of the telo24 G-quadruplex in the green band increases in a way that is directly proportional to the concentration of **1**. By using this method of analysis, the complex of telo24 with ligand **1** is directly observed as a green fluorescent band without the need for staining while the red band of lower mobility seen only by staining corresponds to the ligand-free nucleotide (Fig. 2c shows the merged image). In contrast, the EMSA analysis of mixtures of ds-telo24 with **1** shows that no green fluorescent band is produced (Fig. 2d) and only the red band for uncomplexed ds-telo24 exists even when higher concentrations of LIBOD-7OTD are present (Fig. 2e). The findings indicate that no interaction takes place between **2** and ds-telo24 and, as a result, that the interaction of **1** with G-quadruplex is selective and visualizable against double-stranded DNA.

To determine the apparent dissociation constants (K_d) of the complexes of **1** with the GFOs, fluorescent polarization (FP) titration measurements were made. After incubating mixtures of 50 nM LIBOD-7OTD, 50 mM KCl, and various concentrations of the GFOs (0.1-400 nM) for 12 h, the FP values were determined at 25 °C. Since ESI-MS analysis had shown that LIBOD-7OTD and GFOs form 2:1 stoichiometric complexes, the FP-[GFOs] plots were fitted using nonlinear regression analysis (Fig. 3). As the results, **1** was revealed to have potent dissociation constant toward G-quadruplexes with nanomolar level.

In the cases of ds-telo24 and telomut24 (negative control), no interaction with **1** is observed thus it appears that LIBOD-7OTD potently and selectively bound to G-quadruplexes.

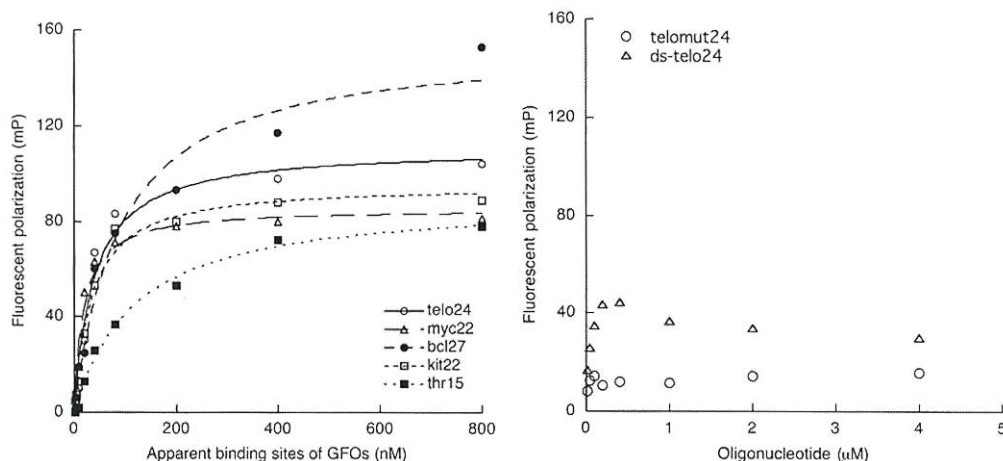


Figure 3. Fluorescent polarization titrations of GFOs. L1BOD-7OTD (**1**) (50 nM) was incubated with various concentrations (1-400 nM) of the GFOs (open circle: telo24, open triangle: myc22, black circle: bcl27, open square: kit22, black square: thr15) at 25 °C for 12 h in the presence of 50 mM KCl, 5 mM Tris-HCl, pH 7.0 and 50% DMSO (v/v). The polarization associated with the emission of **1** was measured at 530 nm (excitation at 500 nm). The fluorescent polarization values are representative of five scans taken at 25°C. All plots result from duplicate assays. telo24 = (TTAGGG)₄; myc22 = GAGGGTGGGG-AGGGTGGGGAAG; bcl27 = CGGGCGCGGGAGGAAGGGGGCGGGAGC; kit22 = AGGGAGGGCGCTGGGAGGAGGG; thr15 = GGTTGGTGTGGTTGG; telomut24 = (TTAGAG)₄.

Discussion & Conclusion

This investigation has led to the development of the fluorescence-labeled macrocyclic heptaaxazole L1BOD-7OTD (**1**), which serves as a novel fluorescent ligand for G-quadruplexes. The macrocyclic heptaaxazole selectively interacts with GFOs by inducing the formation of and stabilizing G-quadruplex structures. It is noteworthy that **1** also selectively interacts with an artificial G-quadruplex aptamer. Interactions of this fluorescent ligand with G-quadruplex structures in genes and artificial nucleotides can be directly visualized as a consequence of the green fluorescence of **1**.

References

- 1) For recent review, see; S. Neidle, *FEBS Journal*, 2010, **277**, 1118, “Human telomeric G-quadruplex: The current status of telomeric G-quadruplex as therapeutic targets in human cancer”.
- 2) M. Tera, K. Iida, H. Ishizuka, M. Takagi, M. Suganuma, T. Doi, K. Shin-ya and K. Nagasawa, *ChemBioChem*, 2009, **10**, 431, “Synthesis of a Potent G-Quadruplex-Binding Macrocyclic Heptaaxazole”.
- 3) M. Tera, K. Iida, K. Ikebukuro, H. Seimiya, K. Shin-ya and K. Nagasawa, *Org. Biomol. Chem.*, 2010, *in press*, “Visualization of G-quadruplexes by using a BODIPY-labeled macrocyclic heptaaxazole”.

Condition clarification and development of new strategy for the treatment of metabolic syndrome: Role of fatty acid composition and long chain fatty acid elongase Elovl6 in energy metabolism

Takashi Matsuzaka

Department of Endocrinology and Metabolism, University of Tsukuba
t-matsuz@md.tsukuba.ac.jp

Keywords: Metabolic syndrome, Liver, Fatty acid elongase

Introduction

Elovl6 is a microsomal enzyme involved in the elongation of saturated and monounsaturated fatty acids with 12, 14 and 16 carbones¹). Mice with targeted disruption in the gene for Elovl6 are resistant to diet-induced insulin resistance despite their hepatosteatosis and obesity being similar to that of the wild-type mice²). Protection against diet-induced insulin resistance in Elovl6KO mice is mainly due to restoration of insulin signaling. To understand the physiological role of Elovl6 in liver, we tried creating liver-specific Elovl6 knockout (LKO) mice.

Results

Es cells, identified as appropriately targeted by a vector with loxP sites flanking exon 5 of the mouse Elovl6 gene, were used to generate chimeric mice. Animals carrying the targeted allele transmitted this locus through the germline to yield mice heterozygous for the targeted allele (lox^{+/-}). The C57BL/6J lox^{+/-} mice were interbred to generate mice homozygous for Elovl6 alleles (lox^{+/+}). The lox^{+/+} mice are phenotypically indistinguishable from wild-type mice and showed normal Elovl6 expression, indicating the loxP sites did not interfere with Elovl6 expression. To generate liver-specific Elovl6 knockout mice, we crossed lox^{+/+} mice to an albumin promoter Cre recombinase-expressing strain on C57BL/6J background to obtain initially heterozygotes (lox^{+/-}, AlbCre⁺). The lox^{+/-}, AlbCre⁺ progeny was interbred to obtain lox^{+/+}, AlbCre⁺ mice that are expected to contain lox^{+/+}, AlbCre⁺ (Elovl6LKO).

To confirm deletion of the Elovl6 gene, we analyzed the expression of Elovl6 by Northern blotting in liver RNA. The native Elovl6 transcripts were detected in the liver RNA from control mice, but not in LKO mice. Elovl6 expression was unaffected in white adipose tissue, brown adipose tissue, and brain of LKO mice.

Discussion & Conclusion

The aim of this study is to determine the role of liver Elovl6 produced long chain fatty acids in lipid metabolism and energy homeostasis. To understand the role of Elovl6 in the liver, we generated liver-

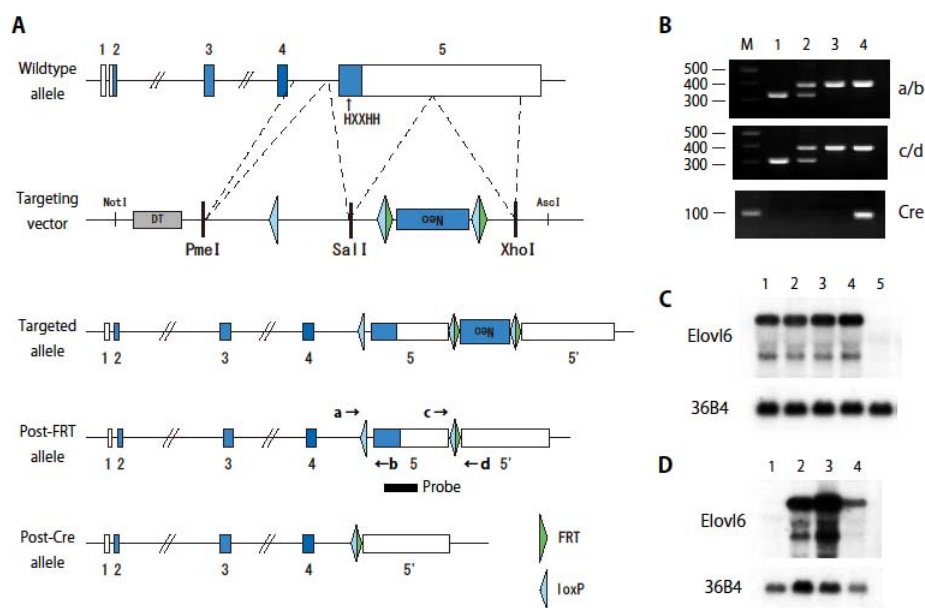


Figure 1 generation of liver-specific Elov6 knockout mice

(A) Scheme of targeting construct design. (B) PCR-based genotyping of tail DNA to distinguish *lox*^{-/-} (lane 1), *lox*^{+/-} (lane 2), *lox*^{+/+} (lane 3), and *lox*^{+/+}, albumin-Cre⁺ (lane 4) using primers indicated in A. (C) Northern blot analysis for liver RNA from *lox*^{-/-} (lane 1), *lox*^{-/-}, albumin-Cre⁺ (lane 2), *lox*^{+/-} (lane 3), *lox*^{+/+} (lane 4), and *lox*^{+/+}, albumin-Cre⁺ (lane 5) with Elov6 specific probe. (D) Northern blot analysis of Elov6LKO RNA from liver (lane 1), white adipose tissue (lane 2), brown adipose tissue (lane 3), and brain (lane 4) with Elov6 specific probe.

specific Elov6 knockout mice. Elov6LKO mice are apparently normal and breed like wild-type. Based on the liver DNA and Northern blotting of the liver RNA, the deletion of Elov6 was essentially complete in Elov6LKO mice. By analyzing the phenotype of Elov6LKO mice in various nutritional conditions (fasting/ refeeding, high sucrose-fat free diet feeding, high fat-high sucrose diet feeding), we want to clarify the molecular mechanism of energy metabolism controlled by the changes of the cellular fatty acid composition.

References

- 1) Matsuzaka, T., Shimano, H., Yahagi, N., Yoshikawa, T., Amemiya-Kudo, M., Hasty, AH., Okazaki, H., Tamura, Y., Iizuka, Y., Ohashi, K., Osuga, J., Takahashi, A., Yato, S., Sone, H., Ishibashi, S. & Yamada, N. : Cloning and characterization of a mammalian fatty acyl-CoA elongase as a lipogenic enzyme regulated by SREBPs. *J Lipid Res.* **43** : 911-920, 2002.
- 2) Matsuzaka, T., Shimano, H., Yahagi, N., Kato, T., Atsumi, A., Yamamoto, T., Inoue, N., Ishikawa, M., Okada, S., Ishigaki, N., Iwasaki, H., Iwasaki, Y., Karasawa, T., Kumadaki, S., Matsui, T., Sekiya, M., Ohashi, K., Hasty, AH., Nakagawa, Y., Takahashi, A., Suzuki, H., Yatoh, S., Sone, H., Toyoshima, H., Osuga, J. & Yamada, N. : Crucial role of a long-chain fatty acid elongase, Elov6, in obesity-induced insulin resistance. *Nat Med.* **13** :1193-1202, 2007.

Molecular mechanisms of endoplasmic reticulum stress response in skeletal tissues and development of its regulation.

Kazunori Imaizumi

Division of Molecular and Cellular Biology, Department of Anatomy,
Faculty of Medicine, University of Miyazaki
imaizumi@med.miyazaki-u.ac.jp

Keywords: ER stress, bone, cartilage

Introduction

Eukaryotic cells have signaling pathways from the endoplasmic reticulum (ER) to cytosol and nuclei, to avoid excess accumulation of unfolded proteins in the ER. We previously identified new types of ER stress transducers, OASIS and BBF2H7, bZIP transcription factors, which are members of the CREB/ATF family. In this project, I explored the in vivo functions of these ER stress transducers using knockout mice.

Results

- 1) OASIS deficient mice exhibited severe osteopenia, involving a decrease in type I collagen, Col1a1, as a target of OASIS. OASIS activates the transcription of Col1a1 through an unfolded protein response element-like sequence in the osteoblast-specific Col1a1 promoter region. Moreover, expression of OASIS in osteoblasts is induced by BMP2 (bone morphogenetic protein 2), the signaling of which is required for bone formation. Additionally, activation of OASIS is accelerated by BMP2 signaling, which causes mild ER stress.
- 2) BBF2H7 deficient mice showed severe chondrodysplasia and died by suffocation shortly after birth because of an immature chest cavity. The cartilage showed a lack of typical columnar structure in the proliferating zone and decrease in the size of hypertrophic zone, resulting in a significant reduction of extracellular matrix proteins. Interestingly, proliferating chondrocytes showed abnormally expanded ER, containing aggregated type II collagen and cartilage oligomeric matrix protein. We identified Sec23a, which encodes a coat protein complex II component responsible for protein transport from the ER to the Golgi, as a target of BBF2H7. When Sec23a was introduced to BBF2H7 deficient chondrocytes, the impaired transport and secretion of cartilage matrix proteins was totally restored, indicating that by activating protein secretion the BBF2H7-Sec23a pathway has crucial role in chondrogenesis.

Discussion & Conclusion

Our studies show that OASIS and BBF2H7 are critical for bone and cartilage formation through the transcription of *Col1a1* and *Sec23a* respectively, and they reveal new mechanisms by which ER stress-induced signaling mediates osteogenesis and chondrogenesis.

References

- 1) Murakami T, Saito A, Hino S-I, Kondo S, Kanemoto S, Chihara K, Sekiya H, Tsumagari K, Ochiai K, Yoshinaga K, Saitoh M, Nishimura R, Yoneda T, Kou I, Furuichi T, Ikegawa S, Ikawa M, Okabe M, Wanaka A, and Imaizumi K.: Signalling mediated by the endoplasmic reticulum stress transducer OASIS is involved in bone formation. *Nature Cell Biology* **11**:1205-1211, 2009.
- 2) Saito A, Hino S-I, Murakami T, Kanemoto S, Kondo S, Saitoh M, Nishimura R, Yoneda T, Furuichi T, Ikegawa S, Ikawa M, Okabe M, and Imaizumi K.: Regulation of endoplasmic reticulum stress response by a BBF2H7-mediated *Sec23a* pathway is essential for chondrogenesis. *Nature Cell Biology* **11**:1197-1204, 2009.

Structural Analysis of Biomolecules by A Combined Method of Azaelectrocyclization-based Microscale Labeling /Fluorescence Detected Circular Dichroism (FDCCD)

Katsunori Tanaka

Osaka University

ktzenori@chem.sci.osaka-u.ac.jp

Abstract

Protein/ligand and/or protein/protein interactions were efficiently achieved through the combined methods of rapid 6π -azaelectrocyclization & fluorescence-detected circular dichroism (FDCCD) analysis. Thus, a specific lysine of human serum albumin (HSA) was selectively labeled by the electrocyclization probe in “non-destructive” manner, and the interaction with the albumin hydrophobic ligands and/or cytokines were investigated afterwards by FDCCD.

Keywords: Rapid 6π -azaelectrocyclization; Site-selective labeling; Fluorescence-detected circular dichroism (FDCCD)

Introduction

The purpose of the research is (i) to establish the “site-selective” and “non-destructive” labeling of the proteins through the rapid 6π -azaelectrocyclization, that this researcher has developed previously, and then (ii) to detect the interaction of the labeled proteins with the ligands and/or proteins based on the fluorescence-detected circular dichroism (FDCCD) with high sensitivity and fluorescence-selectivity. This researcher has initially investigated the human serum albumin (HSA) as a model protein for this purpose.

Results

Human serum albumin (HSA) is the most abundant protein constituent of blood plasma and serves as a major protein storage component for endogenous and external compounds. HSA has three homologous domains (named I, II, III), one of which strongly interacts with the hydrophobic natural products (hydrophobic binding site). This researcher has investigated the site-selective and non-destructive protein labeling based on the rapid 6π -azaelectrocyclization, using HSA as a model protein (Figure 1); site-selective modification of HSA was achieved by directing reactive groups to a hydrophobic binding site using a coumarin ligand (hydrophobic ligand) of the HSA protein. Thus, the incubation of HSA with probe **1**, which loads the coumarin ligand through the ester linkage, lead to the selective labeling of a specific lysine situated close to the coumarin binding site through Schiff base formation (stage **A**) followed by rapid azaelectrocyclization (stage **B**). It was also observed that the 1,2-dihydropyridine derivative as the electrocyclization product readily aromatized to the pyridinium ion by auto-oxidation (stage **C**), which in turn accelerate the hydrolysis of the ester

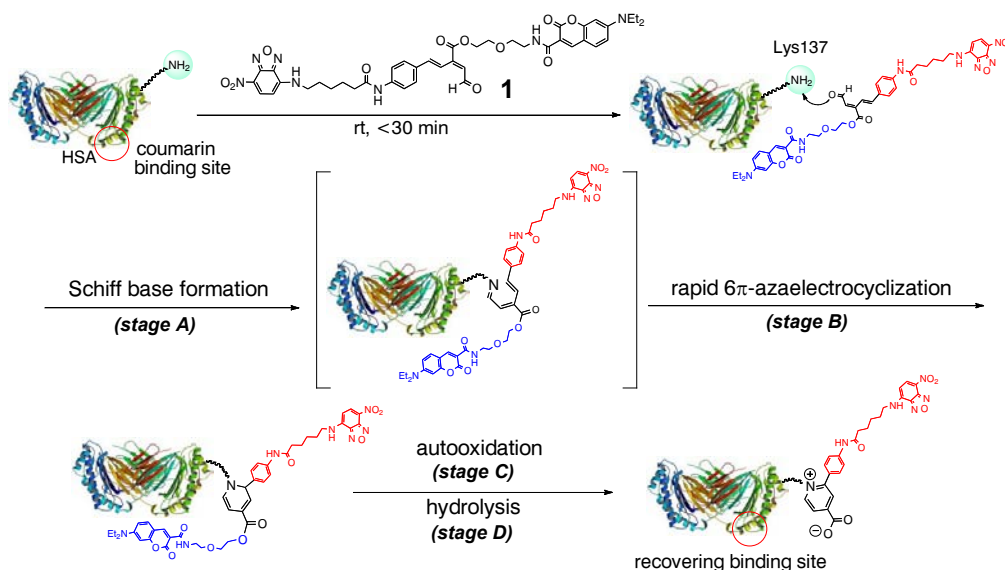


Figure 1. “Site-selective” and “non-destructive” labeling by 6 π -azaelectrocyclization.

linkage (condition **D**) to produce the Zwitterion. Such cascade process of oxidation-hydrolysis at the same time, recovered the hydrophobic binding site in the labeled protein, and therefore, the site-selective and non-destructive protein labeling (modification) were achieved.

Both “selectively”-labeled and “non-selectively”-labeled albumins were subsequently subjected to the interaction with coumarin ligand and these interactions were analyzed by FDCD (Figure 2). This researcher clearly observed the interaction of the coumarin ligand with both albumins on the basis of the changes in FDCD signals; Additional FRET analysis only detected the interaction for the “selectively”-labeled albumin, thus confirming the “site-selective”-labeling performed above at the coumarin-binding-site. On the other hands, the conventional absorbance-based CD failed in detecting these interactions. The interactions of the “selectively”-labeled albumin with the cytokines could also be analyzed by the fluorescence-based FDCD analysis.

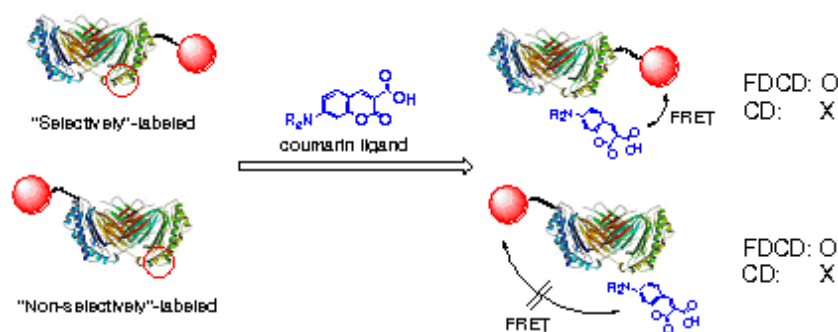


Figure 2. FDCD analysis of protein/ligand interactions.

Discussion & Conclusion

The evidence that the conventional CD failed in detecting the faint signal-changes (induced FDCD signals) during the protein/ligand interaction, due to the inhibition by the intense UV signals at around 200 nm (amides and dyes’ absorbance), proves the efficiency of the present method. The

results clearly show the advantageous features of FDCD in achieving the highly sensitive and/or fluorescence-selective detection. It will be noted that the exciton coupled FDCD could be applied to the case when only the single fluorophore is available and therefore the FRET is not applicable. Thus, the site-selective and non-destructive labeling in combination with the highly sensitive and selective fluorescence detection by FDCD would expand the investigation on protein/ligand as well as protein/protein interactions.

References

- 1) To be submitted: Tanaka, K.; Nehira, T.; Minami, K.; Shiotsuki, S.; Fukase, K. submitted. "Fluorescence-selective Detection of Induced CD Signals on Protein-ligand Interaction by Fluorescence Detected CD."

Significance of Transcriptional Control in Vascular Development, Function and Disease

Osamu Nakagawa

Nara Medical University Advanced Medical Research Center
nakagawa-nmu@umin.ac.jp

Keywords: Transcription factor, Cardiovascular system

Introduction

Transcriptional regulation plays essential roles in tissue-specific gene expression for proper embryonic development and mature organ function. Transcription factors form multi-protein complexes, and such complexes, not individual transcription factors, dictate the specificity of downstream gene expression. Since transcription factors act as “molecular switches” for downstream genes, it is critical to analyze the functions of the genes that directly regulate cellular functions downstream of transcriptional control. Characterization of those genes may provide a link from basic studies of transcriptional regulation to the etiologies of human diseases. We have identified a novel family of transcription factors, Hrt1, Hrt2 and Hrt3, which is highly expressed in the cardiovascular system (Figure 1). In this study, we have attempted to clarify the significance of the Hrt family of transcription factors in vascular development and disease.

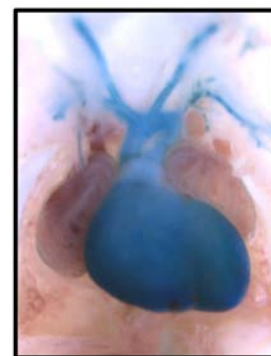


Figure 1: Cardiovascular expression of the Hrt2 gene (Knock-in LacZ expression)

Results

In this study, we employed a conditional knockout mouse system to study cell-type-specific and developmental-stage-specific function of the Hrt family transcription factors. Among three family members, Hrt1 and Hrt2 are predominantly expressed in developing vascular endothelium and smooth muscle cells, and it was reported that the double knockout mice of the Hrt1 and Hrt2 genes die in utero due to the deficiency of vascular formation. However, it has been unclear whether endothelial- or smooth-muscle-specific function of Hrt1 and Hrt2 is essential for vascular development. Therefore, we first generated endothelial-specific Hrt1/Hrt2 knockout mice and found that these mice die showing similar abnormalities observed in the Hrt1/Hrt2 double knockout mice. This result indicated that Hrt1 and Hrt2 expressed in the vascular endothelium play indispensable roles during development. We have also attempted to study the significance of Hrt1 and Hrt2 in adult vascular formation. For that purpose, we established a mouse line in which the deficiency of Hrt1 and Hrt2 can be induced by the Tamoxifen administration. We are currently examining the efficiency of Cre-mediated excision of the floxed Hrt2 allele in adult mice.

Discussion & Conclusion

Our data indicated that the function of the Hrt family of transcription factors in the vascular endothelium is essential for proper embryonic development. Ongoing studies will also clarify whether the Hrt transcription factors play essential roles in the vascular formation at adult stages. These studies will lead to better understanding of transcriptional regulation and intracellular signaling pathways in vascular development and disease.

References

- 1) Nakagawa O, Nakagawa M, Richardson JA, Olson EN, Srivastava D. *HRT1, HRT2, HRT3*: a new subclass of bHLH transcription factors marking specific cardiac, somitic and pharyngeal arch segments. *Dev. Biol.* **216**(1): 72-84, 1999.
- 2) Nakagawa O, McFadden DG, Nakagawa M, Yanagisawa H, Hu T, Srivastava D, Olson EN. Members of the HRT family of bHLH proteins act as transcriptional repressors downstream of Notch signaling. *Proc. Nat. Acad. Sci. USA* **97**(25): 13655-13660, 2000.
- 3) Kathiriya IS, King IN, Murakami M, Nakagawa M, Astle JA, Gardner KA, Gerard RD, Olson EN, Srivastava D, Nakagawa O. Hairy-related transcription factors inhibit GATA-dependent cardiac gene expression through a signal-responsive mechanism. *J. Biol. Chem.* **279**(52): 54937-54943, 2004.
- 4) Nakagawa O, Arnold M, Nakagawa M, Hamada H, Shelton JM, Kusano H, Harris TM, Childs G, Campbell KP, Richardson JA, Nishino I, Olson EN. Centronuclear myopathy in mice lacking a novel muscle-specific protein kinase transcriptionally regulated by MEF2. *Genes Dev.* **19**(17): 2066-2077, 2005.
- 5) King IN, Kathiriya IS, Murakami M, Nakagawa M, Gardner KA, Srivastava D, Nakagawa O. Hrt and Hes negatively regulate Notch signaling through interactions with RBP-Jkappa. *Biochem. Biophys. Res. Commun.* **345**(1):446-452, 2006.
- 6) Xin M, Small EM, van Rooij E, Qi X, Richardson JA, Nakagawa O, Olson EN. Essential roles of the bHLH transcription factor Hrt2 in repression of atrial gene expression and maintenance of postnatal cardiac function. *Proc. Nat. Acad. Sci. USA* **104**(19):7975-7980, 2007.

Severe Dyslipidemia, Atherosclerosis, and Sudden Cardiac Death in Mice Lacking All NO Synthases Fed a High-Fat Die

Masato Tsutsui

Department of Pharmacology, Faculty of Medicine, University of the Ryukyus
nakagawa-nmu@umin.ac.jp

Abstract

Objective: The precise role of the nitric oxide synthase (NOS) system in lipid metabolism remains to be elucidated. We addressed this point in mice that we have recently developed that lack all three NOS isoforms.

Methods and Results: Wild-type, singly, doubly, and triply NOS^{-/-} mice were fed either a regular or high-cholesterol diet for 3-5 months. The high-cholesterol diet significantly increased serum low-density-lipoprotein (LDL) cholesterol levels in all the genotypes as compared with the regular diet. Importantly, when compared with the wild-type genotype, the serum LDL cholesterol levels in the high-cholesterol diet were significantly and markedly elevated only in the triply NOS^{-/-} genotype, but not in any singly or doubly NOS^{-/-} genotypes, and this was associated with remarkable atherosclerosis and sudden cardiac death, which occurred mainly in 4-5 months after the high-cholesterol diet. Finally, hepatic LDL receptor expression was markedly reduced only in the triply NOS^{-/-} genotype, accounting for the diet-induced dyslipidemia in the genotype.

Conclusions: These results provide the first direct evidence that complete disruption of all NOS genes causes severe dyslipidemia, atherosclerosis, and sudden cardiac death in response to a high-fat diet in mice in vivo through the down-regulation of the hepatic LDL receptor, demonstrating the critical role of the whole endogenous NOS system in maintaining lipid homeostasis.

Keywords: nitric oxide synthase, atherosclerosis, high fat diet, sudden death, lipid

Introduction

Nitric oxide (NO) plays an important role in maintaining cardiovascular homeostasis.¹⁻⁴ Three distinct NO synthase (NOS) isoforms exist and are encoded by three distinct genes, including neuronal (nNOS or NOS1), inducible (iNOS or NOS2) and endothelial NOS (eNOS or NOS3). Initial NO studies indicated that nNOS and eNOS are constitutively expressed mainly in the nervous system and the vascular endothelium, respectively, synthesizing a small amount of NO in a calcium-dependent manner both under basal conditions and upon stimulation, and that iNOS is induced only when stimulated by microbial endotoxins or certain proinflammatory cytokines, producing a greater amount of NO in a calcium-independent manner.¹⁻⁴ However, recent studies have revealed that both nNOS and eNOS are also subject to expressional regulation, and that iNOS is constitutively expressed even under physiological conditions.⁴ Furthermore, it has become apparent that in addition to eNOS and iNOS, nNOS is also expressed in the cardiovascular system, exerting important cardiovascular

actions.⁴ Thus, NO research is taking a new turn.

The roles of the NOS system in vivo have been investigated in pharmacological studies with NOS inhibitors and in studies with NOS-isoform deficient mice. However, because of the non-specificity of the NOS inhibitors and the compensatory interactions among the NOS isoforms, the authentic roles of the entire NOS system still remain to be fully elucidated. To address this important issue, we have recently developed mice in which all three NOS isoforms are completely deleted.⁵⁻⁶ The triply nNOS/iNOS/eNOS-deficient (n/i/eNOS^{-/-}) mice are unexpectedly viable and appear normal, but their survival and fertility rates are markedly reduced as compared with wild-type (WT) mice. The triply NOS^{-/-} mice also exhibit marked hypotonic polyuria, polydipsia, and renal unresponsiveness to an antidiuretic hormone, vasopressin, all of which are characteristics consistent with nephrogenic diabetes insipidus.⁵⁻⁶ In addition, we have recently revealed that the triply NOS^{-/-} mice spontaneously develop myocardial infarction.⁷⁻⁸ However, the role of the NOS system in the regulation of lipid metabolism is not fully understood. Thus, in this study, we examined the effect of a Western-type cholesterol-rich diet on lipid metabolism in our triply mutant mice.

Results

Severe Dyslipidemia in Triply n/i/eNOS^{-/-} Mice Fed a High-Cholesterol Diet

We first investigated the effect of the Western-type cholesterol-rich diet for 3 months on the serum lipid profiles in the 8 strains (WT C57BL/6, singly nNOS^{-/-}, iNOS^{-/-}, eNOS^{-/-}, doubly n/iNOS^{-/-}, n/eNOS^{-/-}, i/eNOS^{-/-}, and triply n/i/eNOS^{-/-} mice). The high-cholesterol diet significantly increased the serum levels of total cholesterol (Figure 1A), LDL cholesterol (Figure 1B), and small dense LDL particles (Figure 1C) in all the genotypes studied as compared to the regular diet. Intriguingly, when compared with the WT genotype, the serum levels of total cholesterol, LDL cholesterol, and small dense LDL particles in the high-cholesterol diet were all significantly and markedly higher only in the triply n/i/eNOS^{-/-} genotype, but not in any singly or doubly NOS^{-/-} genotypes, and these levels were similar to those in apoE^{-/-} mice that manifest severe hyperlipidemia.¹⁵⁻¹⁶ In contrast, the serum levels of high-density lipoprotein (HDL) cholesterol (Figure 1D) or triglyceride (Figure 1E) in the high-cholesterol diet did not significantly differ in any of the genotypes.

Atherosclerosis in Triply n/i/eNOS^{-/-} Mice Fed a High-Cholesterol Diet

We next examined whether the cholesterol-rich diet would elicit atherosclerotic vascular lesion formation in the 8 strains. Although in the WT, singly, and

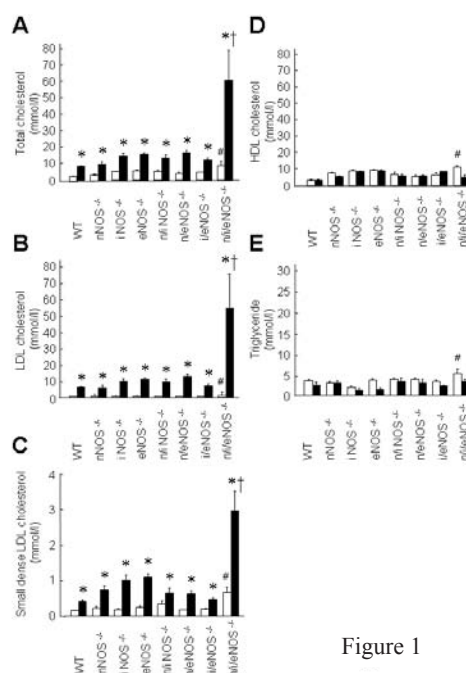


Figure 1

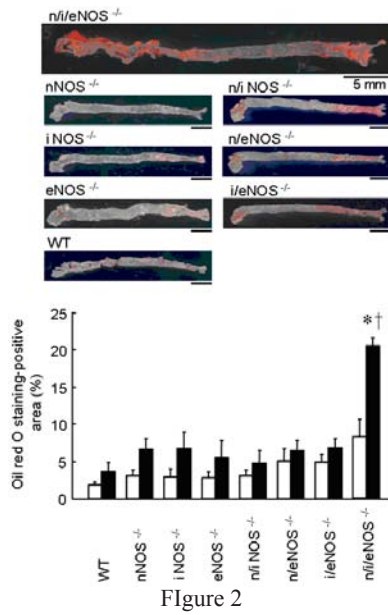


Figure 2

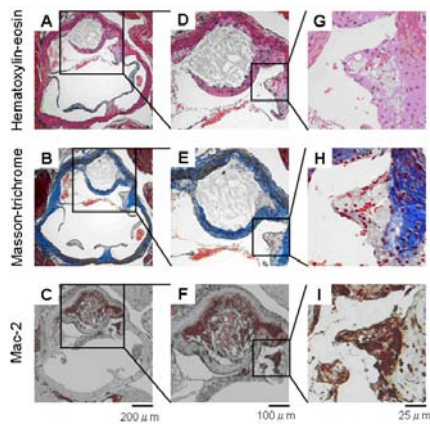


Figure 3

doubly NOS^{-/-} genotypes, the high-cholesterol diet tended to induce lipid accumulation in the aortas, these effects did not reach statistically significant levels (Figure 2). However, in the triply n/i/eNOS^{-/-} genotype, the high-cholesterol diet significantly and markedly caused aortic lipid accumulation (Figure 2). In addition, the high-cholesterol diet also significantly and markedly elicited atheromatous plaque formation in the aortic sinus only in the triply n/i/eNOS^{-/-} genotype (Supplementary Figure 1). In those atheromatous plaque lesions, subendothelial aggregation of Mac-2-positive macrophage-derived foam cells (Figure 3G-I) and a necrotic lipid core covered by a well-formed fibrous cap (Figure 3D-F) were noted.

Reduced Survival in Triply n/i/eNOS^{-/-} Mice Fed a High-Cholesterol Diet

Since we experienced the sudden death of the triply n/i/eNOS^{-/-} mice during the cholesterol-rich feeding, we examined the survival rate. The survival rate with the high-cholesterol diet for 5 months was significantly and markedly reduced only in the triply n/i/eNOS^{-/-} genotype (37.5% [15/40]) as compared with the WT genotype (Figure 4A). We then performed a postmortem histopathological analysis of the 15 dead triply n/i/eNOS^{-/-} mice to identify the cause of death. In all the dead mice,

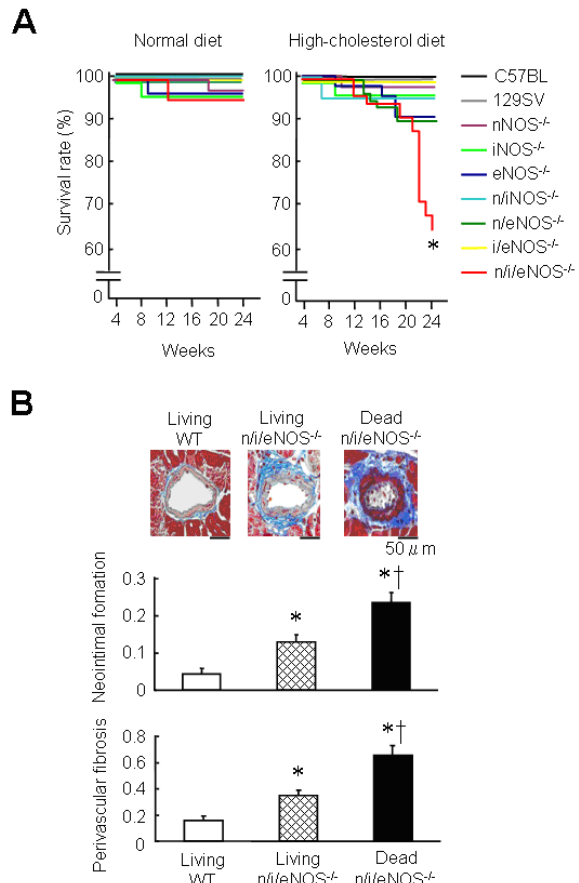


Figure 4

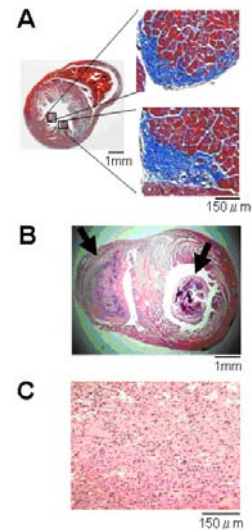
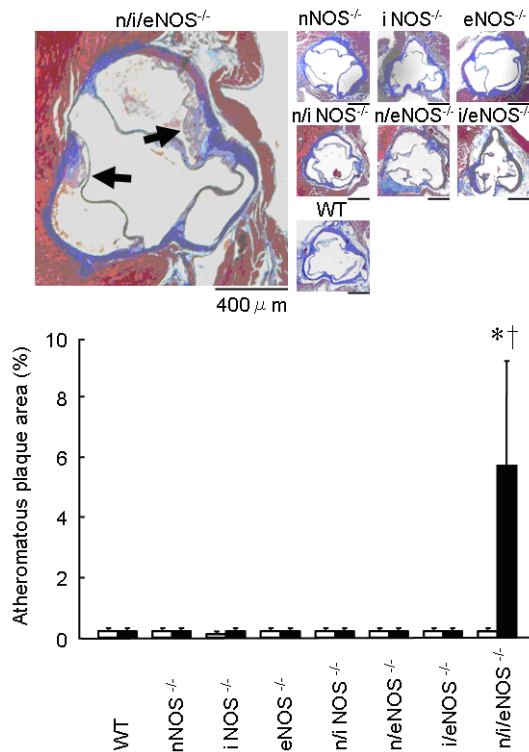
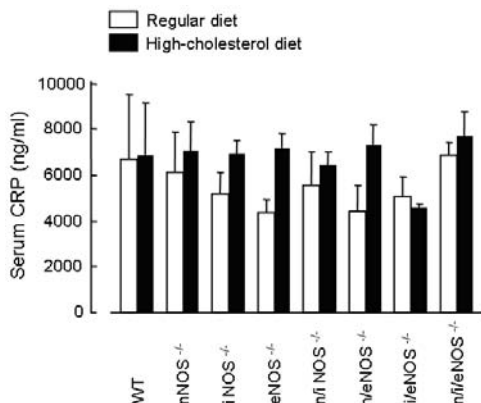


Figure 5

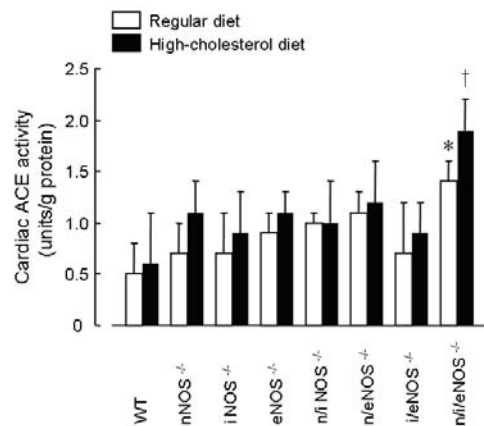


Supplementary Figure I. Atherosclerotic plaque formation in the aortic sinus of triply *n/i/eNOS*^{-/-} mice fed a high-cholesterol diet (Masson-trichrome staining) (*n*=6-11). White and black bars indicate the regular and high-cholesterol diets, respectively. **P*<0.05 vs. the regular diet; †*P*<0.05 vs WT mice fed the high-cholesterol diet.

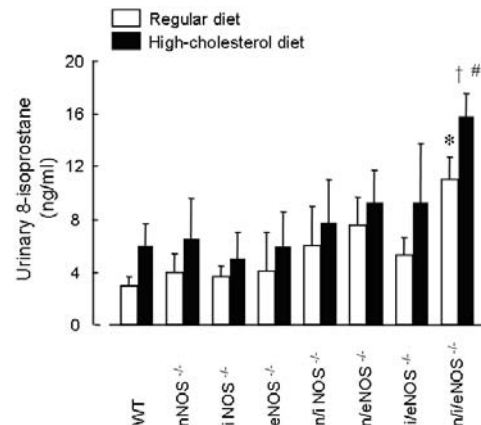


Supplementary Figure IV. Serum CRP levels in WT and *NOS*^{-/-} mice fed either the regular or high-cholesterol diet for 3 months (*n*=5-6). WT, C57BL/6.

marked neointimal formation and perivascular fibrosis of the coronary artery were noted, and their extents were both significantly greater when compared with living control WT mice fed the regular diet and with living triply *n/i/eNOS*^{-/-} mice fed the high-cholesterol diet (Figure 4B). Furthermore, old myocardial infarction was detected in 1 mouse (Figure 5A), giant organized thrombi in both the left and right ventricles were seen in 2 mice (Figure 5B), and pulmonary congestion was observed in all the dead mice (Figure 5C). On the other hand, no pathological finding that explains the cause of death was present in the brain, kidney, or spleen.



Supplementary Figure II. Cardiac ACE activity in WT and *NOS*^{-/-} mice fed either the regular or high-cholesterol diet for 3 months (*n*=4-6). WT, C57BL/6. **P*<0.05 vs. WT mice fed the regular diet; †*P*<0.05 vs. WT mice fed the high-cholesterol diet.



Supplementary Figure III. Urinary 8-isoprostane levels in WT and *NOS*^{-/-} mice fed either the regular or high-cholesterol diet for 3 months (*n*=4-6). WT, C57BL/6. **P*<0.05 vs. WT mice fed the regular diet; †*P*<0.05 vs. WT mice fed the high-cholesterol diet; #*P*<0.05 vs. *n/i/eNOS*^{-/-} mice fed the regular diet.

Blood Pressure in WT and NOS^{-/-} Mice Fed a High-Cholesterol Diet

Arterial blood pressure (mmHg) was significantly elevated in the eNOS^{-/-} (118.4±2.5), i/eNOS^{-/-} (117.8±1.2), n/eNOS^{-/-} (123.4±5.9), and n/i/eNOS^{-/-} mice (126.7±11.2) as compared with the WT mice (103.4±5.2) (n=7-9, each *P*<0.05). There was no significant difference in the hypertension levels among those genotypes.

Cardiac ACE activity in WT and NOS^{-/-} Mice Fed a High-Cholesterol Diet

We next examined whether or not the renin-angiotensin system is activated in the high-cholesterol diet-fed triply n/i/eNOS^{-/-} mice. The cardiac ACE activities in the high-cholesterol diet were significantly enhanced only in the triply n/i/eNOS^{-/-} genotype, but not in any singly or doubly NOS^{-/-} genotypes, as compared with the WT genotype (Supplementary Figure II). In the triply n/i/eNOS^{-/-} genotype, the cardiac ACE activities tended to increase in the high-cholesterol diet than in the regular diet, although the difference did not reach a statistically significant level (Supplementary Figure II).

Urinary 8-Isoprostane Level in WT and NOS^{-/-} Mice Fed a High-Cholesterol Diet

The urinary levels of 8-isoprostane, a marker of oxidative stress, in the high-cholesterol diet, were also significantly increased only in the triply n/i/eNOS^{-/-} genotype compared with the WT genotype (Supplementary Figure III). In the triply n/i/eNOS^{-/-} genotype, the urinary 8-isoprostane levels were significantly higher in the high-cholesterol diet than in the regular diet (Supplementary Figure III).

Serum CRP Level in WT and NOS^{-/-} Mice Fed a High-Cholesterol Diet

There was no significant difference in the serum CRP levels, a marker of inflammation, in the WT or NOS^{-/-} genotypes fed the regular or high-cholesterol diet (Supplementary Figure IV). This negative result might be because CRP is a useful marker of inflammation in humans, but not in mice.¹⁷

Serum ApoE Levels and Small Intestinal Cholesterol Transporter Expression in Triply n/i/eNOS^{-/-} Mice Fed a High-Cholesterol Diet

We finally studied the mechanism(s) for the diet-induced dyslipidemia in the triply n/i/eNOS^{-/-} mice. There was no significant difference in serum apoE levels in the WT and triply n/i/eNOS^{-/-} genotypes.

Also, no significant difference was noted in the expression levels of the cholesterol transporter NPC1L1 in the small intestine in the two genotypes (Figure 6B).

Hepatic LDL Receptor Expression and SREBP-2 Activity in Triply n/i/eNOS^{-/-} Mice Fed a High-Cholesterol Diet

Notably, the expression levels of the hepatic LDL receptor, which introduces circulating LDL into hepatocytes, were significantly and markedly reduced only in the triply n/i/eNOS^{-/-} genotype, but not in

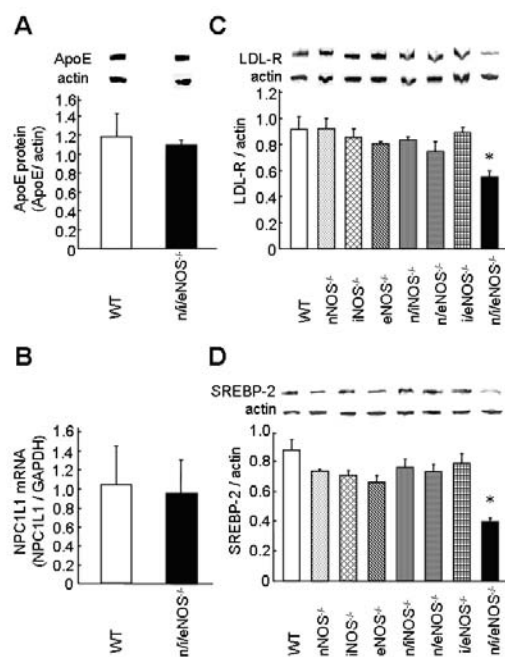


Figure 6

any singly or doubly NOS^{-/-} genotypes, as compared with the WT genotype (Figure 6C). Furthermore, the activity of SREBP-2 (68-kDa, activated form), which regulates the expression of the LDL receptor, was also significantly lower only in the triply *n/i/eNOS*^{-/-} genotype (Figure 6D).

Discussion & Conclusion

The major novel findings of the present study are that mice devoid of all three NOS genes develop severe diet-induced dyslipidemia, atherosclerotic vascular lesion formation, and cardiovascular death via reduced expression of the hepatic LDL receptor. To the best of our knowledge, this is the first study that demonstrates that the defective NOS system is linked to the pathogenesis of diet-induced dyslipidemia.

Role of the NOS System in the Regulation of Lipid Metabolism

Non-selective L-arginine analogues, such as *N*^ω-nitro-L-arginine (L-NNA) or *N*^ω-nitro-L-arginine methyl ester (L-NAME), have been widely used as pharmacological tools to inhibit NO synthesis derived from the whole NOS system. Although the role of the NOS system in lipid metabolism has been studied with those L-arginine analogues, the obtained results are conflicting, such that the NOS system has been suggested to be both essential¹⁸ and nonessential¹⁹ for lipid metabolism in rats. This inconsistency may be due to their multiple non-specific actions.²⁰⁻²³ Indeed, we clarified the NO-independent vascular actions of L-arginine analogues. Although long-term treatment with L-arginine analogues had long been believed without doubt to simply inhibit vascular NO synthesis and cause arteriosclerotic vascular lesion formation, we found that the long-term vascular effects of L-arginine analogues are not solely mediated by the simple inhibition of NO synthesis.^{9,24} Activation of the tissue renin-angiotensin system and increased oxidative stress, independent of endogenous NO inhibition, are involved in the long-term vascular effects of those analogues.^{9,24} These findings questioned the previous theory regarding the effects of L-arginine analogues, and warranted re-evaluation of previous studies using those analogues.^{9,24} Thus, the authentic role of the NOS system in lipid metabolism still remains to be fully elucidated.

In this study, in response to the high-cholesterol diet, the triply NOS^{-/-} mice, but not the singly or doubly NOS^{-/-} mice, exhibited marked increases in serum total cholesterol levels. These increases were due to alterations in the serum levels of LDL cholesterol and small dense LDL particles, both of which are important cardiovascular risk factors,²⁵ but not alterations in the serum levels of HDL cholesterol or triglyceride. These results indicate that the whole NOS system plays a key role in the regulation of lipid metabolism. Consistent with the evidence, NO supplementation by overexpression of the eNOS gene in transgenic mice decreases plasma total and LDL cholesterol levels.²⁶

Several lines of evidence suggest the association of the defective NOS system with dyslipidemia in humans. First, it has been reported that plasma NO_x (nitrite plus nitrate) levels, which are markers of NO production derived from all three types of NOS in vivo, are reduced in patients with hyperlipidemia.²⁷ Second, it has been revealed that lower plasma NO_x levels are significantly correlated with higher plasma total and LDL cholesterol levels.²⁷ Finally, plasma concentrations of

asymmetric dimethylarginine, which is an endogenous NOS inhibitor, have been shown to be elevated in hypercholesterolemic individuals.²⁸ These results may imply the clinical significance of the present findings with the triply mutant mice.

The reason why the singly or doubly NOS^{-/-} mice fed the high-cholesterol diet did not show significant dyslipidemia may be due to a compensatory mechanism by other NOSs that are not disrupted genetically. Indeed, we have revealed that other NOSs are expressed in the singly and doubly NOS^{-/-} mice,^{5,29} and that NOS activity and NOx production are fairly well preserved in those genotypes.⁵

Atherosclerosis and Sudden Cardiac Death in Triply NOS^{-/-} Mice Fed a High-Cholesterol Diet

Since atherogenic lipoproteins were increased in the triply NOS^{-/-} mice, we next studied atherosclerotic vascular lesion formation. Cholesterol deposits, atheromatous plaques, conglomerated foamy macrophages, and necrotic lipid cores with fibrous caps were present in the aorta of the triply NOS^{-/-} mice fed the high-cholesterol diet, all of which findings are recognized in both the early and advanced stages of human atherosclerosis. Thus, the features of the atherosclerotic lesions that were developed in the triply NOS^{-/-} mice are similar to those described in humans,³⁰ and therefore represent an important model for human dyslipidemia and atherosclerosis.

Since some triply NOS^{-/-} mice died during the cholesterol-rich feeding, we then performed a postmortem histopathological analysis to identify the cause of death. Markedly accelerated coronary vascular lesion formation and pulmonary congestion were noted in all the dead triply NOS^{-/-} mice, and old myocardial infarction and giant organized thrombi in both ventricles were found in some of them. Thus, it is likely that the triply NOS^{-/-} mice died due to the cause of cardiovascular death, such as myocardial ischemia-evoked malignant arrhythmia or heart failure.

Considerations of Statin Therapy in Triply NOS^{-/-} Mice Fed a High-Cholesterol Diet

Statins (3-hydroxy-3-methylglutaryl coenzyme A reductase inhibitors) are potent blockers of cholesterol biosynthesis, and widely used in the treatment of hypercholesterolemia. A number of large clinical trials have demonstrated their clinical usefulness for preventing cardiovascular events, such as myocardial infarction and sudden cardiac death. Thus, it is interesting to speculate the potential effect of statin therapy in the triply NOS^{-/-} mice. However, our preliminary study indicated that long-term treatment with a statin did not significantly decrease plasma LDL cholesterol levels in the triply NOS^{-/-} mice (unpublished observations). Previous studies also reported that statins do not reduce, but rather elevates, plasma LDL levels in high-cholesterol diet-fed apoE^{-/-} mice.³¹ Whether statin therapy is beneficial in the treatment of atherosclerosis and cardiovascular death in the triply NOS^{-/-} mice fed the high-cholesterol diet through lipid lowering-independent actions remains to be examined in a future study.

Mechanism for Diet-Induced Atherosclerosis in Triply n/i/eNOS^{-/-} Mice

Whereas blood pressure was significantly elevated in the eNOS-disrupted singly, doubly, and triply NOS^{-/-} mice to a comparable extent, significant atherosclerosis was noted only in the triply NOS^{-/-} genotype, suggesting a minor role of hypertension in the development of the diet-induced

atherosclerosis in the genotype. On the other hand, significant increases in cardiac ACE activities and urinary 8-isoprostane levels were noted in the high-cholesterol diet-fed triply NOS^{-/-} mice. Thus, it is conceivable that the activation of the renin-angiotensin system and increased oxidative stress may be involved in the diet-induced atherosclerosis.

Mechanism for Diet-Induced Dyslipidemia in Triply n/i/eNOS^{-/-} Mice

Finally, we examined the mechanism(s) for dyslipidemia in the triply NOS^{-/-} mice fed the cholesterol-rich diet. Since the extent of the diet-induced dyslipidemia in the triply NOS^{-/-} mice was equivalent to that in apoE^{-/-} mice, we first analyzed the serum apoE levels. However, no defect of serum apoE was seen in the triply NOS^{-/-} mice. We next examined the kinetics of the cholesterol absorption and degradation machineries. Dietary cholesterol is absorbed into the body through the cholesterol transporter NPC1L1 in the small intestine, and circulating LDL cholesterol in the blood is bound to the LDL receptor in the liver, taken up and broken down by hepatocytes. The expression levels of the small intestinal NPC1L1 were not altered in the triply NOS^{-/-} mice, whereas the expression levels of the hepatic LDL receptor were markedly reduced only in the triply NOS^{-/-} mice, in parallel with alterations in the serum LDL cholesterol levels. SREBP-2 was discovered as a transcriptional factor that controls LDL receptor gene expression.³² The activity of SREBP-2 was also diminished only in the triply NOS^{-/-} mice. Thus, it is possible that the lower expression of the hepatic LDL receptor mediated by reduced SREBP-2 activity is involved in the diet-induced dyslipidemia in the triply NOS^{-/-} genotype.

In conclusion, we were able to prove that complete disruption of the entire NOS system causes severe diet-induced dyslipidemia, lipid-rich atherosclerotic lesion formation, and sudden cardiac death in mice in vivo through the down-regulation of the hepatic LDL receptor, demonstrating the critical role of the whole endogenous NO/NOS system in the regulation of lipid metabolism.

References

- 1) Ignarro LJ. Biosynthesis and metabolism of endothelium-derived nitric oxide. *Annu Rev Pharmacol Toxicol* 1990;**30**:535-560.
- 2) Moncada S, Palmer RMJ, Higgs EA. Nitric oxide: physiology, pathophysiology, and pharmacology. *Pharmacol Rev* 1991;**43**:109-142.
- 3) Murad F. What are the molecular mechanisms for the antiproliferative effects of nitric oxide and cGMP in vascular smooth muscle? *Circulation* 1997;**95**:1101-1103.
- 4) Tsutsui M, Shimokawa H, Otsuji Y, Ueta Y, Sasaguri Y, Yanagihara N. Nitric oxide synthases and cardiovascular diseases: insights from genetically modified mice. *Circ J* 2009;**73**:986-993.
- 5) Morishita T, Tsutsui M, Shimokawa H, Sabanai K, Tasaki H, Suda O *et al.* Nephrogenic diabetes insipidus in mice lacking all nitric oxide synthase isoforms. *Proc Natl Acad Sci U S A* 2005;**102**:10616-10621.
- 6) Tsutsui M, Shimokawa H, Morishita T, Nakashima Y, Yanagihara N. Development of genetically engineered mice lacking all three nitric oxide synthases. *J Pharmacol Sci* 2006;**102**:147-154.

- 7) Nakata S, Tsutsui M, Shimokawa H, Suda O, Morishita T, Shibata K *et al.* Spontaneous myocardial infarction in mice lacking all nitric oxide synthase isoforms. *Circulation* 2008;**117**:2211-2223.
- 8) Tsutsui M, Nakata S, Shimokawa H, Otsuji Y, Yanagihara N. Spontaneous myocardial infarction and nitric oxide synthase. *Trends Cardiovasc Med* 2008;**18**:275-279.
- 9) Suda O, Tsutsui M, Morishita T, Tanimoto A, Horiuchi M, Tasaki H *et al.* Long-term treatment with N(omega)-nitro-L-arginine methyl ester causes arteriosclerotic coronary lesions in endothelial nitric oxide synthase-deficient mice. *Circulation* 2002;**106**:1729-1735.
- 10) Usui S, Hara Y, Hosaki S, Okazaki M. A new on-line dual enzymatic method for simultaneous quantification of cholesterol and triglycerides in lipoproteins by HPLC. *J Lipid Res* 2002;**43**:805-814.
- 11) Morishita T, Tsutsui M, Shimokawa H, Horiuchi M, Tanimoto A, Suda O *et al.* Vasculoprotective roles of neuronal nitric oxide synthase. *FASEB J* 2002;**16**:1994-1996.
- 12) Gharavi NM, Baker NA, Mouillesseaux KP, Yeung W, Honda HM, Hsieh X *et al.* Role of endothelial nitric oxide synthase in the regulation of SREBP activation by oxidized phospholipids. *Circ Res* 2006;**98**:768-776.
- 13) Bradford MM. A rapid and sensitive method for the quantitation of microgram quantities of protein utilizing the principle of protein-dye binding. *Anal Biochem* 1976;**72**:248-254.
- 14) Duval C, Touche V, Tailleux A, Fruchart JC, Fievet C, Clavey V *et al.* Niemann-Pick C1 like 1 gene expression is down-regulated by LXR activators in the intestine. *Biochem Biophys Res Commun* 2006;**340**:1259-1263.
- 15) Plump AS, Smith JD, Hayek T, Aalto-Setälä K, Walsh A, Verstuyft JG *et al.* Severe hypercholesterolemia and atherosclerosis in apolipoprotein E-deficient mice created by homologous recombination in ES cells. *Cell* 1992;**71**:343-353.
- 16) Zhang SH, Reddick RL, Piedrahita JA, Maeda N. Spontaneous hypercholesterolemia and arterial lesions in mice lacking apolipoprotein E. *Science* 1992;**258**:468-471.
- 17) Pepys MB, Hirschfield GM. C-reactive protein: a critical update. *J Clin Invest* 2003;**111**:1805-1812.
- 18) Khedara A, Kawai Y, Kayashita J, Kato N. Feeding rats the nitric oxide synthase inhibitor, L-N(omega)-nitroarginine, elevates serum triglyceride and cholesterol and lowers hepatic fatty acid oxidation. *J Nutr* 1996;**126**:2563-2567.
- 19) Navarro J, Sanchez A, Saiz J, Ruilope LM, Garcia-Estan J, Romero JC *et al.* Hormonal, renal, and metabolic alterations during hypertension induced by chronic inhibition of NO in rats. *Am J Physiol* 1994;**267**:R1516-1521.
- 20) Buxton ILO, Cheek DJ, Eckman D, Westfall DP, Sanders KM, Keef KD. N^G-nitro-L-arginine methyl ester and other alkyl esters of arginine are muscarinic receptor antagonists. *Circ Res* 1993;**72**:387-395.
- 21) Heim KF, Thomas G, Ramwell PW. Effect of substituted arginine compounds on superoxide production in the rabbit aorta. *J Pharmacol Exp Ther* 1991;**257**:1130-1135.
- 22) Peterson DA, Peterson DC, Archer S, Weir EK. The nonspecificity of specific nitric oxide synthase inhibitors. *Biochem Biophys Res Commun* 1992;**187**:797-801.

- 23) Thomas G, Ramwell PW. N^{ϵ} -nitro-L-arginine benzyl ester, a potent irreversible inhibitor of endothelium dependent relaxation. *Biochem Biophys Res Commun* 1991;**179**:1677-1682.
- 24) Suda O, Tsutsui M, Morishita T, Tasaki H, Ueno S, Nakata S *et al.* Asymmetric dimethylarginine produces vascular lesions in endothelial nitric oxide synthase-deficient mice. *Arterioscler Thromb Vasc Biol* 2004;**24**:1682-1688.
- 25) Sniderman AD, Furberg CD, Keech A, Roeters van Lennep JE, Frohlich J, Jungner I *et al.* Apolipoproteins versus lipids as indices of coronary risk and as targets for statin treatment. *Lancet* 2003;**361**:777-780.
- 26) van Haperen R, de Waard M, van Deel E, Mees B, Kutryk M, van Aken T *et al.* Reduction of blood pressure, plasma cholesterol, and atherosclerosis by elevated endothelial nitric oxide. *J Biol Chem* 2002;**277**:48803-48807.
- 27) Tanaka S, Yashiro A, Nakashima Y, Nanri H, Ikeda M, Kuroiwa A. Plasma nitrite/nitrate level is inversely correlated with plasma low-density lipoprotein cholesterol level. *Clin Cardiol* 1997;**20**:361-365.
- 28) Boger RH, Bode-Boger SM, Szuba A, Tsao PS, Chan JR, Tangphao O *et al.* Asymmetric dimethylarginine (ADMA): a novel risk factor for endothelial dysfunction: its role in hypercholesterolemia. *Circulation* 1998;**98**:1842-1847.
- 29) Takaki A, Morikawa K, Tsutsui M, Murayama Y, Tekes E, Yamagishi H *et al.* Crucial role of nitric oxide synthases system in endothelium-dependent hyperpolarization in mice. *J Exp Med* 2008;**205**:2053-2063.
- 30) Libby P. The vascular biology of atherosclerosis. In: Libby P, Bonow R, Mann D, Zipes D, eds. Braunwald's Heart Disease. Philadelphia: Saunders Elsevier, 2008:985-1002.
- 31) Nachtigal P, Jamborova G, Pospisilova N, Pospechova K, Solichova D, Zdansky P *et al.* Atorvastatin has distinct effects on endothelial markers in different mouse models of atherosclerosis. *J Pharm Pharm Sci* 2006;**9**:222-230.
- 32) Hua X, Yokoyama C, Wu J, Briggs MR, Brown MS, Goldstein JL *et al.* SREBP-2, a second basic-helix-loop-helix-leucine zipper protein that stimulates transcription by binding to a sterol regulatory element. *Proc Natl Acad Sci U S A* 1993;**90**:11603-11607.

Mechanism of chromosome segregation control by molecules involved in spindle assembly checkpoint

Kozo Tanaka

Institute of Development, Aging and Cancer, Tohoku University

k.tanaka@idac.tohoku.ac.jp

Abstract

Proper chromosome segregation at each cell division is essential for maintenance of genetic information. Among mechanisms for accurate chromosome segregation, the spindle assembly checkpoint (SAC) is a mechanism to prevent anaphase onset until proper kinetochore-microtubule interaction is established on all the chromosomes. Many of the SAC-related molecules were involved in forming proper kinetochore-microtubule interaction as well. We searched for molecules associated with the SAC-related molecules to find novel regulators for chromosome segregation. A novel protein, C13orf8, was found as an interacting molecule with MAD2L2, one of the homologues of the yeast SAC component, MAD2. C13orf8 is a zinc-finger protein and localizes on both chromosomes and the spindle. We found that mitotic cells increased after knockdown of C13orf8, and many chromosomes did not align on the metaphase plate. In immunofluorescence analyses of C13orf8-depleted cells, we observed kinetochores in metaphase cells not properly attaching to microtubules, and decreased sister-kinetochore distance, suggesting that C13orf8 is involved in kinetochore-microtubule attachment. Live-cell imaging revealed that in C13orf8-depleted cells, many chromosomes once aligned on, but then delocalized from the metaphase plate, concomitantly with the disconnection of kinetochore-microtubule attachment. These data imply that C13orf8 is involved in maturation of microtubules attaching to kinetochores (K-fibers) or maintenance of kinetochore-microtubule interaction when tension is exerted between sister kinetochores.

Keywords: chromosome segregation, kinetochore, microtubule, spindle

Introduction

Proper chromosome segregation at each cell division is essential for maintenance of genetic information. Among mechanisms for accurate chromosome segregation, the spindle assembly checkpoint (SAC) is a mechanism to prevent anaphase onset until proper kinetochore-microtubule interaction is established on all the chromosomes¹. The SAC mechanism is well conserved from yeast to human, but it is regulated more finely in human cells, partly by human-specific molecules. Dysfunction of such a fine regulation may lead to oncogenic transformation through the induction of chromosomal instability. In addition, it has recently been revealed that many SAC-related molecules are not only involved in arresting cells at mitosis in the presence of defective kinetochore-microtubule attachment, but also in the establishment of correct kinetochore-microtubule attachment itself. Therefore, we screened for molecules interacting with known SAC-related molecules in human

cells using proteomic approach. We isolated a novel protein, C13orf8, as an interacting protein with MAD2L2, one of the homologues of the yeast SAC component, Mad2, and investigated the functions of the protein.

Results

C13orf8 is a zinc-finger protein containing several characteristic repeat motifs (Fig. 1). C13orf8 localizes on both chromosomes and spindle (Fig. 2), and is phosphorylated mainly in mitosis. C13orf8 was not involved directly in the SAC like MAD2L2, as C13orf8-depleted cells arrested in mitosis in the presence of nocodazole or taxol. Instead, early cell death was induced in mitotically-arrested C13orf8-depleted cells, suggesting a role of C13orf8 in cell survival in the SAC-activated

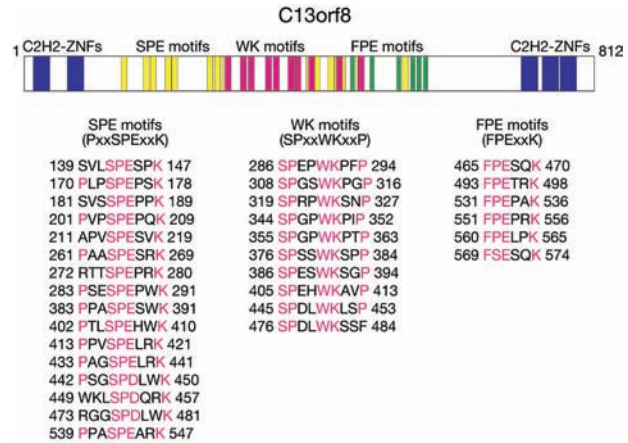


Figure 1 Structure of C13orf8

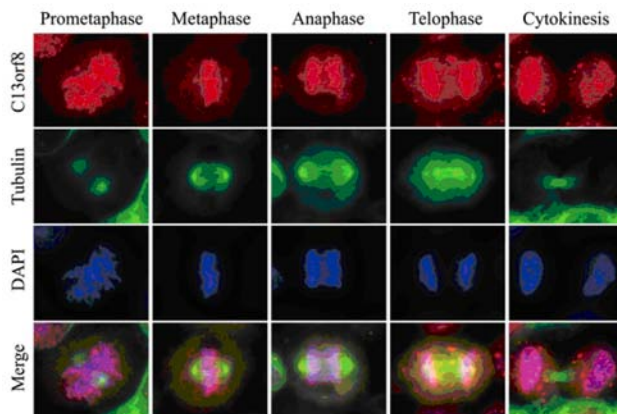


Figure 2 Localization of C13orf8 in mitotic cells

cells. Interestingly, many chromosomes in C13orf8-depleted cells did not align on the metaphase plate in mitosis. In immunofluorescence analyses of C13orf8-depleted cells, we found that kinetochores did not properly attach to microtubules in mitotic cells, suggesting that C13orf8 is involved in kinetochore-microtubule attachment (Fig. 3). Live-cell imaging revealed that in C13orf8-depleted cells, many chromosomes once aligned on, but then delocalized from the metaphase plate, concomitantly with the disconnection of kinetochore-microtubule attachment.

Discussion & Conclusion

In this study, we reported the identification of a previously uncharacterized molecule, C13orf8, as a novel player involved in kinetochore-microtubule attachment. We found that C13orf8 is a phosphoprotein that localizes on chromosomes and spindle. C13orf8-depleted cells were arrested in mitosis and could not maintain chromosome

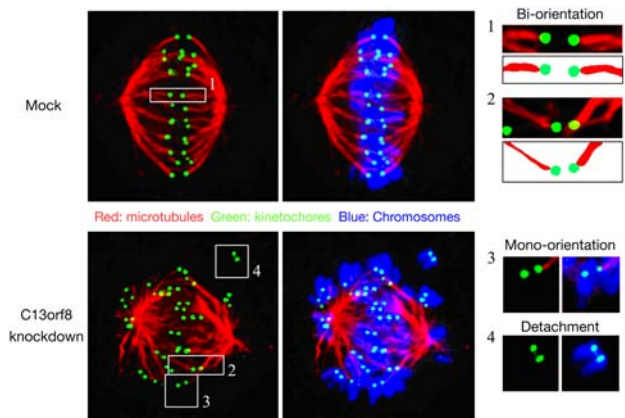


Figure 3 Kinetochore-microtubule attachment in C13orf8-knockdown cells

alignment during the mitotic arrest. Our data imply that C13orf8 is involved in maturation of microtubules attaching to kinetochores (K-fibers) or maintenance of kinetochore-microtubule interaction when tension is exerted between sister kinetochores (Fig. 4). C13orf8 also plays a role in maintaining cell viability during mitotic arrest. As C13orf8 is conserved only among vertebrates, it is probably involved in a fine regulation of chromosome segregation in higher eukaryotes. We are now investigating the functions of C13orf8 further.

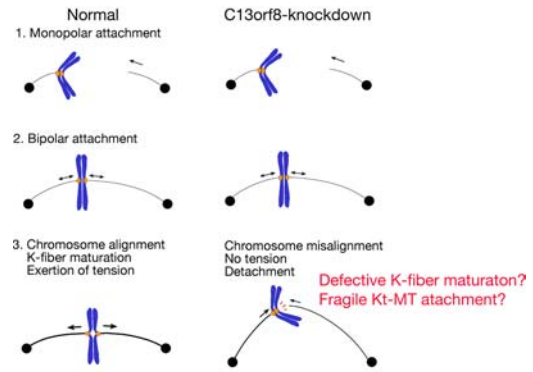


Figure 4 Putative role of C13orf8 in mitotic progression

References

- 1) Tanaka, K, and Hirota, T. Chromosome segregation machinery and cancer. *Cancer Sci* (2009) **100**, p1158-1165.

Molecular mechanism of trans-association of Tie2, a receptor for angiopoietin-1, and its biological significance

Shigetomo Fukuhara

National Cerebral and Cardiovascular Center Research Institute

fuku@ri.ncvc.go.jp

Abstract

Angiopoietin-1 (Ang1) regulates both vascular quiescence and angiogenesis through the receptor tyrosine kinase Tie2. We have recently shown that Ang1 and Tie2 form distinct signaling complexes at cell-cell and cell-matrix contacts, and further demonstrated that the former selectively induces expression of Krüppel-like factor 2 (KLF2), a zinc finger family of transcription factor involved in vascular quiescence. Here, we investigated the mechanism how trans-associated Tie2 induces KLF2 expression to clarify the role of KLF2 in trans-associated Tie2-mediated vascular quiescence. We found that Ang1 induces KLF2 expression through a phosphoinositide 3-kinase (PI3K)/Akt-dependent activation of myocyte enhancer factor 2 (MEF2), and that Ang1-induced KLF2 expression attenuates vascular endothelial growth factor-mediated inflammation. Collectively, these findings indicate that trans-associated Tie2 stimulates transcriptional activity of MEF2 through a PI3K/AKT pathway, thereby inducing KLF2 expression and contributing to the maintenance of vascular quiescence.

Keywords: Angiopoietin-1, Tie2, vascular quiescence

Introduction

Angiopoietin-1 (Ang1) is a ligand for endothelium-specific receptor tyrosine kinase Tie2. Mice deficient in either Ang1 or Tie2 exhibit embryonic lethality because of the impaired vascular maturation, revealing the essentiality of Ang1/Tie2 signal for developmental vascular formation(1;2). In adult vasculature, Ang1/Tie2 signaling is thought to regulate both maintenance of vascular quiescence and promotion of angiogenesis(1;2). However, it has been unknown how Tie2 signal regulates these distinct biological functions. Recently, we have reported that Ang1 assembles distinct Tie2 signaling complexes in the presence or absence of cell-cell junctions(3). Ang1 bridges Tie2 at cell-cell contacts, resulting in *trans*-association of Tie2 in the presence of cell-cell contacts. In clear contrast, in the isolated cells, extracellular matrix (ECM)-bound Ang1 locates Tie2 to cell-substratum interface. Furthermore, trans-associated Tie2 at cell-cell junctions preferentially activates phosphoinositide 3-kinase (PI3K)/Akt signaling pathway, thereby promoting endothelial cell survival and vascular stability. On the other hand, ECM-anchored Tie2 at cell-substratum contacts stimulates Erk1/2 signaling pathway leading to enhanced endothelial cell migration and proliferation, which are responsible for angiogenesis.

We further performed DNA microarray analyses to identify the genes regulated by trans-associated Tie2 and ECM-anchored Tie2. Ang1 regulated distinct sets of genes in the presence or absence of

cell-cell contacts(3). It is noteworthy that, in the presence of cell-cell contacts, Ang1 up-regulated the genes involved in vascular stabilization, which include *Krüppel-like factor 2 (KLF2)*, *zinc finger protein 36*, *C3H type-like 2*, *connexin 40*, *delta-like1* and *delta-like 4(3)*. KLF2 is a zinc finger-family of transcription factor that maintains vascular quiescence by regulating the genes involved in angiogenesis, inflammation and thrombosis. In this study, we investigated the signaling mechanism involved in trans-associated Tie2-induced KLF2 expression and its role in vascular stabilization.

Results

Trans-associated Tie2 induces KLF2 expression.

To confirm the data of DNA microarray analyses, we performed quantitative real time-PCR and western blot analyses. COMP-Ang1, a potent activator for Tie2, induced KLF2 mRNA and protein expression in human umbilical vein endothelial cells (HUVECs) under confluent culture condition, but not under sparse condition. These results suggest that KLF2 expression is selectively induced by trans-associated Tie2, but not by ECM-anchored Tie2.

KLF2 expression by trans-associated Tie2 involves MEF2 transcription factor, but does not require Erk5.

Laminar shear stress potently induces KLF2 expression in endothelial cells. It has been reported that shear stress-induced KLF2 expression occurs through phosphorylation of myocyte enhancer factor 2 (MEF2), a MADS-box family of transcription factor, by Erk5 kinase. Thus, we examined whether trans-associated Tie2 also induces KLF2 expression by stimulating an Erk5-MEF2 signaling pathway. COMP-Ang1-induced KLF2 expression was prevented by knocking down of MEF2. Consistently, COMP-Ang1 stimulated KLF2 promoter activity in a MEF2-binding element-dependent manner. However, COMP-Ang1 did not induce Erk5 activation under confluent condition. In addition, depletion of Erk5 by siRNA did not affect COMP-Ang1-induced KLF2 expression. These results indicate that KLF2 expression by trans-associated Tie2 involves MEF2, but is not mediated by Erk5.

Trans-associated Tie2 induces KLF2 expression through PI3K/Akt signaling axis.

We investigated the involvement of PI3K/Akt signaling axis in trans-associated Tie2-induced KLF2 expression, since Ang1 stimulates PI3K/Akt pathway selectively in the presence of cell-cell contacts. Inhibitors for PI3K and Akt and the depletion of Akt by siRNA blocked COMP-Ang1-induced KLF2 expression, indicating that a PI3K/Akt pathway is indispensable for trans-associated Tie2-induced KLF2 expression.

PI3K/Akt pathway induces KLF2 expression by stimulating the transcriptional activity of MEF2.

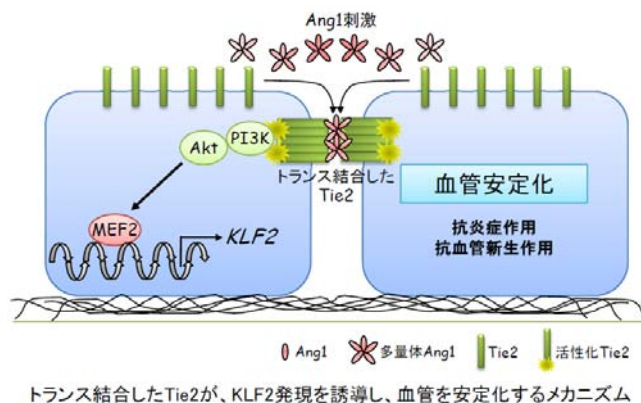
We performed luciferase reporter assay to investigate whether PI3K/Akt pathway stimulates the transcriptional activity of MEF2. Constitutive active mutants of PI3K (PI3K-CA) and Akt (Akt-CA) induced luciferase expression in the HUVECs transfected with the plasmid encoding luciferase reporter gene under the control of a single MEF2 site (MEF2-Luc). To further investigate the effect of PI3K-CA and Akt-CA on the transcriptional activity of MEF2, we fused full-length MEF2C with

DNA-binding domain of Gal4 (Gal4-MEF2C). PI3K-CA and Akt-CA significantly stimulated the transcriptional activity of Gal4-MEF2C, but not that of Gal4. COMP-Ang1 also increased in the transcriptional activity of Gal4-MEF2C. These findings indicate that trans-associated Tie2 enhances the transcriptional activity of MEF2 through a PI3K/Akt signaling pathway.

We further investigated whether PI3K/Akt pathway enhances KLF2 promoter activity by stimulating the transcriptional activity of MEF2. PI3K-CA and Akt-CA stimulated the KLF2 promoter activity, and these stimulatory effects were significantly augmented by the co-expression of MEF2C. Furthermore, adenovirus-mediated over-expression of Akt-CA potently induced both mRNA and protein expression of KLF2 in HUVECs. Collectively, these results suggest that trans-associated Tie2 induces KLF2 expression through a PI3K/Akt/MEF2 signaling axis.

Trans-associated Tie2 inhibits vascular endothelial growth factor-mediated inflammation through KLF2.

Ang1/Tie2 signal is known to inhibit the inflammatory responses mediated by vascular endothelial growth factor (VEGF). It has been also shown that KLF2 has potent anti-inflammatory effects on the vascular endothelium. Therefore, we hypothesized that trans-associated Tie2 inhibits VEGF-induced inflammation through KLF2. To address this possibility, we examined the effect of siRNA-mediated KLF2 depletion on the anti-inflammatory function of Ang1/Tie2 signal. VEGF induced expression of vascular cell adhesion molecule-1 (VCAM1) and enhanced the adhesion of monocytes to HUVECs. COMP-Ang1 partially inhibited VEGF-induced VCAM1 expression and VEGF-induced monocyte adhesion to HUVECs. However, these inhibitory effects of COMP-Ang1 were blunted by depletion of KLF2. These results reveal that trans-associated Tie2 attenuates VEGF-induced inflammation through induction of KLF2.



Discussion & Conclusion

In this study, we found that trans-associated Tie2 at cell-cell junctions induces KLF2 expression by stimulating the transcriptional activity of MEF2 through a PI3K/Akt axis in endothelial cells(4). In addition, KLF2 expression by trans-associated Tie2 inhibits VEGF-induced inflammation(4). KLF2 not only has anti-inflammatory effect but also acts as an inhibitor of angiogenesis. Indeed, it has been reported that KLF2 inhibits VEGF-induced angiogenesis. Therefore, KLF2 may be involved in the

maintenance of vascular quiescence mediated by trans-associated Tie2. Further examination is required for clarifying the in vivo role of KLF2 in trans-associated Tie2-mediated vascular stabilization.

References

- 1) Fukuhara S., Sako K., Noda K., Nagao K., Miura K., Mochizuki N.: Tie2 is tied at the cell-cell contacts and to extracellular matrix by Angiopoietin-1. *Exp. Mol. Med.* **41**:133-139, 2009
- 2) Fukuhara S., Sako K., Noda K., Zhang J., Minami M., Mochizuki N.: Angiopoietin-1/Tie2 receptor signaling in vascular quiescence and angiogenesis. *Histol. Histopathol.* **25**:387-396, 2010
- 3) Fukuhara S., Sako K., Minami T., Noda K., Kim H. Z., Kodama T., Shibuya M., Takakura N., Koh G. Y., Mochizuki N.: Differential function of Tie2 at cell-cell contacts and cell-substratum contacts regulated by angiopoietin-1. *Nat. Cell Biol.* **10**:513-526, 2008
- 4) Sako K., Fukuhara S., Minami T., Hamakubo T., Song H., Kodama T., Fukamizu A., Gutkind J.S., Koh G.Y., Mochizuki N.: Angiopoietin-1 induces Kruppel-like factor 2 expression through a phosphoinositide 3-kinase/AKT-dependent activation of myocyte enhancer factor 2. *J. Biol. Chem.* **284**:5592-5601, 2009

III.

Reports from the Recipients of Grants for International Meetings

2009 29th INTERNATIONAL SYMPOSIUM ON CANCER

1. Representative

Masanori Hatakeyama

2. Opening period and Place

July 13-14, 2009 / The Hokkaido University conference hall Sapporo, Japan

3. Number of participants / Number of participating countries and areas

Number of participants: 100

Number of participating countries: 9

Areas: Japan, USA, UK, Germany, Canada, Australia, Singapore, New Zealand, Indonesia

4. Total cost

¥11,208,066JPY

5. Main use of subsidy

Invitation fee

6. Result and Impression

The 29th Sapporo Cancer Seminar Symposium entitled “*Helicobacter pylori* and Gastric Cancer” was held in July 13-14, 2009 at the Conference Hall of Hokkaido University, with 100 participants including 20 participants from abroad.

The symposium consisted of 6 Scientific Sections. In Session 1, genetic and epigenetic factors involved in gastric carcinogenesis such as *Helicobacter pylori* infection, EB virus infection and E-cadherin mutation were discussed. Session 2 focused on the nature of gastric cancer stem cells. In Session 3, the role of inflammation in the development of gastric cancer was extensively discussed. In this session importance of inflammatory cytokines and their down-stream targets in carcinogenesis was emphasized. Also, importance of host genetic factors in determining susceptibility to gastric cancer was discussed. Furthermore, systemic analysis for the epigenetic changes in genome during chronic *H. pylori* infection was presented. In Session 4, roles of *H. pylori* virulence factors such as VacA, OipA and DupA in the mucosal damages were discussed. Section V aimed to uncover the role of *H. pylori* oncoprotein CagA in the transformation of gastric epithelial cells, particularly focusing on the molecular mechanisms of CagA delivery and intracellular signaling pathways perturbed by host cell-injected CagA, with the use of state-of-arts real-time imaging system, *Drosophila* genetics and genetically engineered mice. In Session 6, clinical prevention of gastric cancer by eradication of *H. pylori* was discussed. In this session,

clinical application of CagA polymorphism in identifying high-risk populations for gastric cancer was also considered. Throughout the symposium, scientific levels of presentations were extremely high and the discussions were substantial, exciting and fruitful. In the afternoon of July 13, 20 posters were presented by young researchers. During coffee breaks and banquet, participants had a chance to know each other and to develop scientific relationship, which will be helpful for future collaborations. I concluded that the symposium was one of the best symposiums on Gastric Cancer to be held in Japan in recent years.

*5th International Symposium on Autophagy:
Molecular mechanism, cellular and physiological functions, and diseases*

1. Representative

Yasuyoshi Sakai, Ph.D.

2. Opening period and Place

September 24th ~ 28th, 2009, Otsu Prince Hotel, Otsu, Japan

3. Number of participants / Number of participating countries and areas

231 participants/ 22 countries and areas

4. Total cost

¥28,844,505JPY

5. Main use of subsidy

Traveling fees for Dr. Beth Levine (USA) and Dr. Patrice Codogno (France)

6. Result and Impression

We are happy to state that the 5th International Symposium on Autophagy (ISA) ended in a perfect success. This symposium was originally held in 1997, and since then a growing number of researchers have come to attend the series of its following meetings. This is mostly owing to the rapid development of autophagy research in the last decade, especially regarding the elucidation of its molecular mechanism. At the same time, the physiological importance of autophagy has been revealed to a great extent, such as its involvement in metastasis, neurogenic disorders, or developmental processes. These progresses led to a boost for the participation of both basic researchers and medical workers in this symposium.

In the 5th ISA, there was an outstanding increase in the participation numbers from Asian nations, namely P. R. China, Taiwan, and South Korea. Three oral presentations were done by the distinguished researchers in this region (Dr. Hong Zhang and Wei-Pang Huang as programmed oral speakers, and Dr. Li Yu as a selected speaker from Poster applications). Interestingly, all of their presentations belonged to basic science field, giving us strong impression of their growing contributions to this field.

As a new trend of this symposium, we set a session specialized in autophagy studies on plant physiology and pathology. This included a talk by Dr. Nicholas Talbot from UK, who worked very extensively on the pathogenesis of some fungi species to rice plants. The talk told us much about the importance of autophagy in cell differentiation of the fungi, in good

analogy with other kingdoms of living things.

In addition to the fundamental research of autophagy, some pioneering studies are now heading for the discovery of chemical substances that affect autophagic activities. In the last session of our symposium, we had a good opportunity to have two presentations by Dr. David Rubinsztein (from UK) and Dr. William A. Dunn Jr. (fromUSA), both of which showed remarkable progresses in identifying autophagy inducers or inhibitors. These data gave us a positive perspective that the medical applications of autophagy will be tested in the near future. In this sense, we realized the importance of holding meetings on autophagy that involves both basic and medical researchers.

7. Additional description

We are planning to hold 6th International Symposium on Autophagy in 2012.

The 9th Annual Meeting of the Protein Science Society of Japan

1. Representative

Yuriko Yamagata (Faculty of Medical and Pharmaceutical Sciences Kumamoto University)

2. Opening period and Place

May 20(Wed.)-May 22(Fri.), ANA Hotel Kumamoto Newsy, Kumamoto, Japan

3. Number of participants / Number of participating countries and areas

810 attendees from 7 countries (UK, USA, South Korea, China, Singapore, Thailand and Japan)

4. Total cost

¥15,306,790JPY(excluding banquet cost)

5. Main use of subsidy

Printing Cost

6. Result and Impression

The 9th annual meeting of the Protein Science Society of Japan (PSSJ) was held at ANA Hotel Kumamoto Newsy for 3 days from May 20 to May 22, 2009. It gathered 810 researchers including 20 oversea participants. The meeting was consisted of various programs, such as 4 history reviews, 3 symposia, 17 workshops, 8 luncheon seminars and 418 posters. Especially the poster session had the largest number of presentations the PSSJ meeting ever had.

The field of protein science has rapidly developed in recent years, through the influence of genome projects. The purpose of the 9th Annual Meeting of the Protein Science Society of Japan was to announce new findings and analyze future perspectives in the field, as well as to attract young researchers in the post-genome era to this promising field.

Symposia featured world's distinguished researchers. At the disease-related protein session, Dr. G. Schertler, who was from UK and is well known for his successful research on the X-ray structure analysis of adrenergic receptors, gave an excellent lecture and made a deep impression on the audience. Another session, under the theme of the development of new protein science techniques, urged active discussions which inspired the participants. The 3rd session was for young scientists. Talented 10 fresh researchers made great presentations and the best 3 presenters were awarded the young scientist prizes. To encourage students, the meeting also awarded the poster prizes to the selected 10 presenters

for their excellent works.

This meeting was a great success with many attendees and presentations with high quality. It was not only a good chance to hear the latest discoveries, but also a great place to share thoughts and discuss with rivals and other talents. It gave us hints for the next step to go forward. We believe that most of the attendees were satisfied with what they acquired at this meeting. This meeting contributes to the further development of protein science in Japan.

In this serious recession, we anticipated to have financial problems. We also worried about the effect of swine flu that was going around the world. Despite all our anxieties, we could successfully conclude the meeting through efforts of many PSSJ members. We appreciate all the supports and aids from various organizations. Especially we would like to thank the Novartis Foundation (Japan) for the Promotion of Science for its generous contribution.

The 11th International Symposium on Exocrine Secretion, Tokushima 09
Exocrine Secretion-Mechanism and Disease

1. Representative

Kazuo Hosoi, Ph.D., Professor of Physiology
Department of Molecular Oral Physiology, Institute of Health Bioscience,
The University of Tokushima Graduate School

2. Opening period and Place

July 23-25, 2009 (3 days)
Kuramoto Campus, the University of Tokushima (3-18-15, Kuramoto-cho, Tokushima-shi,
Tokushima 770-0939)

3. Number of participants / Number of participating countries and areas

33 from oversea (participating countries were USA, Canada, Australia, England, Germany,
Denmark, China, Korea, and Russia)
117 from within the country (Japan) (Japanese 100 and foreigner 17)
Total number of participants, 150

4. Total cost

¥9,641,000 JPY

5. Main use of subsidy

- 1)Preparation of lecture auditorium and the place for poster presentation
Signboards on the campus entrance, auditorium stage, hall ways, campus passage
Cloth panel for poster presentation
- 2)Cost of printings (partial)
Program and Abstract book, Poster, Envelop, Certificate of Attendance

6. Result and Impression

The 11th International Symposium on Exocrine Secretion (ISES; Chairman, Kazuo Hosoi, the University of Tokushima, vice chairs, Masataka Murakami, Institute for Physiological Sciences and Ivana Novak, University of Copenhagen) was held in Kuramoto Campus, the University of Tokushima during July 23-25, 2009. The places for symposium and poster presentations were at Nagai Memorial Hall and Information Plaza of the Graduate School of Pharmaceutical Sciences, respectively. In the opening ceremony on the 1st day, Dr. Toshihiro Aono, the president of the University of Tokushima, and Dr. Yuji Sano (as a

representation of Kamon Iizumi, the governor of Tokushima prefecture), a vice-director of the Department of Health Policy and Health Service, Tokushima Prefectural Government presented their message to the ISES participants. Mr. Hideki Hara, the Mayor of Tokushima City also sent the telegram of the message of celebration.

Besides the The ISES office received 35 symposium papers (oral presentation) and 45 papers for poster presentations. Thirty three scientists from oversea and 117 from within the country attended the ISES. The participating countries were USA, Canada, England, Germany, Denmark, China, Korea, Australia, Russia and Japan. In the 3rd day afternoon the strong shower was fallen, but weather on the first and second days was very nice. On July 26th, the ISES served the “After-Convention Tour,” and those who want to attend the IUPS meeting visited several spots in Tokushima before leaving for Kyoto. The bus brought these participants to Kyoto after this excursion.

Aquaporins (AQPs), the water channel proteins, are strongly involved in the water secretion by exocrine gland; professor Verkman however said in his plenary lecture that these channel proteins have physiological functions other than the function to permeate the water. This was explored by the experiments in which AQP knock out mice were used; various physiological functions are altered in these mice. Professor Melvin showed in his keynote lecture that Cl-channel and Na⁺,K⁺,2Cl⁻ co-transporter as well as AQPs are important in the water secretion by the exocrine gland. This was again shown by using knock out mice. Estrogenic action has been suggested to be responsible for the strong female preponderance of many autoimmune diseases, including systemic lupus erythematosus (SLE), scleroderma, rheumatoid arthritis (RA), and Sjögren’s syndrome (SS). SS is a T cell-mediated autoimmune disorder characterized by lymphocytic infiltrates and destruction of the salivary and lacrimal glands. Professor Hayashi reported in his keynote lecture that retinoblastoma-associated protein RbAp48 induces tissue-specific apoptosis in the salivary glands depending on the level of estrogen deficiency, and discussed its molecular mechanism.

In the symposium and poster presentation, it was expected that every participant understand more about the mechanism of exocrine secretion by mutual exchange of the scientific information. Although working on the different tissues, scientists are interested in mechanism and function of exocrine secretion, and disease caused by malfunction and/or failure of the exocrine gland. We, therefore, had a lot of discussion and argument to establish a new idea and principle. It was expected also that this symposium contributes to the development of new medical cures and the promotion of public health. The ISES organizer considered that junior scientists or graduate students are important for the development of this field, and therefore granted partial supports for these young scientists. During the period of the symposium, the committee members evaluated the posters. Five

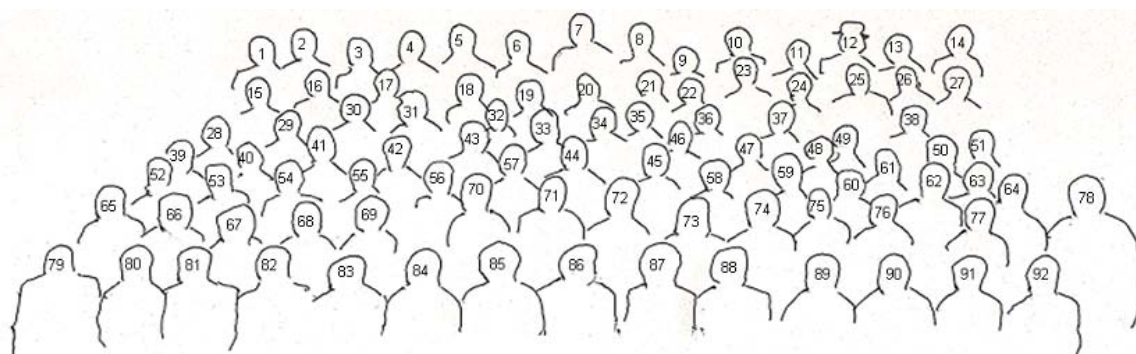
excellent posters, including the best one, were selected by the strict evaluation by these members; the poster awards were given to these presenters at the farewell party on the 3rd day. Lastly, we, the organizer believe that this international symposium was successful if it could contribute to the development of the science in the field of the exocrine gland.

7. Additional description

The following is a group photograph taken on the 2nd day in front of the Nagai Memorial Hall, the University of Tokushima, where the symposium was held.



**The 11th International Symposium on Exocrine Secretion, Tokushima 09
Nagai Memorial Hall, the University of Tokushima
July 23-25, 2009, Tokushima, Japan**



1. T. Mukaibo 2. Y. Kondo 3. K. Satoh 4. T. Hasegawa 5. T. Iida 6. S. Nakamura 7. AK. Stewart
8. H. Silke 9. Y. Otsuki 10. Y. Kitanaka 11. K. Ishibashi 12. C. Korbmacher 13. DI. Cook
14. T. Hayashi 15. M. Kidokoro 16. MG Guo 17. C. Wang 18. D. Wang 19. S. Ying 20. L. Yi
21. M. Tsukamoto 22. Y. Sakane 23. M. Yamaguchi 24. H. Nakashima 25. JH. Hanrahan
26. A. Dinudom 27. Y. Kadoya 28. T. Morita 29. A. Tanimura 30. A. Nezu 31. J. Leipziger
32. MV. Sørensen 33. P. Javkhlan 34. P. Poronnik 35. WA. Kruger 36. S. Hammami 37. M. Hayashi
38. T. Nakamoto 39. B. Qi 40. JS. Yoon 41. MC. Steward 42. G. Chen 43. DL. Bovell
44. J. Putney 45. Y. Sahara 46. SL. Alper 47. H. Ishiguro 48. K. Park 49. N. Koyama
50. M. Kashimata 51. MA. Cátalan 52. S. Ko 53. S. Muallem 54. MG Lee 55. Y. Hieda
56. A. Shitara 57. Y. Hayashi 58. Y. Shiba 59. C. Hirono 60. H. Ichikawa 61. A. Inagaki
62. T. Narita 63. H. Uneyama 64. N. Yamada 65. T. Hosoi 66. S. Hashimoto 67. A. Ahmad
68. C. Yao 69. Y. Ishikawa 70. T. Lukmanee 71. S. Naruse 72. Y. Seo 73. M. Fukushima
74. O. Katsumata-Kato 75. J. Yoshigaki 76. H. Sugiyu 77. M. Kawai 78. VA. Zolotarev
79. S. Matsuo 80. Y. Hiroshima 81. T. Akamatsu 82. K. Inenaga 83. Y. Hayashi 84. E. Gresik
85. AS. Verkman 86. K. Hosoi 87. I. Novak 88. M. Murakami 89. IS. Ambudkar 90. J. Melvin
91. AM. San Gabriel 92. M. Fukano

16th International Conference on Cytochrome P450

1. Representative

Hirofumi Shoun

2. Opening period and Place

June 21 - June 25, 2009

Bankoku Shinryokan (1792 Kise Nago, Okinawa 905-0026)

3. Number of participants / Number of participating countries and areas

207 Participants / 19 Countries

Japan (103), USA (40), UK (10), Korea (10), Germany (8), Australia (6), Sweden (6), Czech Republic (5), France (4), Canada (2), Denmark (2), Slovenia (2), India (2),

Taiwan (2), Russia (1), Finland (1), Switzerland (1), China (1), Nepal (1)

4. Total cost

¥24,412,112 JPY

5. Main use of subsidy

Shuttle buses (Between hotels and the venue and every morning and night during the conference for participants.)

6. Result and Impression

The 16th International Conference on Cytochrome P450 was held in the last June in Okinawa, as noted above. In spite of the recent world wide bad economy and epidemic of flu, more than 100 persons from abroad have attended the meeting. We had 2 plenary lectures, 52 invited lectures, and 117 posters, which covered almost all of recent important findings and results in this field for these couple of years. Professor Shigeaki Kato presented a lecture on the expression of CYP genes regulated by nuclear vitamin D and dioxin receptors. Prof. Frances Arnold of California Institute of Technology had a lecture on artificial selection (directed evolution) of cytochrome P450s. These two plenary lectures gave deep impression to the audience. Dr. D. Ghosh (Roswell Park Cancer Institute, USA) reported their important result on the structure of aromatase (CYP19), which was just published in Nature in this year. The result is very important because it can be applied to the development of anti-breast cancer drugs. Prof. A. W. Munro of University of Manchester presented a lecture on the P450 systems in the human pathogen Mycobacterium tuberculosis, which shows a new aspect on the curatives for tuberculosis. Prof. E. F. Johnson of the

Scripps Research Institute, USA, who gave a breakthrough in determining the crystal structures of human drug-metabolizing P450s, had a lecture on the structure of human P450 2C9. Importance of P450 is now expanding into various fields of life sciences. The theme we emphasized this time is Biotechnology and Environment. We had two sessions on this theme. Prof. H. Ohkawa of Fukuyama Univ. reported on phytomonitoring and phytoremediation utilizing recombinant P450s. Prof. T. Sakaki of Toyama prefecture Univ. presented Construction of P450 species for production of active vitamin D3. Dr. Y. Tanaka of Suntory Ltd reported on flower color modification (creation of blue rose).

In addition to the presentations by these “big names”, we had many exciting poster presentations by young scientists. Dr. Tsuneo Omura and the selection committee afforded a poster award (with 100,000 JPY) to five young scientists. Further, we presented travel support to many domestic and foreign students and young scientists as much as possible. The meeting was very active and successfully closed. We could therefore concentrate these scientific properties and inherit them to future.

7. Additional description

Conference venue was constructed for the millennium Okinawa Summit in 2000. Therefore it has incomparable environment and gorgeous buildings. However, its location is remote, which we mostly worried. So we gave transportation service as much as possible, which was performed smoothly. As the results, many participants, in particular from abroad, appreciated and admired the selection of venue and administration of the meeting. They also enjoyed very much the excursion to Nakijin castle (the World heritage) and Churaumi aquarium. So we also contributed to the advertisement of Okinawa that depends on tourists.

Satellite Symposium, XXXVIth International Union of Physiological Sciences (IUPS)

1. Representative

Name: Gozoh Tsujimoto

Institution: Department of Genomic Drug Discovery Science, Graduate School of
Pharmaceutical Sciences Kyoto University

Faculty of Pharmaceutical Sciences, Kyoto University

2. Opening period and Place

Opening Period: July 27—August 1, 2009

Place: Kyoto International Conference Center

3. Number of participants / Number of participating countries and areas

Number of participants: Approximately 150

Number of participating countries: Approximately 10~15

U.S.A, U.K, Canada, China and others.

4. Total cost

¥4,039,000JPY

5. Main use of subsidy

Traveling fee for overseas invited speakers.

Expenses for reception.

6. Result and Impression

The central research theme of this Satellite Symposium is the study of network dynamics across various time scales, including temporal changes in both network state and structure. Invited research groups exemplify the type of multi-disciplinary, multi-investigator research in this field. Prof. Michel Fill (Loyola University Chicago, USA) presented “Calsequestrin regulation of Signal ryanodine receptor Calcium Release Channels”, Prof. Frances Zorzato (Basel University Hospital, Switzerland) presented “Modulation of skeletal muscle excitation-contraction coupling by protein components of the sarcoplasmic reticulum functional face membrane.”. Prof. Richard Steinhardt(University of California Berkeley, USA) presented “Membrane Repair – Ca entry and vesicle trafficking”. Prof. Jian Ma(University of Medicine and Dentistry, New Jersey, USA) presented “MG53, a molecular sensor of the acute membrane repair process in striated muscle.”. Prof. Toshio Tanaka (Mie University, Japan) presented “Pharmacogenomics networks in human disease

models and therapeutic target”. And Prof. Shouhei Mitani(Tokyo Women’s medical University, Japan) presented “Systematic isolation of mutants defective in transcription factors in *C. elegans*”.

第 23 期 (2009 年度) 助成事業報告

当財団は、1987年9月3日に文部大臣より認可を受けて設立して以来、寄附行為に定めた研究助成を中心とした事業を行ってきました。2009年度は、下記に示したノバルティス研究奨励金、研究集会助成、海外留学生受入れ助成の総額3,700万円の助成を行っております。

ノバルティス研究奨励金	30件 (1件	100万円)	3,000万円
研究集会助成	5件 (1件	40万円)	200万円
海外留学生受入れ助成	3件 (1件100～200万円)		500万円
			総額 3,700万円

2009 年度ノバルティス研究奨励金贈呈者

この事業は、生物・生命科学およびそれに関連する化学の領域において、我が国で行われる創造的な研究に対し、助成することを目的としています。

(受付順、敬称略、所属・職位は申請時。助成金額：1件100万円)

番号	氏名	研究機関名	役職	研究テーマ
1	北村 ゆかり	群馬大学 生体調節研究所	グローバル COE 研究員	FoxO1 による ChREBP の O-グリコシル化調節を介した糖、脂質代謝制御機構の解明
2	森田 啓行	東京大学 大学院医学系研究科	特任准教授	心筋転写ネットワーク破綻による心筋症・心不全発症の機序解明～ヒト拡張型心筋症を惹起する HOP 遺伝子変異からのアプローチ～
3	古橋 真人	札幌医科大学 内科学第二講座	助教	心血管代謝疾患における脂質シヤペロン・炎症・小胞体ストレス応答の解明
4	鈴木 敏彦	琉球大学 大学院医学研究科	教授	Nod 様受容体 NLRP3 を介した宿主炎症誘導の分子機構
5	江島 亜樹	京都大学 生命科学系キャリアパス形成 ユニット	特定助教	求愛行動を制御する嗅覚系バックグラウンド・キャンセリング機構の研究
6	林 郁子	横浜市立大学 大学院生命ナノシステム科学 研究科	准教授	細胞移動を制御する超小管伸長端結合蛋白質 CLASP 2 の分子基盤
7	阿部 郁朗	東京大学 大学院薬学系研究科 天然物化学教室	教授	ステロイド系抗生物質の生合成工学
8	大塚 稔久	山梨大学大学院 医学工学総合研究部	教授	アクティブゾーンタンパク質 CAST/ELKS ファミリーの生理機能
9	大島 正伸	金沢大学 がん研究所	教授	消化管腫瘍発生における Sox17 の作用
10	今泉 美佳	杏林大学 医学部生化学	准教授	インスリン開口放出の 4D イメージング解析
11	小内 伸幸	東京医科歯科大学 難治疾患研究所	講師	ヒト樹状細胞サブセットの分化・ホメオスターシス機構の解明
12	堀内 久徳	京都大学 大学院医学研究科	講師	低分子量 GTP 結合蛋白質 Ral を介した細胞癌化および浸潤・転移に関する研究

番号	氏名	研究機関名	役職	研究テーマ
13	太田 嗣人	金沢大学 フロンティアサイエンス機構	特任助教	リポドミクスによる脂肪酸プロファイルを指標とした非アルコール性脂肪肝炎の病態解明
14	宮武 昌一郎	東京都医学研究機構 東京都臨床医学総合研究所	プロジェクト リーダー	ウイルスの出芽を抑制する分子 CD317/ tetherin の個体レベルでの機能解析
15	上口 裕之	理化学研究所 脳科学総合研究センター	チーム リーダー	神経軸索ガイダンスの駆動機構：成長円錐での非対称性膜動態の研究
16	松岡 雅雄	京都大学 ウイルス研究所附属 エイズ研究施設	教授	ヒトT細胞白血病ウイルス1型の病原性発現機構
17	長束 俊治	新潟大学 理学部生物学科	教授	糖鎖シーケンシングのための化学的フラグメンテーション法の開発
18	鳶巣 守	大阪大学 大学院工学研究科	特任講師	含窒素ヘテロ芳香環の炭素-水素結合の直接官能基化反応の開発
19	此木 敬一	東北大学 大学院農学研究科	准教授	天然毒貯蔵生物がもつ自己耐性機構
20	依光 英樹	京都大学 大学院理学研究科	准教授	パラジウム触媒による多置換エポキシドの不斉合成
21	丸本 朋稔	九州大学 高度先端医療センター	特任講師	コモンマーモセットを用いた新規霊長類脳腫瘍モデルの作成
22	水波 誠	北海道大学 大学院先端生命科学 科学研究院	教授	昆虫に学ぶ匂い情報処理アルゴリズムの研究
23	増富 健吉	国立がんセンター 研究所	プロジェクト リーダー	ヒト RNA 依存性 RNA ポリメラーゼとがん幹細胞
24	松尾 勲	大阪府立病院機構 大阪府立母子保健総合医療 センター研究所	主任研究員	分泌性シグナル因子による哺乳動物胚パターン形成機構
25	柳田 素子	京都大学 生命科学系キャリアパス形成 ユニット	講師	BMP とその調節因子が織りなす慢性腎臓病の素因決定および進展メカニズムの解明
26	内匠 透	広島大学大学院 医歯薬学総合研究科	教授	自閉症ヒト型モデルマウスを用いた社会性行動の分子解析
27	中屋敷 均	神戸大学大学院 農学研究科	准教授	DNA 修復系から RNAi への新たなシグナルフロー
28	岡崎 拓	徳島大学 疾患ゲノム研究センター	教授	自己免疫疾患モデルマウスを用いたゲノム解析
29	高橋 将文	自治医科大学 分子病態治療研究センター	教授	心筋虚血再灌流障害における炎症惹起機構の解明：新規自然免疫経路インフラマソームを中心とした解析
30	広常 真治	大阪市立大学 大学院医学研究科	教授	カルパイン阻害剤を用いた滑脳症治療への新戦略

2010 年度研究集会助成金贈呈集会

この事業は、生物・生命化学およびそれに関連する化学の領域において、我が国で開催される国際性豊かな研究集会の運営費の一部を援助することを目的としています。

(受付順、敬称略、所属・職位は申請時。助成金額：1 件 40 万円)

番号	研究集会名	開催期日 (開催地)	助成先代表者	
			所属・職位	氏名
1	第 5 回国際フィロウイルス シンポジウム	2010.4.18 ~ 4.21 (東京)	東京大学 医科学研究所 教授	河岡 義裕
2	タンパク質社会に関する国際会議	2010.9.12 ~ 9.16 (奈良)	名古屋大学 大学院理学研究科 教授	遠藤 斗志也
3	第 17 回国際 RUNX ワークショップ 2010	2010.7.11 ~ 7.14 (神奈川)	理化学研究所 免疫・アレルギー科学 総合研究センター チームリーダー	谷内 一郎
4	2010 国際ポリアミン会議 - 医学・生命科学への展開 -	2010.6.14 ~ 6.18 (静岡)	東京慈恵会医科大学 教授	松藤 千弥
5	第 16 回国際分化学会国際会議	2010.11.14 ~ 11.18 (奈良)	自然科学研究機構 基礎生物学研究所 教授	上野 直人

2009 年度海外留学生助成金贈呈者

この事業は、生物・生命科学およびそれに関連する化学の領域において、創造的な研究に携わるアジアの国々および地域から日本への留学生（留学中を含む）に対して、旅費・滞在費を助成することを目的としています。

(受付順、敬称略、所属・職位は申請時。助成金額：1 件 100 ~ 200 万円)

番号	氏名	国名	職位	所属機関	研究テーマ
1	カルクザマン エムディ KHALEQUZZAMAN Md.	Bangladesh	Graduate student	名古屋市立大学 大学院医学研究科 [教授上島 通浩]	発展途上国における室内空 気汚染の実態と子供の健康 への影響の解明
2	スラジ エカ ウイドリアン Suradji Eka Widriani	インドネシア	Graduate student	群馬大学 大学院医学研究科 [教授小山 洋]	抗マalaria薬の新規ターゲッ トとしてのセレンによるマラリ ア原虫アポトーシス誘導メカ ニズムの解明
3	グナワルダナ エゴダハ ゲダラワセナ GUNAWARDANA Egodaha Gedara Wasana	Sri Lanka	Student	東京大学 大学院新領域 創成科学研究科 [准教授佐藤 弘泰]	下水処理水中に出現する微 生物群集の種構成とその経 時変動

第23期（2009年度）財務報告

貸借対照表

2009年3月31日現在

(単位：円)

科 目	金 額
I 資産の部	
1. 流動資産	
現金預金	18,285,394
未収収益	10,802,098
未収金	5,733
有価証券	1,184,342
前払費用	260,566
流動資産合計	30,538,133
2. 固定資産	
(1) 基本財産	
投資有価証券（指定）	724,680,000
投資有価証券（一般）	45,690,000
基本財産合計	770,370,000
(2) その他固定資産	
什器備品	174,912
電話加入権	76,440
その他有価証券	35,145,002
その他固定資産合計	35,396,354
固定資産合計	805,766,354
資産合計	836,304,487
II 負債の部	
1. 流動負債	
未払金	35,107,634
預り金	24,500
流動負債合計	35,132,134
負債合計	35,132,134
III 正味財産の部	
1. 指定正味財産	
指定正味財産合計	724,680,000
(うち基本財産への充当額)	(724,680,000)
2. 一般正味財産	76,492,353
(うち基本財産への充当額)	(45,690,000)
正味財産合計	801,172,353
負債及び正味財産合計	836,304,487

収支計算書

2008年4月1日から2009年3月31日まで

(単位：円)

科 目	決 算 額
I 事業活動収支の部	
1. 事業活動収入	
基本財産運用収入	24,623,656
寄付金収入	40,078,000
雑収入	1,695,081
事業活動収入計	66,396,737
2. 事業活動支出	
事業費支出	48,613,776
管理費支出	4,621,687
事業活動支出計	53,235,463
事業活動収支差額	13,161,274
II 投資活動収支の部	
1. 投資活動収入	0
2. 投資活動支出	20,000
投資活動収支差額	△ 20,000
III 財務活動収支の部	
1. 財務活動収入	0
2. 財務活動支出	0
財務活動収支差額	0
当期収支差額	13,141,274
前期繰越収支差額	△ 17,735,275
次期繰越収支差額	△ 4,594,001

役員名簿（理事・評議員・選考委員）

理 事 会

2010年10月1日現在（順不同、敬称略）

職名	氏名	現 職	就任年月日	常勤・非常勤
理事長	金子 章道	畿央大学大学院健康科学研究科教授 慶應義塾大学名誉教授	2003年6月10日	非常勤
理 事	浅野 茂隆	早稲田大学理工学術院教授 東京大学名誉教授	1999年6月4日	非常勤
	石川 裕子	ノバルティス ファーマ株式会社 常務取締役 人事・コミュニケーション本部長	2004年6月7日	非常勤
	大島 泰 郎	共和化工株式会社 環境微生物学研究所長 東京工業大学名誉教授	1997年6月8日	非常勤
	黒 川 清	政策研究大学院大学教授 東京大学名誉教授	1999年6月4日	非常勤
	眞崎 知生	筑波大学名誉教授 京都大学名誉教授	1999年6月4日	非常勤
	マックス・ブルガー	ノバルティス サイエンスボード議長 バーゼル大学教授	1987年9月16日	非常勤
	眞弓 忠 範	神戸学院大学薬学研究科教授 大阪大学名誉教授	2004年6月7日	非常勤
	三谷 宏 幸	ノバルティス ファーマ株式会社 代表取締役社長	2007年9月5日	非常勤
	村崎 光 邦	CNS薬理研究所長 北里大学名誉教授	2001年6月1日	非常勤
	森 美 和 子	北海道医療大学客員教授 北海道大学名誉教授	2005年6月13日	非常勤
監 事	中嶋 徳 三	中嶋徳三公認会計士事務所 公認会計士	2006年6月5日	非常勤
	松本 秀三郎	元ノバルティス ファーマ株式会社 常勤監査役	1998年2月10日	非常勤

評 議 員 会

2010年10月1日現在（順不同、敬称略）

職名	氏名	現職	就任年月日	常勤・非常勤
評議員会議長	黒岩 常祥	立教大学極限生命情報センター長 東京大学名誉教授	2002年2月7日	非常勤
評議員	赤池 紀扶	熊本保健科学大学リハビリテーション学科教授 銀杏学園理事・副学長 九州大学名誉教授	1999年6月4日	非常勤
	赤沼 安夫	財団法人朝日生命成人病研究所名誉所長	2001年6月1日	非常勤
	浅島 誠	東京大学大学院総合文化研究科客員教授 東京大学名誉教授	1999年6月4日	非常勤
	遠藤 政夫	山形大学名誉教授	1997年6月8日	非常勤
	小川 聡	国際医療福祉大学三田病院長 慶應義塾大学名誉教授	2001年6月1日	非常勤
	川寄 敏祐	立命館大学糖鎖工学研究センター長 京都大学名誉教授	1999年6月4日	非常勤
	川島 博行	元新潟大学大学院医歯学総合研究科教授	2001年6月1日	非常勤
	北 徹	神戸市立医療センター中央市民病院 病院長	1999年6月4日	非常勤
	後藤 勝年	JST サテライト茨城センター長	2001年6月1日	非常勤
	榊 佳之	豊橋技術科学大学学長 東京大学名誉教授	2001年6月1日	非常勤
	柴崎 正勝	財団法人微生物化学研究会 微生物化学研究所長	2005年6月13日	非常勤
	富永 健	昭和大学附属豊洲病院乳癌検診・治療センター 元センター長・教授	1998年6月5日	非常勤
	中西 重忠	財団法人大阪バイオサイエンス研究所所長 京都大学名誉教授	1999年6月4日	非常勤
	長田 敏行	法政大学生命科学部学部長 東京大学名誉教授	2005年6月13日	非常勤
	西川 武二	慶應義塾大学名誉教授 日本ワックスマン財団常務理事	2001年6月1日	非常勤
	西宗 義武	大阪大学微生物病研究所特任教授	1999年6月4日	非常勤
	水野 美邦	順天堂大学医学部教授	1999年6月4日	非常勤

選考委員会

2010年10月1日現在（順不同、敬称略）

職名	氏名	現職	就任年月日
選考委員長	満屋 裕明	熊本大学医学部教授	2007年6月 4日
選考委員	石川 冬木	京都大学大学院生命科学研究科教授	2007年6月 4日
	梅田 真郷	京都大学大学院工学研究科教授	2007年6月 4日
	岡 芳知	東北大学大学院医学系研究科教授	2008年6月20日
	貝淵 弘三	名古屋大学大学院医学研究科教授	2009年6月19日
	狩野 方伸	東京大学大学院医学系研究科教授	2009年6月19日
	斎藤 能彦	奈良県立医科大学教授	2007年6月 4日
	笹井 芳樹	理化学研究所発生・再生総合研究センター グループディレクター	2008年6月20日
	笹井 宏明	大阪大学産業科学研究所教授	2010年6月18日
	佐田 政隆	徳島大学大学院ヘルスバイオサイエンス 研究部教授	2009年6月19日
	竹内 勤	慶應義塾大学医学部教授	2009年6月19日
	中山 俊憲	千葉大学大学院医学研究院教授	2007年6月 4日
	西田 篤司	千葉大学大学院薬学研究科教授	2009年6月19日
	西村 いくこ	京都大学大学院理学研究科教授	2007年6月 4日
	長谷部 光泰	自然科学研究機構 基礎生物学研究所教授	2009年6月19日
	福田 恵一	慶応義塾大学医学部教授	2008年6月20日
	福永 浩司	東北大学大学院薬学研究科教授	2007年6月 4日
	峯岸 敬	群馬大学大学院医学系研究科教授	2010年6月18日
	宮園 浩平	東京大学大学院医学系研究科教授	2009年6月19日
	村田 道雄	大阪大学大学院理学研究科教授	2008年6月20日

事務局便り

ご寄附のお願い

当財団は、生物・生命科学およびそれに関連する化学の領域における創造的な研究および研究集会を助成し、学術の進展と福祉の向上に寄与することを目的としております。

これらの事業は、基本財産の運用益および寄附金にて行われており、当財団は事業の趣旨にご賛同いただける方々からのご寄附を募っております。

なお、当財団はご寄附をいただく方々へご配慮するために、特定公益増進法人の認定を受けております。

特定公益増進法人とは、公益法人等のうち教育または科学の振興、文化の向上、社会福祉への貢献その他公益の増進に著しく寄与するものとして認定された法人をいいます。

これらの法人に対して、個人または法人が寄附を行った場合は、下記の税法上の優遇措置を受けることができます。

優遇措置の概略

- 個人：支出した寄附金（その年の総所得額の40%を限度とする）のうち、5千円を超える部分について寄附金控除が認められます。
また、上記の寄附金控除の対象になっている寄附金は、個人住民税の寄附金控除が受けられます。
- 法人：支出した寄附金は、通常一般の寄附金の損金算入限度額と同額まで、別枠で損金に算入できます。

ご寄附は、随時受付けております。

詳しくは、財団事務局までお問合せ下さい。

（電話：03-5464-1460、Eメール：novartisfound.japan@novartis.com）

事務局より

平成22年度の財団年報を発行できることは、助成を受けられた皆様および財団関係者のご尽力の賜物です。厚く御礼申し上げます。

財団法人の制度が改定され、当財団も新しい公益法人に移行する必要が出てまいりました。

慣れない申請準備の作業で戸惑っている点がありますが、助成事業の方は学術の発展に寄与できる喜びを胸に例年通り着実に進めていきたいと考えております。

今後ともご指導、ご支援の程よろしくお願い申し上げます。

事務局長 松田光陽

財団法人 ノバルティス科学振興財団

〒106-0031 東京都港区西麻布4-16-13

西麻布28森ビル

Tel:03-5464-1460 Fax:03-5467-3055

E-メール：novartisfound.japan@novartis.com

ホームページ：<http://www.novartisfound.or.jp>